# CHANNEL CHARACTERIZATION AND FORWARD ERROR CORRECTION CODING FOR DATA COMMUNICATIONS ON INTRABUILDING ELECTRIC POWER LINES

by

Morgan Hing Lap Chan

B.A.Sc., University of Ottawa, 1983
M.A.Sc., University of British Columbia, 1985

A THESIS SUBMITTED IN PARTIAL FULFILLMENT OF

THE REQUIREMENTS FOR THE DEGREE OF

DOCTOR OF PHILOSOPHY

in

THE FACULTY OF GRADUATE STUDIES

(Department of Electrical Engineering)

We accept this thesis as conforming
to the required standard

THE UNIVERSITY OF BRITISH COLUMBIA

December 1988

© Morgan Hing Lap Chan, 1988

In presenting this thesis in partial fulfilment of the requirements for an advanced degree at the University of British Columbia, I agree that the Library shall make it freely available for reference and study. I further agree that permission for extensive copying of this thesis for scholarly purposes may be granted by the head of my department or by his or her representatives. It is understood that copying or publication of this thesis for financial gain shall not be allowed without my written permission.

Department of _Electrical Engineering_

The University of British Columbia
Vancouver, Canada

Date _17 Apr., 1989_

# Abstract

The use of intrabuilding electric power lines for data communications and local area networking is of growing interest. In this thesis, an original work to study the very important signal propagation and noise characteristics of the complex and hostile power line networks has been completed. Various impairments such as high and varying signal attenuation levels, periodic signal fading and impulse noise were identified. Estimates of the amplitude, pulse width and interarrival distributions of impulse noise were obtained. Communication signal attenuation of power line networks was explored. The effects of electrical loading on these communication channel factors were examined. Implications of the results for intrabuilding communications are addressed.

To combat power line impulse noise, channel fading, attenuation and other impairments, forward error correction (FEC) coding and bit interleaving is proposed and shown to be very effective, and is an essential component for reliable communication over power lines. The performance of interleaved hard and soft decision decoding of repetition codes with or without erasure has been analysed, using a simple first order power line noise model. Various random and burst error correcting block codes have been evaluated, using actual recorded bit error patterns encountered on power line data channels.

Based on studies of the channel and error correction coding, an actual low cost FEC coded communication system for use on intrabuilding power lines was successfully designed, implemented and tested. Real time performance results of coded and uncoded data transmissions on typical power

lines were experimentally determined. Convolutional codes as well as repetition coding and bit interleaving are used to overcome burst errors and other impairments encountered on power line channels. The emphasis is on high speed transmission at bit transmission rates up to 57.6 kbits/s. Typical practical coding gains from 10 to 20 dB were achieved at bit error rate of $10^{-4}$ on various noisy links. It is successfully demonstrated that with appropriate and inexpensive FEC coding, reliable high speed data transmission over power lines is feasible, even at very small interleaving delay.

# Table of Contents

*)*

# List of Tables

# List of Figures

x

xi

# Acknowledgement

# Chapter 1

# Introduction

## 1.1 Communications through Electric Power Lines

Electric power distribution lines have been used by the power industry for communication purposes including remote metering reading, load management and other applications [10,20,26]. Because of the inherent incompatibility of the electric power lines to carry communication signals and the large amount of noise generated by electrical equipment, most of these systems have data rates below 100 bits/s.

Recent developments in local area networks (LAN) and in the advancement of microprocessor controlled equipment motivate the use of power lines as a communication medium for intrabuilding local area networking. The possibility of using power lines for data and voice communications within

1

office buildings, hospitals, warehouses, factories, convention centers, and residential buildings is an exciting proposition. A number of obvious advantages in using power lines for indoor communications includes:

1. Avoidance of the need for custom networks which can be costly or even impossible to install, as well as restrictive in the location of equipment served by the network.

2. Virtual universality of coverage.

3. Ease of network access by a standard electrical wall-socket plug.

4. Flexibility of adding or relocating equipment without the need for time-consuming and costly rewiring.

In fact, the high cost of relocating LAN terminals has generated interest in LAN technologies that require no dedicated cabling. The prospect of power line based communication systems for commercial applications looks promising. A power line network would find applications in home control and management, security and fire alarm monitoring, personal computer and terminal communications, office automation, and point-of-sale networking. Recently, the Electronic Industries Association (EIA) began to draft standards for using intrabuilding electric power lines for home automation control and communications.

During the past few years, several commercial intrabuilding power line communication systems have been developed. These include modems from BSR, NONWIRE, ExpertNet, National Semiconductor and Signetics [2,27,34,36,40]. These products have nominal data rates from 120 bits/s to 1.2 kbits/s, operate at carrier frequencies from 30 kHz to 150 kHz and use amplitude shift keying (ASK) or noncoherent frequency shift keying (FSK) modulation. These modulation schemes are simple to implement, and facilitate manufacture. In addition to these commercial products, several research projects have been reported. Ochsner [37] discussed the suitability of a spread spectrum FSK system at 1.2 kbits/s transmission rate. Van der Gracht [16] presented measured results of an AC zero crossing synchronized peudo noise (PN) spread spectrum modem at 60 bits/s. A potential advantage of spread spectrum signalling is its inherent capacity of simultaneously supporting multiple users using code division multiple access (CDMA). However, there is no reported work on using CDMA with spread spectrum signalling. It is important to note that not all power line modems can operate satisfactorily across phases and under different power line environments.

Channel impairments severely limit the data transmission speed and accuracy achieveable on power line networks. Thus far, because of the hostile communication environment, transmission at 1.2 kbits/s on power lines is often considered to be a practical limit. At these low data rates, the effect of

3

power line impulse noise is relatively small, energy per data bit is relatively high, implementation tolerance is large, and reliable performance can easily be achieved at low transmitter power levels. As the transmission speed increases, the harmful effect of impulse noise also increases. At high data rates ($\geq$ 9.6 kbits/s), it becomes much harder to overcome noise impulses whose durations approach that of a data bit, and system performance can be seriously degraded.

The inadequate performance of present systems together with a growing interest in the use of intrabuilding power lines for data communications requires characterization of this channel for communication purposes. Determination of channel behaviour and proper application of such knowledge for reliable transmission at ever higher data rates is becoming the main focus of increasing research activities in this area. The eventual objective is to develop technology for future commercial developments.

The cost of a power line local area network will be one determinant of its success in real applications. Custom installed communication networks will have a much higher transmission capacity and reliability. It is therefore mandatory that the price of power line LAN facilities be kept as low as possible in order that these facilities can be purchased at a small incremental cost to complement a faster dedicated network, and to support specific lower

speed applications.

## 1.2   Outline of Thesis

A prerequisite to the design of communication systems is knowledge of the communication channel. Important basic parameters including signal attenuation and channel noise require appropriate description.

This thesis begins with a study into the very important signal propogation and noise characteristics of the power line networks, in order to assess signal transmission capability and to identify fundamental limitations on reliable transmission. The results will considerably influence system design by helping to develop appropriate design strategies for combating these impairments.

Potential benefits of using forward error correction (FEC) coding to combat power line channel impairments is of much concern. Initial analytical results indicating the importance and potential performance advantages to be realized with FEC coding over power line channels are presented. However, with FEC care must be exercised to choose a code that matches the channel condition and user requirements. The use of a code with inappropriate error handling ability can increase the error rate of a system, cause unnecessary delay and degrade system throughput. To determine an efficient and reliable

5

code for use on power lines, actual performance of a code when subjected to actual channel errors is of prime importance. Original results from simulation of various random and burst error correcting block codes using real recorded error patterns encountered on power line channels during different kinds of impairment are presented in this thesis.

Following the above investigations, orginal measurement results on practical application of coding to actual systems in operation are presented. A low cost FEC coded data communication system designed for use on intra-building power lines was successfully implemented, and was used to establish real-time performance results of coded and uncoded data transmissions to be realized on real-world power line networks. Convolutional codes as well as repetition coding were examined. The emphasis is on high speed digital transmission and includes results at bit transmission rates up to 57.6 kbits/s which go well beyond the works of others. After this introductory chapter, the thesis is organized as follows:

Chapter 2 describes the topological structure of intrabuilding power line networks, and their interaction with electrical loads.

Chapter 3 details the signal attenuation characteristic of power line net-works, as well as periodic signal fading behaviour. Attenuation data from five different building environments are carefully analysed, followed by a detailed

discussion on the implications of these results for intrabuilding communications.

Chapter 4 presents measurement results on probability distributions for the amplitude, width and interarrival time of noise impulses on intrabuilding power lines. These distributions are useful for designing effective signalling and error control schemes.

Chapter 5 presents explicit bit error rate formulae obtained for interleaved repetition coding with either hard or soft decision decoding and with or without erasure. The results indicate the potential for FEC coding and bit interleaving to greatly improve the performance of a data communication system by combating power line impulse noise, signal fading and other bursty impairments.

Chapter 6 presents original performance results obtained using a number of random and burst error correcting block codes. Actual recorded channel error patterns under various impairments are used to test these codes. Block error rates are measured for these codes, to determine appropriate codes, to assess the effects of variation of block size and to determine a suitable depth of interleaving.

Chapter 7 presents a number of promising FEC convolutional codes for power line communications. An actual FEC coded data communication

system designed for use over power lines was successfully implemented and used to obtain real-time performance results on typical power line channels. Convolutional codes are emphasized. Decoded bit error rate and packet reception rate are obtained for these codes. A practical erasure mechanism is described for power line channel errors. The obtained results show that utitlization of suitable, inexpensive FEC coding schemes can ensure reliable transmisison on otherwise unreliable power line channels.

Finally, Chapter 8 provides some general conclusions drawn from this thesis and suggests some future research directions.

# Chapter 2

# Intrabuilding Power Distribution Circuits as Communication Channels

Intrabuilding power distribution circuits receive power from distribution transformers and carry this power to various loads in either commercial/industrial or residential buildings. To understand the communication characteristics and behaviour of intrabuilding power line networks, it is necessary to first examine the way in which buildings are wired.

## 2.1 Building Wiring Plans

Three-phase electric power is transmitted from generation sites via high voltage lines to substations, from where transmission to distribution transformers occurs via distribution lines at voltage levels ranging from 10 to 50 kV [3,14].

9

The secondary (load) side of the distribution transformer connects to circuit panels in buildings. From a circuit panel power is delivered to electrical loads via intrabuiding branch circuits, as shown in Figs. 2.1 and 2.2.

In residential housing or apartment units, the secondary side of the transformer delivers split-single-phase power to circuit panels by two 120-V lines 180° out of electrical phase and a neutral conductor. The neutral conductor is normally grounded at the circuit panel and is common to all electrical loads. From the circuit panel, general purpose branch circuits consisting of a 120-V line and neutral conductor deliver power to small loads interfaced by means of standard lamp or plug-in recepticles. Some of these loads may be controlled by switches. Each large appliance is individually supplied by a special dedicated branch circuit. Washing machines, refrigerators, home freezers, dishwashers, garbage disposals and forced-air motor drives, all have their own individual branch circuits consisting of a 120-V line and the neutral. Electric range and dryer heating elements are connected directly across two 120-V supply lines (240 V drop) while the dryer motor, as well as dryer and range lamps and timers connect between the 120-V line and neutral. Hot water tanks, which typically draw 3 kW at 240 V, connect across the two 120-V supply lines; there is no connection to neutral in this case.

25 KV POWER LINE

DISTRIBUTION
TRANSFORMER

TO RESIDENCE B

120 V $\underline{/0^\circ}$

NEUTRAL

120 V $\underline{/180^\circ}$

RESIDENCE A

METER

SERVICE PANEL

CIRCUIT
BREAKERS

SWITCHES

LOADS

WATER HEATER

BRANCH CIRCUITS
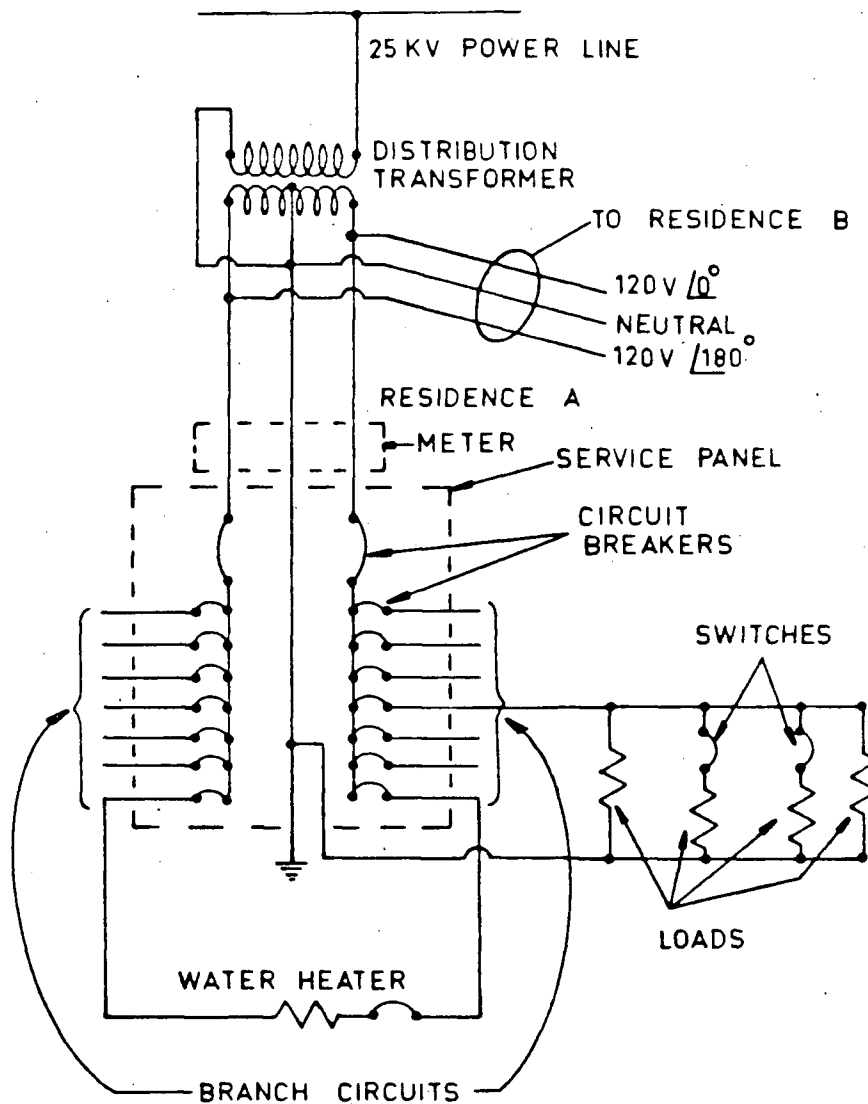
Figure 2.1: Residential power delivery scheme.

DISTRIBUTION TRANSFORMER

3 φ
POWER LINES

METER

CIRCUIT PANEL

BRANCH CIRCUITS
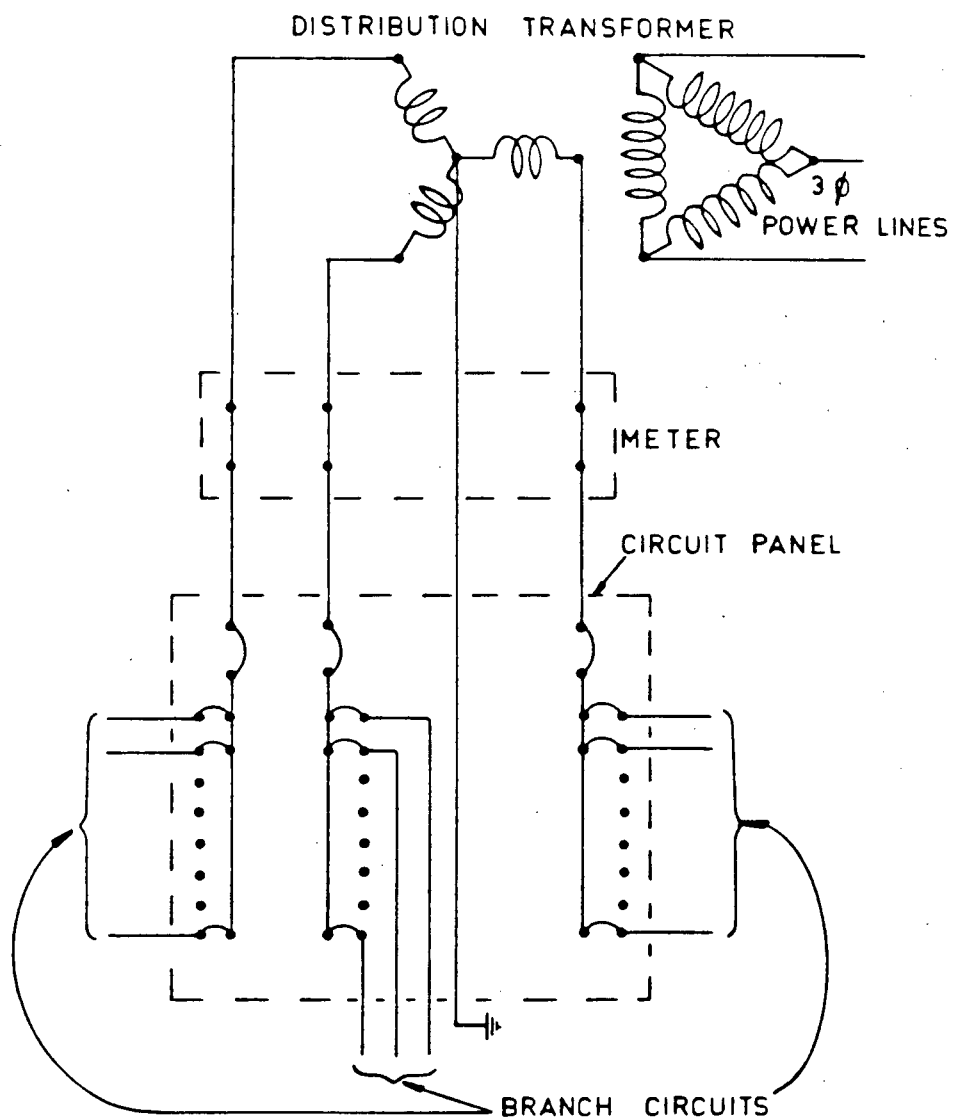
Figure 2.2: Commercial/Industrial three-phase power delivery scheme.

Commercial and industrial buildings are typically supplied with three-phase power as indicated in Fig. 2.2. In large buildings, each floor or floor group may be supplied by separate three-phase transformers. Standard branch circuits consisting of a 120-V and neutral line supply standard electrical loads. Heavier loads are supplied by circuits that deliver either single-phase or polyphase power.

On each power phase, the hot wire directly connects all loads. In addition, electric loads provide signal transmission paths between a 120-V line and the neutral line, and will attenuate communication signal transmissions between two points even if these are on the same 120-V phase. Loads connected across two 120-V supply lines provide signal transmission paths from one phase to another. For signal transmission between points on different 120-V lines, these paths are in addition to the signal transmission path provided by the inherent capactive coupling across the supply transformer secondary. Therefore, phase-to-phase loads can enhance signal transmission between different power phases. Signal attenuation from power line loads would be particularly high on long transmission paths with many loads between the transmitter and receiver, as well as on some transmission paths involving different 120-V phases.

The addition and removal of electrical loads cause frequent changes in

13

signal attenuation between any two intrabuilding circuit nodes. As well, the loading of circuits in Residence B in Fig. 2.1 could affect signal attenuation in Residence A. Finally, transmission-line effects can occur in long wiring runs at high frequencies. For example, at 100 kHz the signal wavelength is 3000 m, and line lengths in excess of approximately 500 m imply possible transmission-line effects including narrow-band signal fades [17,37].

## 2.2  Summary

All the electrical components and loads connected to a power distribution circuit form a part of a power line communication network, and affect signal transmission. An exact signal transmission path is very difficult to determine.

Transformers, power factor correction capacitors, line cables, etc. can cause strong communication signal absorption, reflection, resonance and other distortions. The large variety of electric loads will cause different loading effects on communication signals. When energized, these loads produce significant amounts of noise and other disturbances which severely affect signal reception. Altogether, a power distribution system coupled with varying electric loading give rise to a very complex and hostile communication environment.

# Chapter 3

# Signal Propagation on Intrabuilding Power Lines

Continued and growing interest in the use of intrabuilding electric power distribution circuits for data communications requires determination of the communication characteristics of this channel. Vines *et al* [47] recently provided impedance characteristics of power line circuits over the range 0-20 kHz, while the range 20-100 kHz was examined ealier by others [28,35]. This chapter and a recent paper [5] by this author present in detail the signal propagation characteristics of intrabuilding power lines over the range 20-240 kHz. These results provide important guidance in the design of power line data communication systems and services.

## 3.1 Power Line Attenuation

The complexity and general unavailability of actual intrabuilding wiring schemes as well as the lack of knowledge regarding the specification and location of electrical loads make network analysis of intrabuilding power line circuits virtually impossible, even in a single family home. Measurements on representative buildings provide the sole source of data and a practical means to determine typical attenuation characteristics. Five buildings selected for such measurements are described below:

1. Four floor 70,000 square feet industrial building (the University of British Columbia Electrical Engineering Building), supplied with three-phase power as in Fig. 2.2, from a single transformer in the basement vault. Loads included office equipment, air conditioning equipment with motors for driving forced-air fans, numerous mini and mirco computers, switching power supplies and other electrical and electronic laboratory facilities, lighting equipment, arc welders, copy machines and other machine shop equipment.

2. Large city hospital with 540 beds and a full range of diagnostic, medical, surgical, management and research facilities. Three-phase power is supplied to this building.

3. Low-rise apartment building with four floors and 60 dwelling units. Each dwelling unit is supplied with split-single-phase power.

4. High-rise apartment building with 12 floors and more than 100 dwelling units. Each dwelling unit is supplied with split-single-phase power.

5. Single family house. This house together with 20 others is supplied with split-single-phase power from the same pole-mounted distribution transformer.

### 3.1.1  Measurement Procedure

The measurement set-up appears in Fig. 3.1(a). A single frequency sinewave tone was generated by an Exact Electronics Inc. Model 123A VCF signal generator, and was power amplified using a standard circuit based on IC TDA 2002, with approximately 5 $\Omega$ output resistance. The amplified signal was passed onto the power line by the line coupling network which was essentially a high-pass filter having a 3-dB cut-off at 25 kHz. The coupling network is shown in Fig. 3.1(b). At the receiving node the tone signal was passed through another line coupling network, identical to that at the transmitting node, to a 27 $\Omega$ resistive load. Each line coupling network was connected to a 120-V power line and the neutral conductor.

The attenuation A in dB was determined as follows:
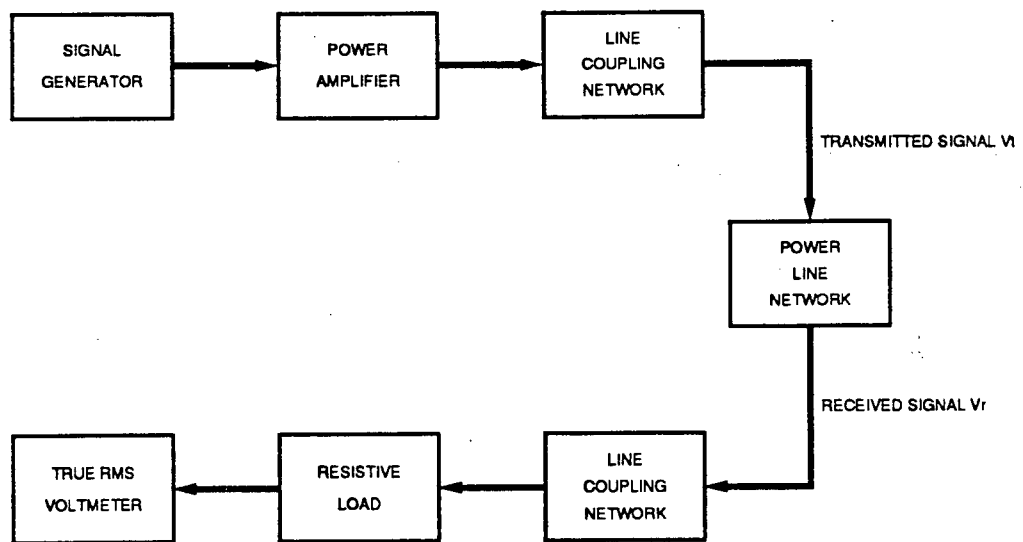
(a)
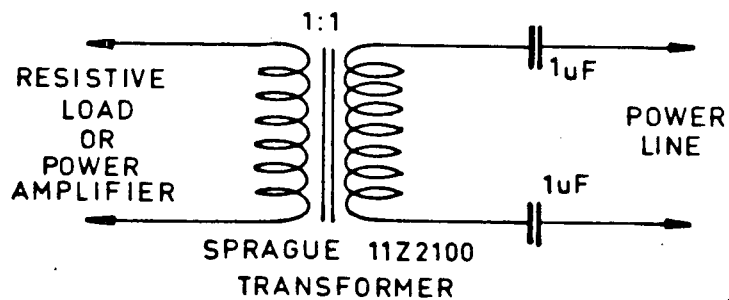


(b)

Figure 3.1: (a) System for measuring signal attenuation on power lines. (b) Line coupling network.

$$A(dB) = 10log_{10}[v_t^2/(\bar{v}_r^2 - \bar{v}_n^2)]  \tag{3.1}$$

In Eqn. (3.1) $v_t$ is the transmitted signal voltage, $v_r$ the received voltage including signal plus noise, and $v_n$ the voltage in the absence of any transmitted signal. The overbar denotes a time average. Eqn. (3.1) reasonably assumes in effect that the received signal and noise are uncorrelated. Measurement of $v_n$ and $v_r$ was alternated to accurately estimate the desired signal power term $\bar{v}_r^2 - \bar{v}_n^2$.

All voltage measurements were obtained using a Brüel and Kjaer Model 2426 (0.5 Hz -0.5 MHz) true rms electronic voltmeter. The transmitted signal voltage level used was maintained at 3.7 $V_{rms}$. Measurements were taken at 16 discrete frequencies from 20 to 240 kHz, inclusive.

## 3.1.2  Measurement Results

The attenuation measurements are plotted in Figs. 3.2-3.7. Each curve represents attenuation as measured between two specific network points during a time interval of approximately half an hour. For easy reference, signal transmission is denoted as in-phase (I) when the transmitter and receiver use the same 120-V power line. Across-phase transmission (A) indicates that the transmitter and receiver use different three-phase 120-V power lines. Opposite-phase transmission (O) applies when the transmitter and receiver

19
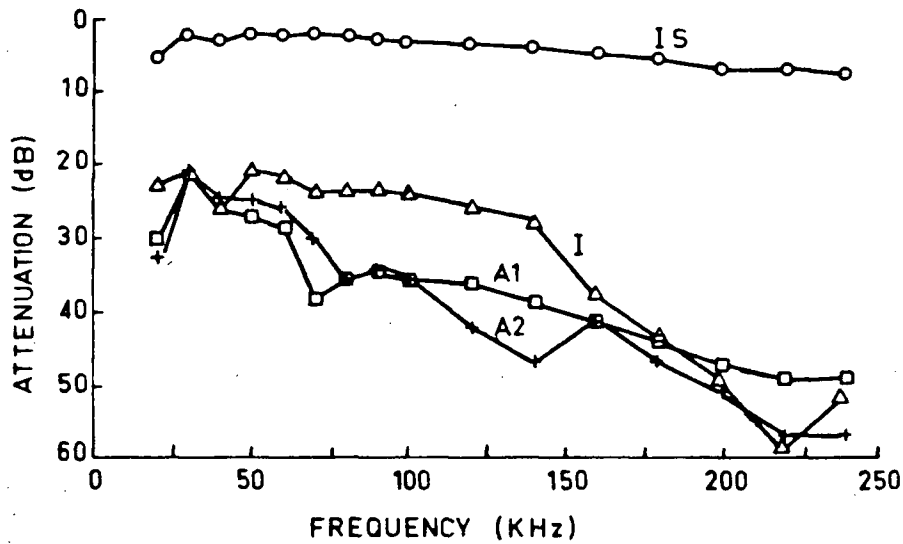
Figure 3.2: Attenuation vs. frequency, industrial building, daytime. IS - short distance, in-phase channel. I-unknown distance, in-phase channel. Al, A2 - across-phase channels.

use different 120-V split-single-phase power lines. In obtaining attenuation measurements within any building the receiver location remained fixed and the transmitter was moved to obtain the results for across-phase or opposite-phase transmission.

Fig. 3.2 shows attenuations measured in the industrial building during normal working hours. In-phase attenuation over a short distance (denoted by IS) is relatively flat and is less than 5 dB over most of the frequency range considered. This known, physically short path (approximately 10 m) was relatively free of electrical loads between the transmission and reception points; curve IS indicates what minimum attenuation might be expected.

20
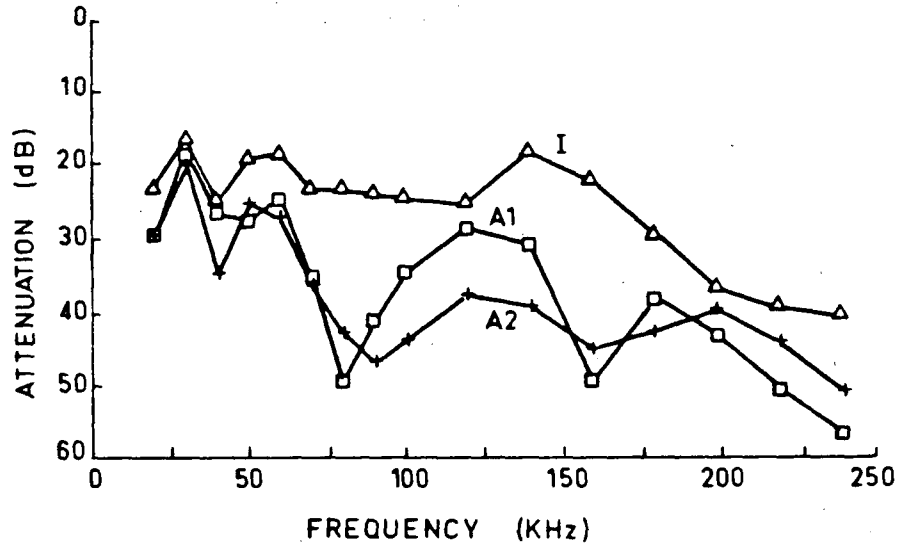
Figure 3.3: Attenuation vs. frequency, industrial building, night-time. I, A1 and A2 as in Fig. 3.2.

Over longer but unknown[1] distances however, attenuation is approximately 25 dB for frequencies below 60 kHz and increases with frequency to approximately 50 dB at 200 kHz. Comparison of the in-phase attenuation curve I with the across-phase curves A1 and A2 shows that across-phase transmission did not always result in larger attenuations than for in-phase transmission. Curves A1 and A2 denote transmission over an unknown distance from phase $\phi_1$ to $\phi_3$ and from $\phi_2$ to $\phi_3$, respectively.

Fig. 3.3 shows results for the same building at night. The transmitter and receiver locations for cases I, A1 and A2 were identical to those used

---

[1]Unknown distances would typically exceed 20 m and could be as long as 500 m.

to obtain the corresponding curves in Fig. 3.2. We do not show the curve IS because it is virtually the same as in Fig. 3.2. In-phase transmission at night shows less attenuation, in general, than for daytime. Across-phase curves show much more fluctuation at night than during the day, with 20 dB fades occurring at night on curve A1 at 80 and 160 kHz. Such fades could result from reactive loads, reflections, multipath propagation or from standing waves which represent energy trapped in the power line network. At any specific frequency, attenuation between two network points is seen to vary by up to 20 dB from day to night. Such variation is caused by differences in network loading.

Fig. 3.4 shows results for the hospital, taken during normal daytime hours. Below 140 kHz in-phase attenuation is approximately 5 dB, but drops sharply by 20 dB at 160 kHz from where it increases more slowly to 27 dB at 240 kHz. The difference in attenuation levels for the three hospital curves is more pronounced than for the industrial building. At 240 kHz, for example, the difference between the I and A1 curves is approximately 20 dB for the hospital, whereas for the industrial building in the daytime the difference between in-phase and across-phase attenuation was 3 dB (I-A1) and 10 dB (I-A2). In Fig. 3.4 there is a 20 dB difference between the A1 and A2 curves above 140 kHz, but almost no difference between 80 and 90 kHz. Attenuation for the hospital is generally lower than for the industrial

22
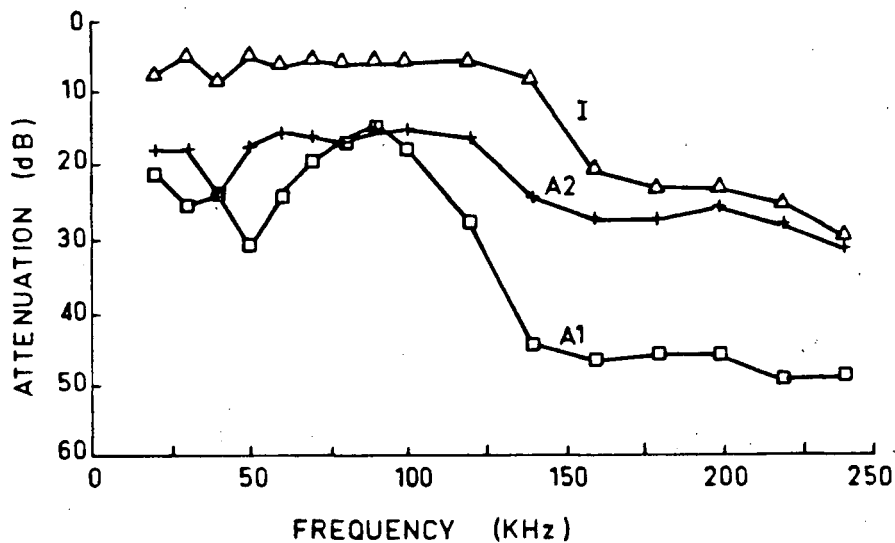
Figure 3.4: Attenuation vs. frequency, hosptial. I, A1, A2 as in Fig. 3.2.

building during daytime hours.

Results for the residential apartment buildings, taken during 6-8 p.m., appear in Fig. 3.5. Above 50 kHz, attenuation in the low-rise building is less than for the high-rise even when low-rise transmissions go to the opposite phase. Above 140 kHz in the high-rise opposite-phase transmission shows several dB less attenuation than in-phase transmission.

Fig. 3.6 shows results for the single-family residence, taken in summer time between midnight and 4 a.m. when virtually all residential electrical loads were switched off. In the absence of loads there is a very large difference between in-phase (I) and opposite-phase (O) transmission, up to 40 dB at 140 kHz. To determine the effects of loading, specific consumer loads were

23
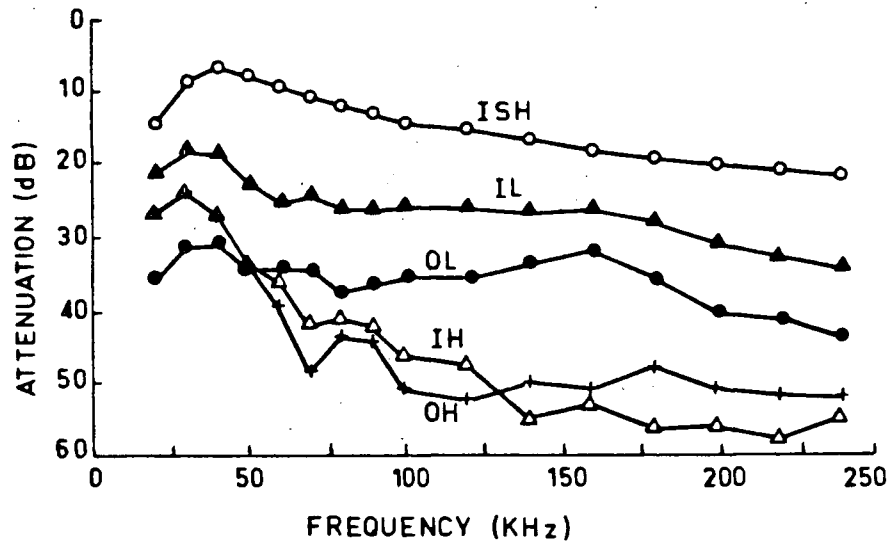
Figure 3.5: Attenuation vs. frequency, residential apartment buildings. IL, OL - in-phase and opposite-phase channels, low-rise. ISH - short in-phase channel, high-rise. IH, OH - in-phase and opposite-phase channels, high-rise.
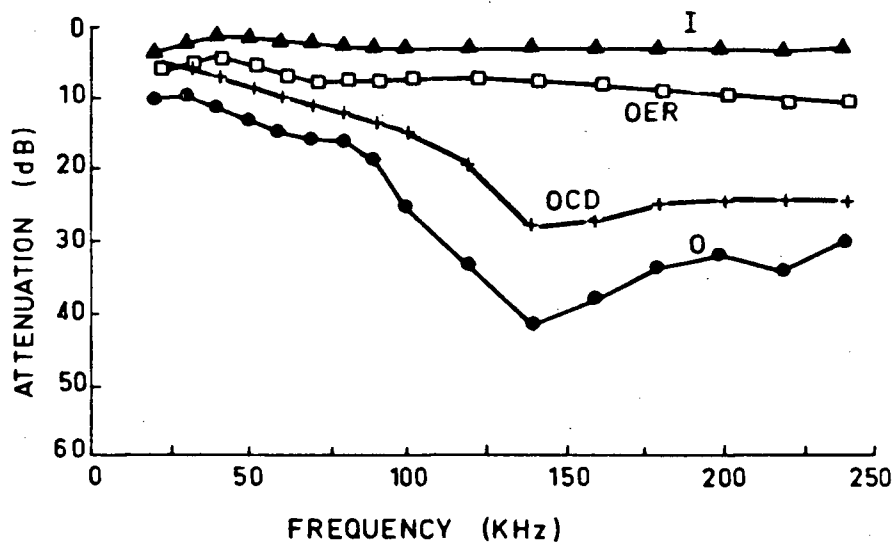


Figure 3.6: Attenuation vs. frequency, single family home. I, O - in-phase and opposite-phase channels with no specific loads. OER and OCD are shown for reference and are defined in Fig.3.7.
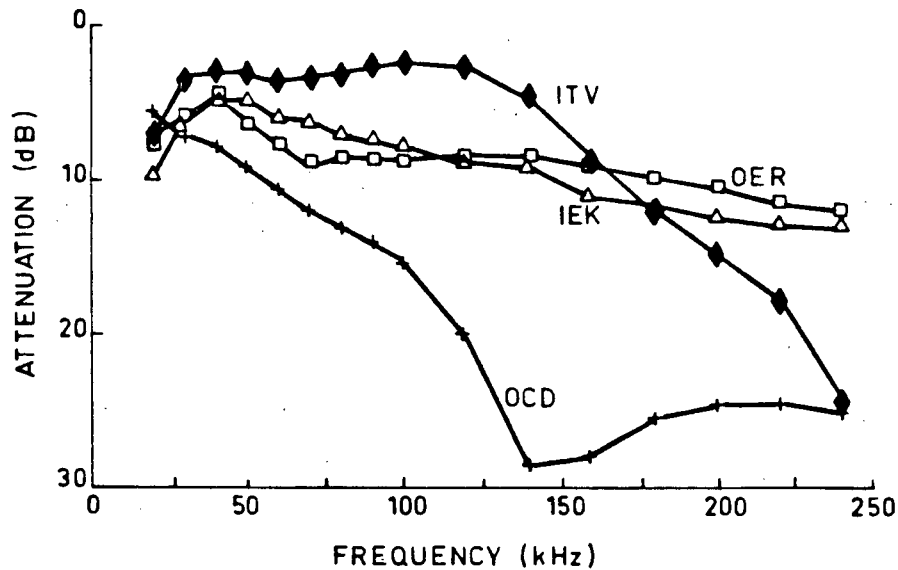
Figure 3.7: Attenuation vs. frequency, single family home with known loads. I, O denote in-phase and opposite-phase channels with loads as follows: TV - television, EK - electric kettle, ER - electric range, CD - clothes dryer.

then applied, one at a time close to and on the same power phase as the receiver. A radio, cassette recorder, vacuum cleaner, razor, sewing machine, fan and flourescent lamp showed no significant effect on the received signal level for either in-phase or opposite-phase transmission. These small loads typicaly draw less than 100 W except for a vacuum cleaner which may draw 400 W. An electric kettle and television receiver each caused some signal level attenuation during both in-phase and opposite-phase transmission. Fig. 3.7 shows the effects of loads. For the kettle an attenuation increase occurred at all frequencies over that shown by the I curve in Fig.3.6. For the television receiver attenuation increased rapidly with frequency, above 140 kHz. Both

appliances provide significant loading between line and neutral. A kettle typically acts as a resistor ($\sim 10 \ \Omega$) while a television receiver provides capacitive loading.

Loading by an electric range or a clothes dryer also caused some attenuation increase for in-phase transmission. However, Figs. 3.6 and 3.7 show that opposite-phase attenuation was actually reduced from the levels shown by the O curve in Fig. 3.6. With the electric range energized the transmission improvement was as much as 32 dB. Both loads provide a low resistance path between the two 120-V lines in addition to the coupling across the supply transformer secondary.

## 3.2  Signal Fading

The curves in Figs. 3.2-3.7 are based on attenuation levels averaged over hundreds of 60 Hz cycles. At times, periodic 120 Hz fading was observed. Fig. 3.8 shows some 120 Hz fading patterns observed in the industrial building. Similar 120 Hz fading was observed, but less frequently, in the other buildings.

Different loads were observed to cause different fading effects in the industrial building. For example, on a long 60 kHz in-phase transmission a 2 dB fade ocurred over 20 per cent of the time cycle as in Fig. 3.8 (a).
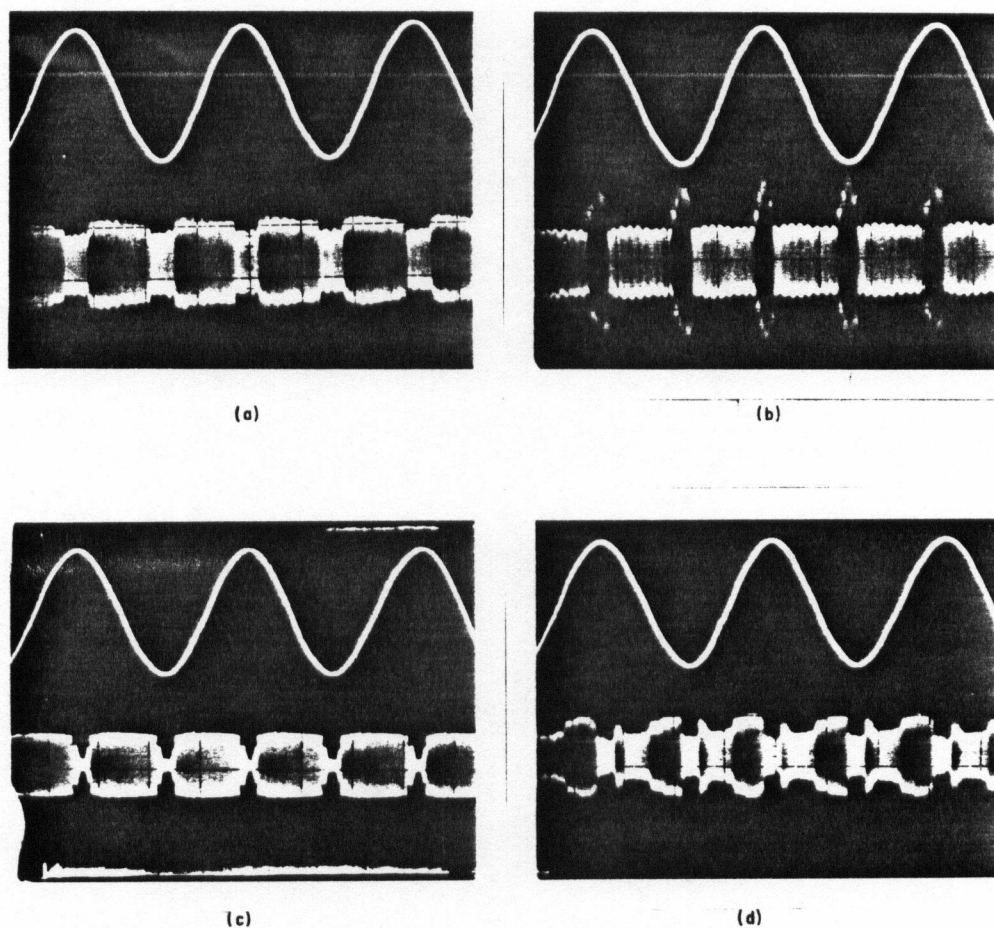
Figure 3.8: Received signal level vs. time, 120 Hz signal impairments. The upper trace is the 60-Hz power line voltage. The lower trace is: (a) Long 60 kHz in-phase transmission (b) Long 60 kHz in-phase transmission with IBM PC loading (c) Long 40 kHz across-phase transmission (d) Long 80 kHz across-phase transmission.

27

However energizing an IBM PC on this circuit near the receiver caused a periodic 5 dB relative gain of the received signal power as shown in Fig. 3.8 (b). At 60 kHz with an IBM PC energized results similar to those in Fig. 3.8 (b) were observed on a long across-phase transmission path as well as for short in-phase and short across-phase transmissions.

Some other 120 Hz fading patterns less common than those in Fig. 3.8(a) and (b) were also observed at different signalling frequencies; two of these appear in Fig. 3.8(c) and (d). In general, it seems difficult to predict the effects of various loads on 120 Hz periodic fading behaviour. The occurrence of periodic signal fading results in periodic degradation of signal to noise ratio (SNR) which can cause burst errors to occur.

Another type of periodic time fading was observed less frequently at approximately 6 Hz frequency as shown in Fig. 3.9. Similarly, relative gain of the received signal can also occur at 6 Hz frequency as shown in Fig. 3.10. Severe fading of this kind have been observed on across-phase transmissions in the industrial building causing large numbers of burst errors. More important, Figs. 3.9 and 3.10 indicate that both 6 Hz and 120 Hz impairments can occur at the same time, thus increasing their individually harmful effects.

Another serious problem associated with signal transmission is possible
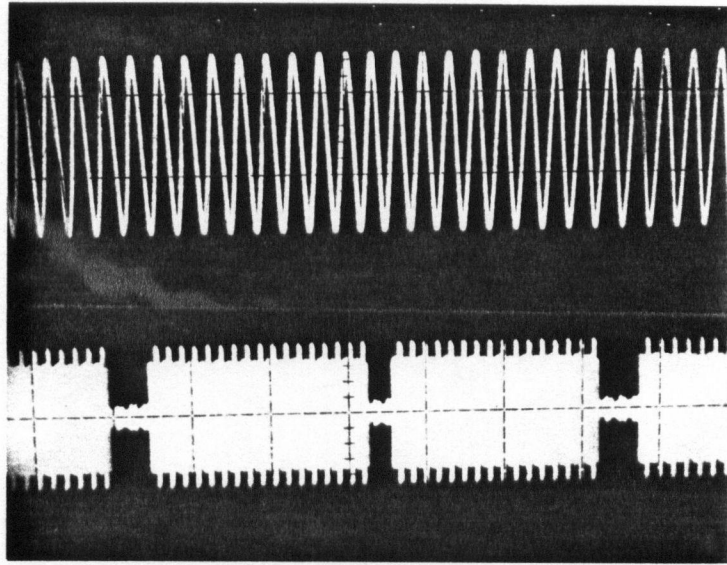
(a)
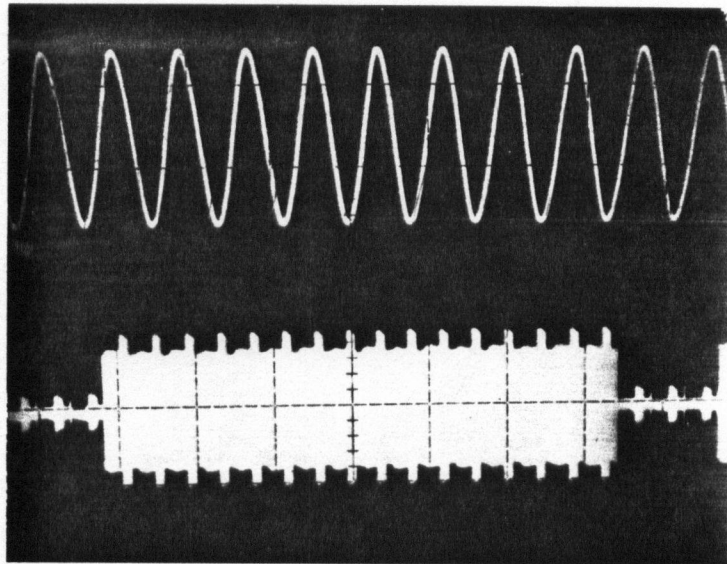


(b)

Figure 3.9: Received signal level vs. time, 6Hz and 120 Hz signal impairments. The upper trace is the 60-Hz power line voltage. The lower trace is: (a) 150 kHz across-phase transmission (b) expanded view.
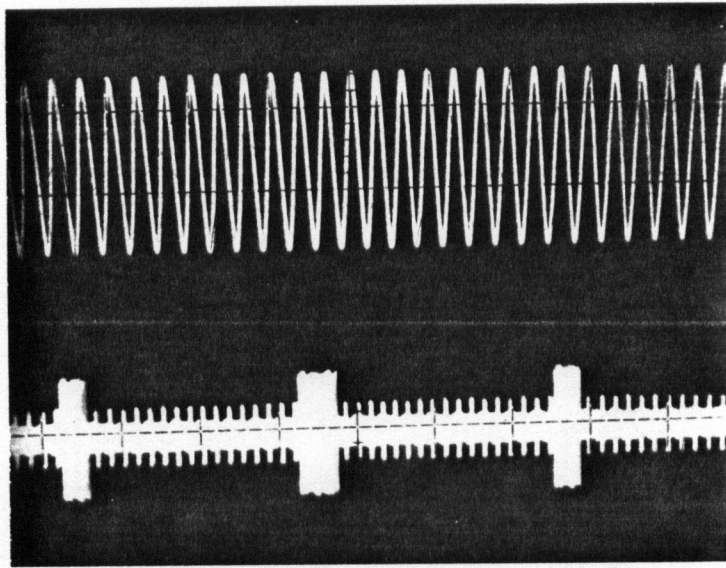
Figure 3.10: Received signal level vs. time, 6 Hz and 120 Hz signal impairments. The upper trace is the 60 Hz power line voltage. The lower trace is 90 kHz across-phase transmission.

occurrence of a sudden phase change at the instants that the signal experiences step change of amplitude. This phenomenon is shown in Fig. 3.11. Line triggering was used to obtain Fig. 3.11(a) while Fig. 3.11(b) was obtained by triggering the scope with the transmitted signal. The effect of this phase distortion can be disastrous as it causes malfunction of timing circuits used in recovering carrier synchronization, thus causing a large block of data detected incorrectly until the timing circuits catch up with the received signal again. Fig. 3.12 shows the occurrence of periodic burst errors when this kind of very rare periodic phase distortion happened. The data was detected incorrectly regardless of the strong received signal.

30
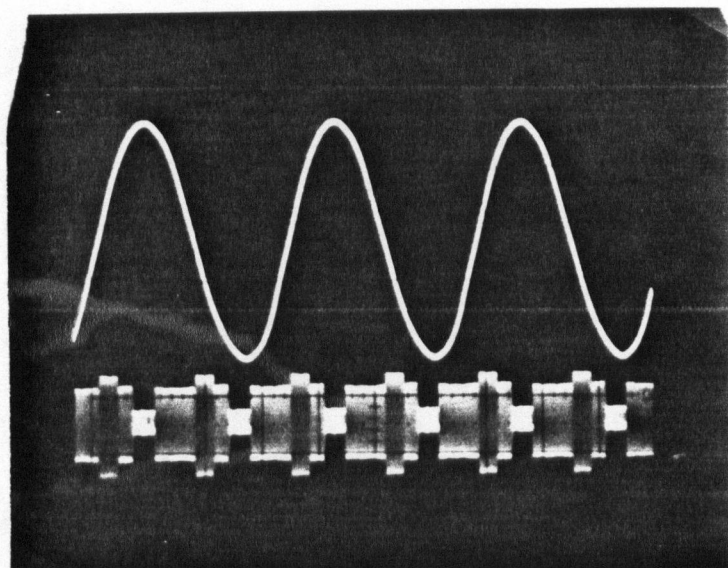
(a)
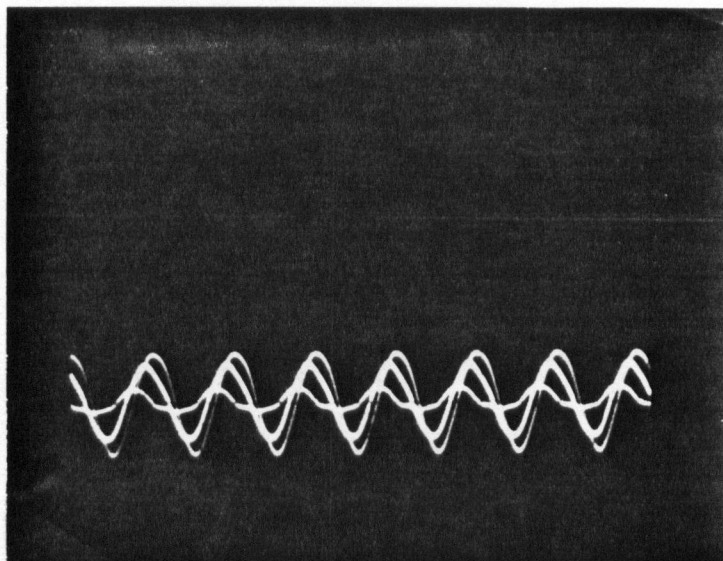


(b)

Figure 3.11: Received signal level vs. time, 70 kHz across-phase transmission
(a) Triggering with line signal (b) Triggering with transmitted signal.
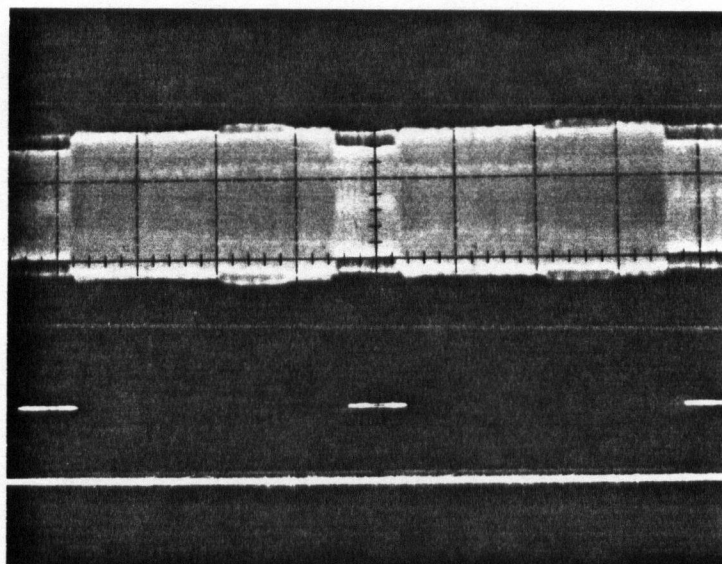
Figure 3.12: Error pattern as a result of phase distortion during step variation of signal amplitude. Coherent FSK transmission at 9.6 kbits/s. The upper trace is the received signal. The lower trace is the error pattern.

## 3.3 Discussion of the Results

### 3.3.1 Discussion of Attenuation Measurement Results

Figs. 3.2-3.7 show wide variations in attenuation vs. frequency behaviour and in actual attenuation levels at any given frequency. Table 3.1 lists attenuation values measured at 50, 120 and 200 kHz. Within a given building, large attenuation differences arise in transmission between different node pairs or between the same node pair at different times. The differences over time arise because of variations in network loading, and can be well in excess of 20 dB. In the single family home at 120 kHz, for example, the attenua-

32

| Network Envirnoment | Attenuation (dB) | | |
|---|---|---|---|
| | 50 kHz | 120 kHz | 200 kHz |
| Industrial Building Daytime (Fig. 3.2) | | | |
| IS | 2.5 | 3.8 | 7.1 |
| I | 20.8 | 25.7 | 48.9 |
| A1 | 27.0 | 36.3 | 47.3 |
| A2 | 24.8 | 42.2 | 51.1 |
| Industrial Building Night (Fig. 3.3) | | | |
| I | 18.7 | 25.6 | 39.6 |
| A1 | 27.6 | 28.7 | 43.2 |
| A2 | 25.4 | 37.8 | 39.8 |
| Hospital (Fig. 3.4) | | | |
| I | 5.6 | 6.2 | 23.9 |
| A1 | 31.6 | 28.4 | 46.7 |
| A2 | 18.1 | 17.1 | 26.6 |
| Apartments (Fig. 3.5) | | | |
| ISH | 8.4 | 15.8 | 20.6 |
| IL | 23.2 | 26.4 | 31.3 |
| OL | 35.2 | 36.0 | 40.6 |
| IH | 34.2 | 48.0 | 56.2 |
| OH | 34.2 | 52.8 | 51.2 |
| Single Family Residence (Figs. 3.6-3.7) | | | |
| I | 2.3 | 3.9 | 4.2 |
| ITV | 3.1 | 2.5 | 14.5 |
| IEK | 4.6 | 8.5 | 12.3 |
| O | 13.6 | 34.0 | 32.5 |
| OER | 6.6 | 8.4 | 10.5 |
| OCD | 9.3 | 19.9 | 24.5 |

Table 3.1: Measured attenuations (dB) from Figs. 3.2-3.7.

tion decreased from 34.0 dB to 8.4 dB when an electric range was energized. These results clearly indicate that signal attenuation on power line is highly variable and unpredictable.

Attenuation tends to increase with frequency although the increase is not monotonic. The measured data was fitted with various curves in order to see whether or not some general invariants could be determined. Table 3.2 shows the results for a best linear mininum mean square error (MMSE) fit of the form

$$\varepsilon = \sum_{i=1}^{N} [A_i - A(f_i)]^2 \qquad (3.2)$$

where $A_i$(dB) denotes the measured attenuation at frequency $f_i$(kHz), N denotes the number of test points (we excluded the high pass filtered 20 kHz point, so N = 15) and

$$A(f_i) = A_0 + (k/100)f_i \qquad (3.3)$$

Constant $A_0$(dB) and $k$(dB/100kHz) were chosen to minimize $\varepsilon$ in (3.2) and appear in Table 3.2. The standard error $S_e$ was also obtained, where $\mu$ is the number of parameters to be determined [49] ($\mu = 2$ for the linear fit case):

$$S_e = \sqrt{\varepsilon/(N-\mu)} \qquad (dB) \qquad (N > 2) \qquad (3.4)$$

34

| Network Environment | Curve-fit Parameters | | | | Error $S_e$ (dB) | |
|---|---|---|---|---|---|---|
| | Linear | | RC | | Linear | RC |
| | $A_0$ | k | $A_0$ | $f_0$ | | |
| Industrial Building Daytime (Fig. 3.2) | | | | | | |
| IS | 1.1 | 2.6 | 2.0 | 154 | 0.6 | 0.5 |
| I | 11.6 | 17.1 | -8.2 | 1 | 4.9 | 8.9 |
| A1 | 22.6 | 12.1 | -3.1 | 1 | 2.9 | 3.7 |
| A2 | 18.1 | 17.0 | -1.7 | 1 | 2.9 | 6.9 |
| Industrial Building Night (Fig. 3.3) | | | | | | |
| I | 13.0 | 11.8 | 10.3 | 15 | 4.3 | 6.0 |
| A1 | 22.3 | 12.4 | -2.9 | 1 | 7.5 | 8.0 |
| A2 | 28.0 | 8.9 | -1.4 | 1 | 6.2 | 5.5 |
| Hospital (Fig. 3.4) | | | | | | |
| I | -1.6 | 12.3 | -3.2 | 16 | 3.9 | 6.0 |
| A1 | 13.8 | 16.0 | -7.2 | 1 | 7.7 | 10.2 |
| A2 | 13.9 | 6.9 | 16.0 | 64 | 3.5 | 3.9 |
| Apartments (Fig. 3.5) | | | | | | |
| ISH | 6.3 | 7.2 | 4.4 | 33 | 1.1 | 0.9 |
| IL | 19.7 | 5.7 | 19.3 | 52 | 1.8 | 1.8 |
| OL | 31.7 | 3.8 | 33.0 | 114 | 2.5 | 2.6 |
| IH | 28.1 | 14.5 | 5.3 | 1 | 4.6 | 5.7 |
| OH | 32.7 | 10.3 | 4.9 | 1 | 6.4 | 5.3 |
| Single Family Residence (Figs. 3.6-3.7) | | | | | | |
| I | 2.6 | 0.8 | 2.5 | 240 | 0.4 | 0.7 |
| ITV | -3.1 | 8.8 | -0.6 | 47 | 3.3 | 4.4 |
| IEK | 3.4 | 4.2 | 4.3 | 92 | 0.7 | 0.6 |
| O | 9.7 | 12.9 | -14.9 | 1 | 6.4 | 6.7 |
| OER | 5.7 | 2.5 | 6.7 | 161 | 0.7 | 0.8 |
| OCD | 5.3 | 10.4 | -22.3 | 1 | 3.6 | 3.4 |

Table 3.2: Linear fit (3.3) and first-order RC fit (3.5) to measured attenuation values.

|  | RC Fit | Linear Fit (p=1) | Polynomial Fit | | | |
|---|---|---|---|---|---|---|
|  |  |  | p=2 | p=3 | p=4 | p=5 |
| $\bar{S}_e$ (dB) | 4.39 | 3.61 | 2.86 | 2.43 | 2.29 | 2.13 |
| $\sigma_e$ (dB) | 2.90 | 2.30 | 2.15 | 1.77 | 1.81 | 1.79 |

Table 3.3: Mean $\bar{S}_e$ and standard deviation $\sigma_e$ of the error $S_e$ for the 21 network envirnoments listed in Table 3.2.

Table 3.2 shows considerable variation for $A_0$ and k, even among networks within the same building or between the same two network points at different times. In the hospital, for example $A_0$ varies from -1.63 to 13.9 while k varies from 6.9 to 16. Within this range, $S_e$ is as high as 7.7 dB. The mean error $\bar{S}_e$ averaged over the 21 $S_e$ values in Table 3.2 appears in Table 3.3, together with the standard deviation $\sigma_e$. The relatively high $\bar{S}_e$ value of 3.61 dB confirms the general inadequacy of a linear fit. The relatively large $\sigma_e$ value indicates considerable variation among the 21 $S_e$ values. Linear fits for two of the cases appear in Fig. 3.13. In both cases the linear fit is not very good.

Also shown in Table 3.2 and Fig. 3.13 is a simple first-order RC network fit to the data points, with $A(f_i)$ in (3.2) given by

$$A(f_i) = A_0 + 10 log_{10}[1 + (f_i/f_0)^2] \qquad (3.5)$$

Table 3.2 shows the MMSE fit in (3.5) to be worse than the linear MMSE

36

FREQUENCY (kHz)

ATTENUATION (dB)

LINEAR FIT

R-C FIT

3$^{rd}$ ORDER
POLYNOMIAL FIT

(a)

FREQUENCY (kHz)

ATTENUATION (dB)

3$^{rd}$ ORDER POLYNOMIAL FIT
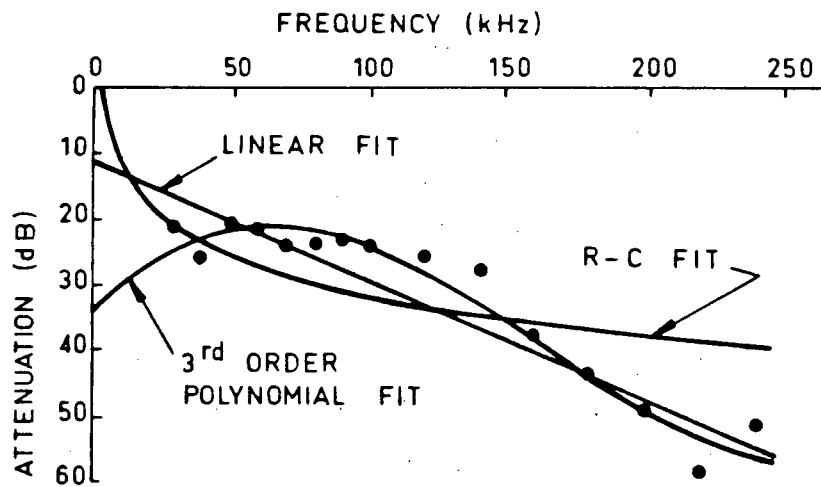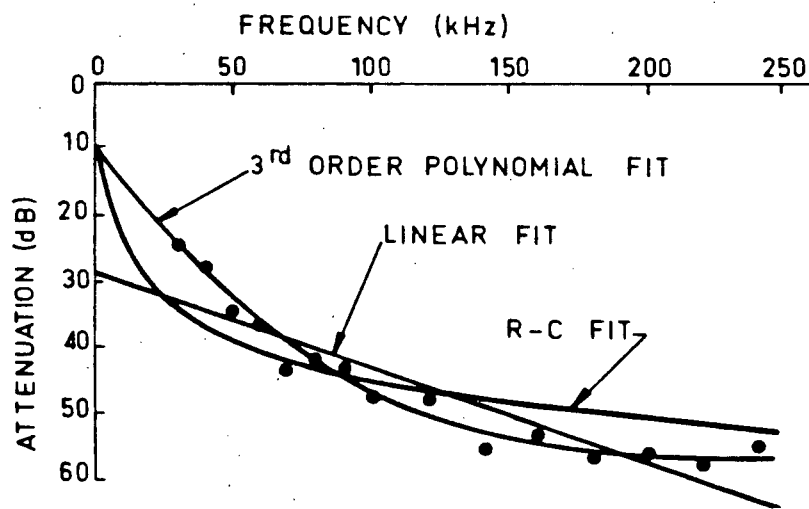
LINEAR FIT

R-C FIT

(b)

Figure 3.13: Linear, RC and third order polynomial fits. (a) Curve I in
Fig.3.2. (b) Curve IH in Fig.3.5.

fit for all but six cases. Table 3.3 shows both $\bar{S}_e$ and $\sigma_e$ to be higher for the RC fit than for the linear fit. Again, Table 3.2 shows considerable variation for the parameters $A_0$ and $f_0$.

To reduce the $S_e$ values obtained using (3.3) and (3.5), a polynomial of the form

$$A(f_i) = \sum_{n=0}^{p} A_n f_i^n \tag{3.6}$$

with p = 1, 2, 3, 4 or 5 and with $A_n$ chosen as MMSE parameters (p = 1 is the linear fit case) was used. In general, $S_e$ decreases as p increases until p = 3 at which point further increases in p do not reduce $S_e$ very much. Table 3.3 confirms that p $\geq$ 3 does not yield much improvement in a MMSE fit to the attenuation data points. With p = 3, $S_e$ = 7.0, 5.5 and 4.9 for the three worst cases. In all other cases $S_e \leq 3.8$. Fig. 3.13 shows $A(f_i)$ as given by (3.6) with p = 3. In the two cases shown, the fit is reasonably good, but the appearance of the two curves is quite different. For each p value in (3.6), considerable variation was observed among the various MMSE curves and parameters sets $A_n$ and there was no obvious systematic pattern among these curves and parameter sets.

There is obvious difficulty in defining a reasonable communication "bandwidth" for intrabuilding power line networks. The simple RC net-

work fit shows that the 3 dB bandwidths $f_0$ in Table 3.2 vary from 1 to 114 kHz for long paths in the industrial building, hospital and apartment buildings. One could argue that the RC network model is too simple, and indeed the results show no obvious choice for "bandwidth". From Figs. 3.2-3.4 one might tentatively conclude that in large buildings, signalling above 150 kHz could be subject to large ($\sim$ 50 dB) attenuation. However the 80 kHz fade in Fig. 3.3, and the sudden increase in attenuation in Fig. 3.5 for the high-rise building indicate that large attenuations can also occur at frequencies between 50 and 150 kHz.

## 3.3.2    Implications for Intrabuilding Communications

The large variations in attenuation imply that a signal transmission level which is adequate for power line networks with moderate attenuation may not be adequate for networks with large attenuation. One could design a signal transmission level for worst case attenuation; however this approach is not practical because attenuation can become extremely high. In addition, a high transmit signal level increases cost, power consumption and interference. Also, an increase of signal transmission level to overcome noise is strictly limited by FCC regulations for conductive and radiated emissions. An appropriate approach for power efficient digital data transmission is to use suitable error control coding (to be addressed in details in Chapters 5-7)

39

which allows for some variation in signal to noise ratio. A further option would be to use repeaters in networks with severe attenuation, so that messages not successfully transmitted to a destination receiver after several tries would be routed through a repeater. Other solutions include perfoming signal bypassing between different power phases at the power entry panel as well as signal isolation of the incoming power lines to confine most of the signal energy within a section of the power line network. Since attenuation is frequency selective, it may be useful to enable a transmitter to select an alternative carrier frequency following unsuccessful attempts using a preferred frequency. A multicarrier receiver would be needed in this case.

At the network level, with a fixed transmitter output power level, the large variation in attenuation implies that individual links of a power line network will have different bit error rate (BER) performance. Furthermore, a small percentage of the links can be particularly bad, with BER values much worse than for the rest of the network. In assessing the performance of a network protocol on power lines, this asymetric BER distribution among all pairs of network users should be incorporated in the analysis in order to give an accurate estimate. A good network protocol for power line LAN should take these realities into consideration.

With multiple users, the large difference in signal attenuation levels

among different network points implies that all users may not be able to hear all other users. This frequent occurrence of hidden users in power line networks has important bearing on the choice of medium access protocol. In some medium access protocols such as carrier sense multiple access (CSMA), collision detection is often used to enhance performance. With collision detection, a sending station listens to its message from the channel while transmitting. If another station is also transmitting on the channel, a collision will be detected and both stations will abort their transmissions. On power lines, a signal from another station is subject to large attenuation. A sending station often receives its own message at a signal level much above that of another station unless the two stations are close to each other. This large difference in signal strength makes a sending station unable to hear another station's transmission, and collision would not be detected.

In contrast to attenuation, noise tends to decrease as frequency increases [43,46]. The choice of signalling frequency therefore involves a compromise between a relatively high noise level with low signal attenuation and a high signal attenuation with reduced noise power. However, high speed data transmission dictates the use of a higher carrier frequency.

When very severe periodic fading occurs digital transmission is subject to periodic burst errors. The overall BER which occurs on such a severe

ERROR FREE SPANS

··· e | 000 ··· 000 | ee O e O ee | 000 ··· 000 | e | 000 ··· 000 | e ···

ERROR BURST REGIONS
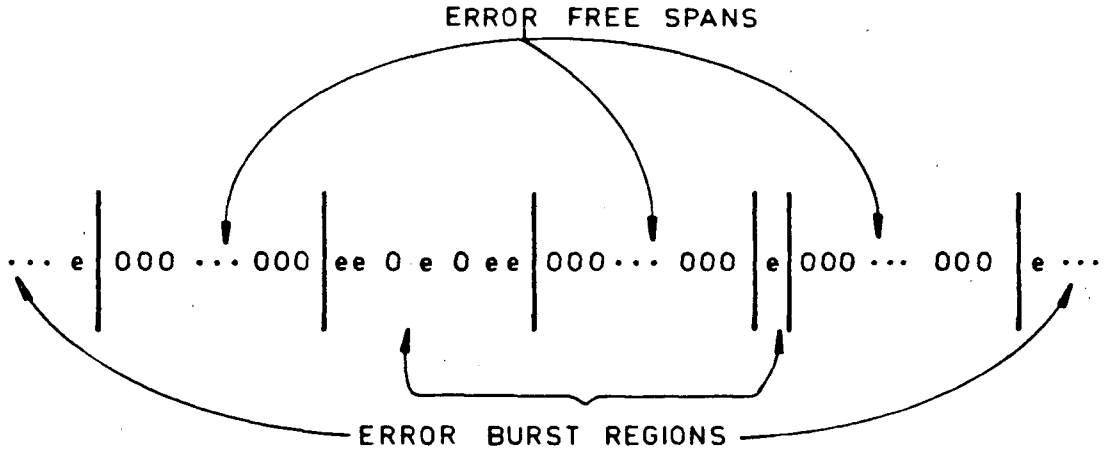
Figure 3.14: Illustrating error bursts and error free spans. Each burst begins and ends with an error, denoted as "e".

fading channel can be approximately given by

$$BER \cong BER_eBL(F/R) \tag{3.7}$$

where    $BER_e$=bit error rate during error bursts

$BL$=nominal burst length in bits

$F$=fading rate

$R$=bit rate

An error burst begins and ends with an incorrect bit. Error burst and error free spans alternated as indicated in Fig. 3.14. Some initial results on burst lengths can be found in [4,5]. During deep fades SNR is badly degraded and $BER_e$ can exceed $10^{-1}$ but is always upper bounded by 0.5. Thus, $0.5BL(F/R)$ upper bounds BER for a fading channel.

42

## 3.4 Summary

The results and observations clearly indicate that power line signal transmission is highly variable and unpredictable and lead to the following general conclusions:

1. Except for short transmission paths, signal attenuation on intrabuilding power lines typically exceeds 20 dB, and can be much higher, even when the transmitter and receiver use the same power phase.

2. When the transmitter and receiver are on the same power phase, attenuation tends to be less than when they are on different phases. However, the differences are not always large relative to absolute attenuation levels.

3. Signal attenuation tends to increase with frequency, although such increases are not always monotonic.

4. Narrowband signal fades can and do occur at specific signalling frequencies.

5. Power line channel bandwidth is limited as the power line cables, power distribution transformers, power factor correction capacitors, magnetic circuit breakers, and other equipment effectively form a low pass filter.

6. Electrical loading greatly affects signal attenuation on intrabuilding power lines. The load profile varies over time and as a result attenuation may vary considerably over time at any given frequency; variations of 20 dB are not unusual.

7. No simple mathematical relationship was found that provided a good general fit to signal attenuation data from various intrabuilding power line networks.

8. Periodic 6 Hz and 120 Hz signal fades can occur; these cause periodic degradation in received signal to noise ratio which in turn causes periodic burst errors in digital transmissions.

# Chapter 4

# Amplitude, Width and Interarrival Distributions for Noise Impulses on Intrabuilding Power Lines

Impulse noise provides a serious source of impairment to intrabuilding power line data transmission circuits and systems [4,44,45]. Such noise requires appropriate description to enable efficient and effective channel utilization. In this chapter and in a recent paper by this author [7], estimates of the probability distributions for the amplitude, width and interarrival time of noise impulses on intrabuilding power line circuits are presented. These estimates are based on measurements in both industrial and residential buildings. The results usefully complement noise spectral density estimates by others [43,46], and are essential for designing effective error control codes and data link pro-

tocols.

## 4.1  Intrabuilding Power Line Noise

Power line noise includes both background and impulsive components. Smith [43] found that the measured spectral density, which he regarded as primarily from background noise, decreases at approximately 29 dB/decade over the 10 kHz to 100 MHz range. Vines *et al* [46] presented measurement results on noise power spectral density of some residential power line noise sources which they categorized as follows:

1. Sources such as silicon rectifiers (SCR) and some power supplies which generate noise in synchronism with the 60 Hz power frequency; this noise has a line spectra with lines at multiples of 60 Hz.

2. Smooth spectrum noise, often caused by loads not synchronous with the power frequency; examples include a universal motor for an electric drill.

3. Single-event impulse noise from lightning, and switching of thermostats and capacitor banks.

4. Nonsynchronous periodic noise, produced for example by television receivers at multiples of the 15.734 kHz horizontal line scanning fre-

46

quency.

Gaussian noise and its effect on communication system performance is well understood. In the case of impulse noise, however, the time-domain characteristics of the impulses have an important bearing on data communication performance. Important time-domain parameters include impulse amplitude, width and interarrival time [19,21,22,23,32,33,42]. The amplitude together with the width defines the impulse energy. The interarrival time defines the impulse frequency, and together with the energy defines the impulse noise power.

## 4.2  Measurement Procedure

The system used for measuring amplitude, width and interarrival time for noise impulses appears in Fig. 4.1. The coupling network was that shown in Fig. 3.1(b). Signal energy from the 120-V power line circuit passed through the line coupling network to a grounded 27 Ω resistive load. The load voltage envelope was captured by a Hewlett Packard (HP) 6944 programmable processor using an HP 69759 analog-to-digital converter board which digitized the signal to 12-bit accuracy at 500,000 samples/s. The programmable analog-to-digital converter has a 126 dB dynamic range, and is capable of measuring voltage amplitudes from 50 $\mu$V to 100 V. The digitized samples

47

```
                    ┌──────────┐    ┌──────────┐    ┌──────────┐    ┌──────────┐
                    │   LINE   │    │ RESISTIVE│    │   A/D    │    │ DIGITAL  │
              ●─────│ COUPLING │───▶│          │───▶│          │───▶│          │
              │     │ NETWORK  │    │   LOAD   │    │CONVERTER │    │ COMPUTER │
         ●────│     └──────────┘    └──────────┘    └──────────┘    └──────────┘
         │    │
         │    │ NEUTRAL
      120-V
```
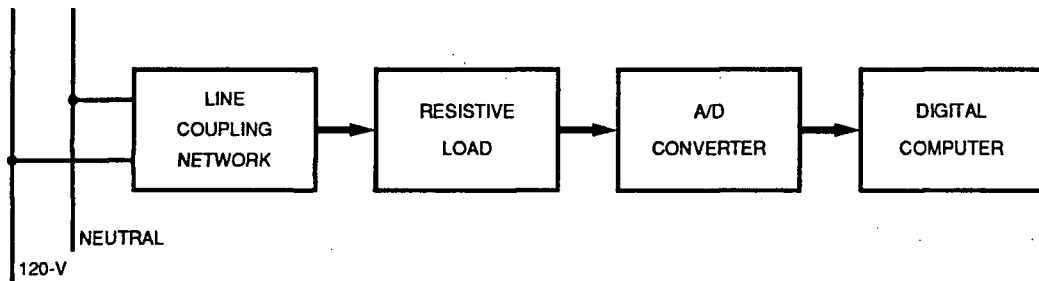
Figure 4.1: System for measuring power line impulse noise.

were transferred to and stored in a HP 9836 computer and then used to
obtain estimates of the probability distributions shown in Figs. 4.2-4.8, in-
clusive. Each curve in these figures is based on at least $5 \times 10^6$ samples.

Measurements were obtained from each of three power phases in the
70,000 square feet industrial building with four floors as described in Chapter
3. The entire building is supplied from a single three-phase transformer.
Measurements were also obtained from a single family residence, with three
floors. This home, together with 14 others, is supplied from a split-single-
phase distribution transformer. Studies were carried out to determine the
characteristics of some common noise sources, and to obtain data under
worst possible situations. All measurement results were obtained during
weekdays, between 9:00 a.m. and 5:00 p.m., between a 120-V line and the
neutral conductor.

Obervations in other buildings indicated power line noise characteristics similar to those observed in the industrial building and the single family home. Power line noise is generated primarily by electrical loads and it is these, rather than the network wiring, which is the primary determinant of noise characteristics.

## 4.3  Measurement Results

### 4.3.1  Amplitude Probability Distribution (APD)

Amplitude probability distribution (APD) results of the noise envelope voltage appear in Figs. 4.2-4.4, inclusive, where the voltage amplitude level relative to the rms amplitude is plotted versus the percentage of time that the ordinate is exceeded [19,31]. The extent to which the APD curve peaks near the vertical axis indicates the extent to which the noise is impulsive.

Two typical APD's measured in the industrial building appear in Fig. 4.2. The noise consists of both background and impulsive components, with the impulse noise being relatively larger on phase 1 than on phase 3. On phase 1, for example, the impulsive component is 14 dB above the background component at 0.01 %, and 13 dB above at 0.1 %.

Some specific loads can generate substantial impulse noise. A photo-
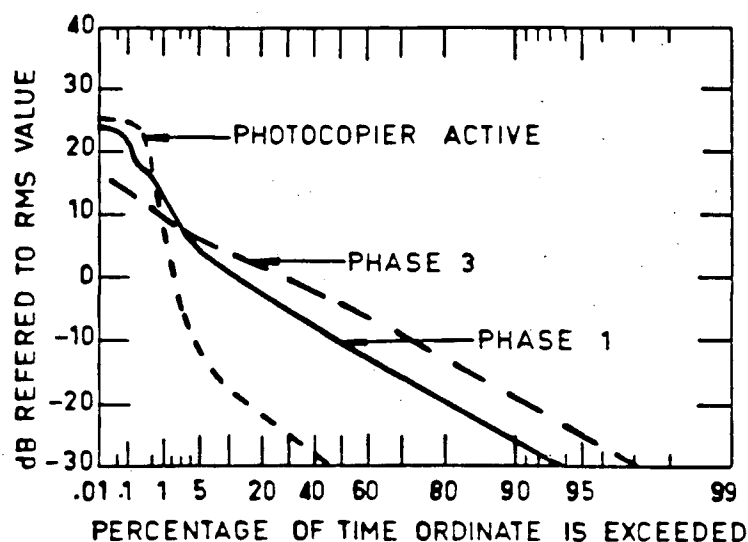
Figure 4.2: APD, industrial building.

copier was found to generate very strong 120 Hz periodic impulse spikes. The strength of the impulse noise in Fig. 4.2 is seen to be approximately 27 dB above the background noise level at 0.01 %.

Fig. 4.3 shows APD's in the industrial building measured in two different frequency bands, namely, 30-40 kHz and 70-80 kHz. A Krohn-Hite model 3342 filter was used to band-limit the noise before it was digitized. In both bands, considerable impulse noise is evident, which indicates that such noise is not confined to narrow bandwidths.

Fig. 4.4 shows APD's measured in a single family residence. The typical APD in Fig. 4.4 with no specific loads is not unlike those in Fig. 4.2 for the industrial building, in the absence of an active photocopier. Fig. 4.4
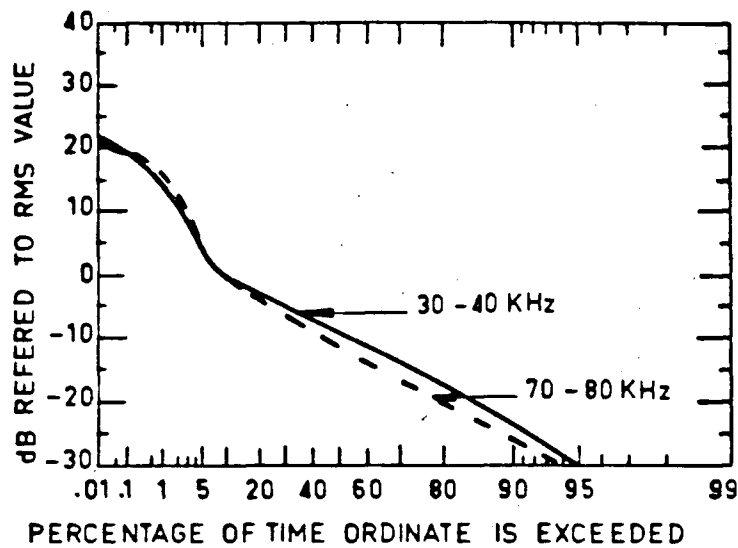
Figure 4.3: APD, industrial building. 10 kHz bandpass filtering.
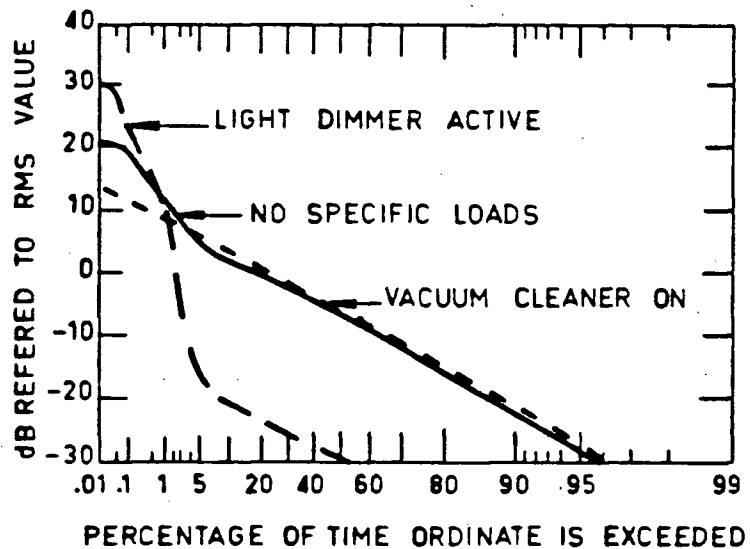


Figure 4.4: APD, residence home.

also indicates the effects of a light dimmer, set at moderate brightness. The SCR switching generates very strong impulse noise which is 40 dB above the background noise level at 0.01 %.

Measurements were taken in the house with other specific consumer appliances, applied individually, on the same phase as the observation point and close to it. A cassette recorder, razor, clothes dryer and flourescent lamp generated insignificant amounts of noise. However, a vacuum cleaner and a blender each increased the background noise level so much that the noise impulses were almost completely masked. Fig. 4.4 indicates that there is virtually no measurable noise impulses with the vacuum cleaner on. A similar APD was obtained with the blender on.

## 4.3.2   Impulse Width Distribution (IWD)

The impulse width depends on the amplitude threshold level used for measurement. We define the measurement point relative to the rms noise level.

Fig. 4.5 shows the impulse width distributions in the industrial building with and without the photocopier activated. With the photocopier on, the impulse width at amplitude level T equal to 5 and 10 times the rms noise level are approximately 70 and 40 $\mu$s, respectively, with probability near one. At amplitude level equal to the rms noise value, another weaker impulse train
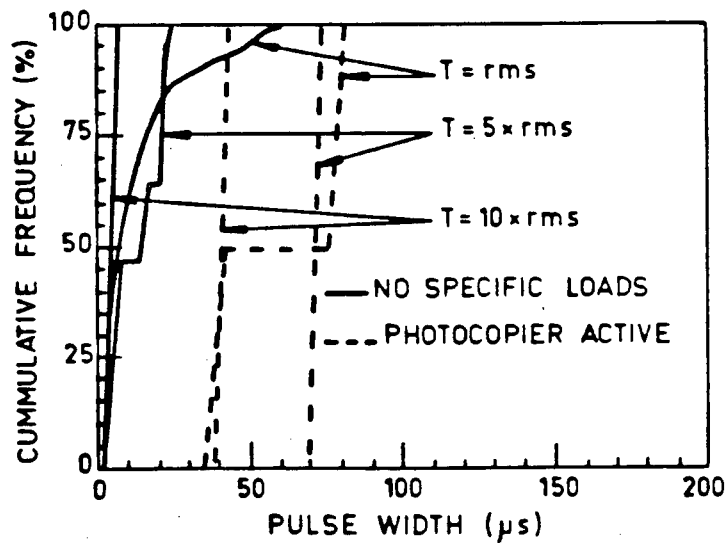
Figure 4.5: IWD, industrial building.

is included. Approximately half of the impulses from the stronger impulse train are 80 $\mu$s wide and the other half from the weaker impulse train are 40 $\mu$s wide.

In the absence of specific loads the results in Fig. 4.5 are different. When the width is measured at the rms noise level, a well defined impulse width is absent. At five times the rms level, widths of 5, 15 and 20 $\mu$s are evident in Fig. 4.5. At 10 times rms, the widths are less than 5 $\mu$s.

Fig. 4.6 shows impulse width distributions in a residential home with the light dimmer activated. In this case, the impulse noise is so strong that well defined impulse widths exist even at an amplitude level equals the rms level, where most impulses are either 95 or 125 $\mu$s wide. At 10 times rms
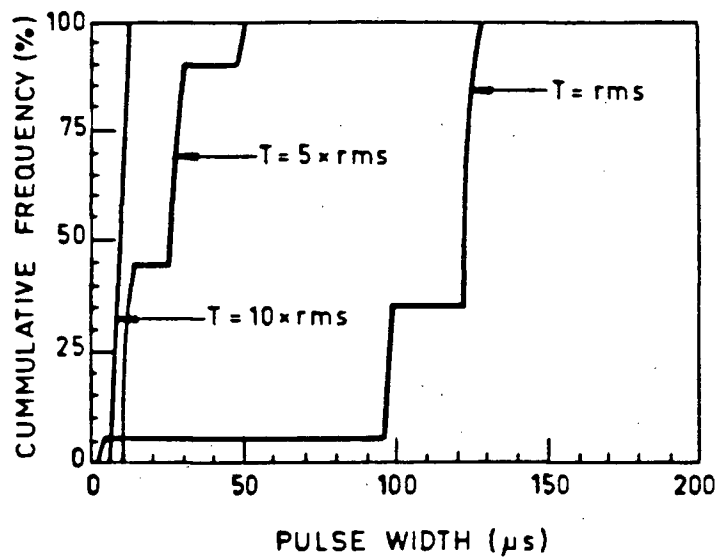
Figure 4.6: IWD, residence home. Light dimmer active.

level, virtually all impulses are approximately 10 $\mu$s wide.

## 4.3.3  Impulse Interval Distribution (IID)

Impulse interval distributions appear in Figs. 4.7 and 4.8. These distributions depend on the amplitude threshold level used to define an impulse. The impulse must exceed the threshold to be counted. The higher the level, the smaller the number of impulses counted per unit time and the larger the time between impulses. Well defined interarrival times occur in the presence of strong, periodic impulse noise.

Fig. 4.7 shows a measured IID in the industrial building with and without the photocopier activated. With the photocopier on and the amplitude
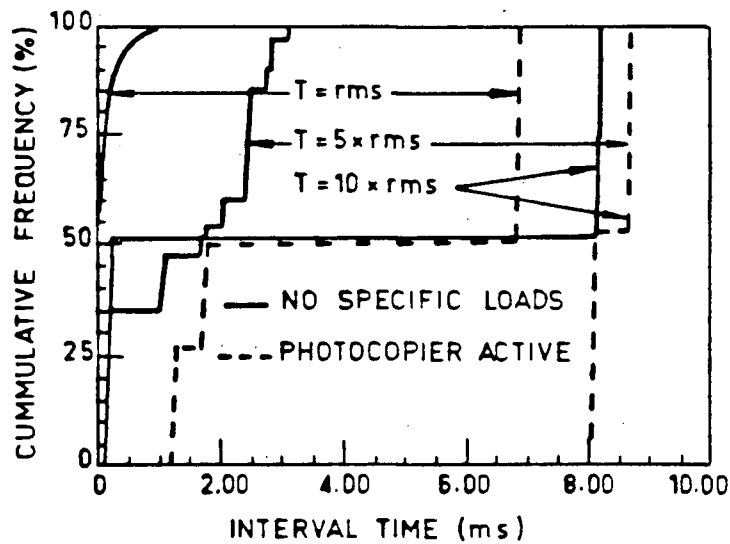
Figure 4.7: IID, industrial building.

threshold level equal to 5 or 10 times the rms noise value, the interarrival time is approximately 8.3 ms, which represents 120 impulses per second. At these two threshold levels, only relatively strong, periodic impulses are observed. At threshold level equal to the rms noise level, the interarrival time is either 1.5 or 6.8 ms, with probability one-half. As mentioned in Fig. 4.5, at this threshold level, two periodic impulse trains one preceded or followed by the other are counted, and the seperation between them alternates between 1.5 ms and 6.8 ms.

In the absence of the strong impulse noise generated by the photocopier, the time between impulses is not well defined, unless the threshold is 10 times the rms noise level. Fig. 4.7 shows, in this case, that a pair of impulses 200
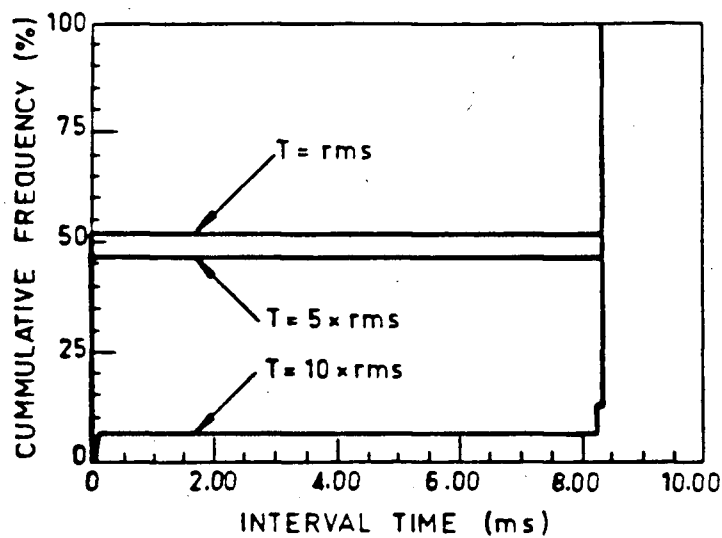
Figure 4.8: IID, residence home. Light dimmer active.

to 300 $\mu$s apart appears at every 8.3 ms period.

Results like those obtained in the industrial building were obtained in the single family residence. Fig. 4.8 shows that, with the light dimmer active, the interarrival time is either extremely short or about 8.3 ms with probablity one-half, for amplitude threshold levels equal to and 5 times the rms noise value. At threshold level 10 times the rms value, the interarrival time is 8.3 ms 90 per cent of the time. Fig.4.6 and 4.8 shows in this case, that a pair of closely located impulses one slightly highly than the other appears at every 8.3 ms period. The results from Figs. 4.7 and 4.8 indicate that, under some conditions, adjacent impulses can occur possibly leading to long burst errors during data transmission.

56

# 4.4  Summary

Orginal measured results on APD, IWD and IID of intrabuilding power line noise under typical as well as severe channel conditions have been obtained. In general, intrabuilding power line noise can be considered to consist of a continuous, relatively low level background noise punctuated by relatively strong noise impulses. The characteristics of the noise impulses are summarized below:

1. Impulse strength is typically more than 10 dB above the background noise level, and can exceed 40 dB. Impulse strength depends on what noise sources are present and the proximity of these noise sources to the receiver.

2. Impulse frequency for the dominant impulse train is typically 120 Hz in synchronism with the positive and negative cycles of the 60 Hz power voltage.

3. Impulse width can vary up to a few percent of the impulse period, for 120 Hz impulse noise.

4. Impulses can occur adjacent to each other which can lead to the formation of long error bursts.

5. When compared to in-phase impulses, impulse noise originating from other phases of a three-phase power system usually have significantly less power.

6. Communication system performance is determined largely by the disturbance caused by the dominant in-phase impulse train.

7. As well as regular periodic impulse noise (from synchronous or phase-controlled loads), high level noise impulses can also result occasionally from random load switching.

8. Because noise as well as wanted signals are subjected to attenuation, noise sources close to the receiver will have the greatest effect on the received noise structure, particularly when the network attenuation is large.

9. Some noise sources will increase the background noise power, others will increase the impulse noise power, and others will increase the power of both noise types.

# Chapter 5

# Combating Impulse Noise and Signal Fading on Intrabuilding Power Lines

On intrabuilding power line channels, synchronous loads and switching devices such as SCR's and triacs produce high level periodic noise impulses which are synchronous and which drift with the 60 Hz power voltage. Since SCR's are an ubiquitous part of every power distribution system, it is these continuous impairments by periodic impulse noise which limit the performance of power line data communication systems. High level impulse noise resulting from random load switching is relatively infrequent, while other noise types are much less harmful than periodic impulse noise. Periodic impulse noise is found to be the major cause of power line channel errors [4] and an impediment to reliable digital transmission.

## 5.1 Overcoming Impulse Noise

Periodic impulse noise can cause power line communication channels to exhibit unacceptably high bit error rates. Consider, for example, the transmission of even a very short 100-bit data packet at 9,600 bits/s, over a channel where the impulse noise is periodic at 120 Hz. Noise pulses occur every 8.3 ms, and since the packet requires a transmission time of 10.4 ms, every packet would be subject to at least one noise impulse. In the absence of some error correction, strong impulse noise would, with high probability, cause at least one bit-error per packet. Under an automatic-repeat-request (ARQ) protocol incorrect packets could be retransmitted; however the retransmission probability is high and the packet throughput low [25]. In addition, acknowledgement packets are also subject to impulse hits further degrading performance. The actual bit error probability during noise impulses would depend on the impulse amplitudes and widths, relative to the received signal level and data bit duration.

Methods have been proposed to estimate and then cancel power line impulse noise using adaptive, on-line filtering techniques [44,45]. The success of this method depends very much on continuous accurate estimation of the fluctuating power line noise. The work only shows an achieved BER of about $10^{-3}$ at 500 bits/s data rate.

Other means to combat impulse noise, based on the use of forward error correction (FEC) coding, are of great interest. With FEC coding, a code matched to the channel conditions is used. Code selection depends on the communication system designer's knowledge of the channel characteristics. One appropriate and practical approach suitable for power line channels involves the use of interleaved repetition coding techniques. The basic idea is to divide in time each data bit into three code bits, transmit the code bits after interleaving, and use the three received code bits that have been spreaded out in time to make a decision on the original data bit. With this scheme a noise impulse can only damage a portion of a data bit, and the undamaged portions can then be used to reconstruct the original data bit.

## 5.1.1 Bit Error Probability of Interleaved Repetition Coding with Hard or Soft Decisions With or Without Erasure

A simple and accurate power line noise model useful for analysis or simulation is currently unavailiable. To test the use of interleaved repetition codes, a simple first order power line noise model consisting of background noise of power spectral density $N_b/2$ and impulse noise of power spectral density $(N_i - N_b)/2$ is proposed, in accordance with our observations as shown in Chapter 4. The impulse noise occurs periodically, and is superimposed on

the background noise in accordance with Duty Factor (DF) which represents the ratio of the impulse noise duration to its period. In other words, $N_i$ respresents the impulse power while DF respresents the impulse width for a fixed impulse period. $N_i$ and DF stay fairly constant over short time period, but they do fluctuate over long times. Both noise types were Gaussian; however, $N_i >> N_b$. Although the modelling is somewhat idealistic, the purpose here is to provide some initial analysis on the potential performance advantages to be realized with error correction on power line channels with periodic impulsive impairments. Realistic tests of codings when subjected to real channel errors are presented in Chapters 6 and 7. In addition, this simple power line noise model can be easily modified to describe periodic signal fading as discussed in Section 5.2. A useful and accurate noise model which can be generally applied to all power line envirnments requires the support of a very large data base and is impossible at this stage.

In accordance with measured power line noise behaviour from Chapter 4, $N_i/N_b$ varied from 20 to 50 dB, and DF varied up to a few percent. This model is used with BPSK signalling, coherent detection and an integrate and dump receiver which is the optimum binary signalling scheme for a simple additive white Gaussian noise channel [50]. Ideal interleaving is assumed so that not more than one of the three code bits is subjected to impulse noise.

Depending on the bit decision and decoding methods used, the following cases are considered.

- Interleaved hard decision - hard binary decisions are made on the integrator output for each of the three code bits and these decisions are used under majority voting to decide the data bit.

- Interleaved soft decision - analog values of the integrator output of the three code bits are summed and the sum determines the data bit.

- Interleaved hard decision with erasure - code bits received during impulse hits are discarded from the majority voting decoding process.

- Interleaved soft decision with erasure - values of code bits received during inpulse hits are discarded from the summation process.

Perfect erasure detection is assumed in the analysis and the results obtained provide a lower bound for decoded bit error probability.

The results of the analysis are shown in Figs. 5.1-5.4 which plot decoded bit error probability $P_e$ vs. $E_b/N_b$, where $E_b$ is the energy per data bit at the receiver. For burst error channels, bit error probability is not a complete description. However, bit error probability is the single most important parameter of any communication channel. To obtain the curves in Figs. 5.1

and 5.2, we assume the impulse noise duration either equals or is an integer multiple of the data bit duration, and that the data bit and impulse noise boundaries coincide. In such case, the bit error probability $P_e$ is given by the following equations in accordance with the explanations given in Appendix A:

(1) Uncoded transmission.

$$P_e = (1 - DF)Q(\sqrt{2E_b/N_b}) + (DF)Q(\sqrt{2E_b/N_i}) \tag{5.1}$$

(2) Interleaved hard decision.

$$
\begin{aligned}
P_e &= (1 - 3DF)\sum_{k=2}^{3}\binom{3}{k}Q(\sqrt{2E_b/3N_b})^k \overline{Q}(\sqrt{2E_b/3N_b})^{3-k} \\
&\quad + 3DF[2Q(\sqrt{2E_b/3N_i})Q(\sqrt{2E_b/3N_b})\overline{Q}(\sqrt{2E_b/3N_b}) \\
&\quad + Q(\sqrt{2E_b/3N_b})^2\overline{Q}(\sqrt{2E_b/3N_i}) + Q(\sqrt{2E_b/3N_b})^2 Q(\sqrt{2E_b/3N_i})] \\
&= (1 - 3DF)\sum_{k=2}^{3}\binom{3}{k}Q(\sqrt{2E_b/3N_b})^k \overline{Q}(\sqrt{2E_b/3N_b})^{3-k} \\
&\quad + 3DF[2Q(\sqrt{2E_b/3N_i})Q(\sqrt{2E_b/3N_b})\overline{Q}(\sqrt{2E_b/3N_b}) \\
&\quad + Q(\sqrt{2E_b/3N_b})^2] \tag{5.2}
\end{aligned}
$$

(3) Interleaved soft decision.

$$P_e = (1 - 3DF)Q(\sqrt{2E_b/N_b}) + 3(DF)Q(\sqrt{6E_b/(N_i + 2N_b)}) \tag{5.3}$$

(4) Interleaved hard decision with erasure.

$$P_e = (1 - 3DF)\sum_{k=2}^{3}\binom{3}{k}Q(\sqrt{2E_b/3N_b})^k \overline{Q}(\sqrt{2E_b/3N_b})^{3-k}$$

$$+3DF[Q(\sqrt{2E_b/3N_b})\overline{Q}(\sqrt{2E_b/3N_b}) + Q(\sqrt{2E_b/3N_b})^2]$$

$$= (1-3DF)\sum_{k=2}^{3}\binom{3}{k}Q(\sqrt{2E_b/3N_b})^k\overline{Q}(\sqrt{2E_b/3N_b})^{3-k}$$

$$+3(DF)Q(\sqrt{2E_b/3N_b}) \qquad\qquad (5.4)$$

(5) Interleaved soft decision with erasure.

$$P_e = (1-3DF)Q(\sqrt{2E_b/N_b}) + 3(DF)Q(\sqrt{4E_b/3N_b}) \qquad (5.5)$$

where

$$Q(x) = \frac{1}{\sqrt{2\pi}}\int_x^\infty e^{-v^2}dy \qquad (5.6)$$

$$\overline{Q}(x) = 1 - Q(x) \qquad (5.7)$$

In all cases (a)-(d) curve (1), which corresponds to uncoded transmission, decreases as $E_b/N_b$ increases for low $E_b/N_b$ values, then levels out as $E_b/N_b$ increases further. If $E_b/N_b$ continues to increase such that the value of $E_b$ becomes comparable to that of $N_i$ , the curve can then begin to slope down again. The impulse noise clearly limits performance by creating an error floor. Curve (3) is worse than curve (1). Even though bit interleaving and repetition coding are used, the soft decision process which involves adding integrator outputs from each code bit can allow large noise impulse in one code bit to damage the overall data bit. A strong impulse which originally widely disturbs one data bit now destroys three data bits. This curve demonstrates that the wrong choice of a coding scheme could make

65
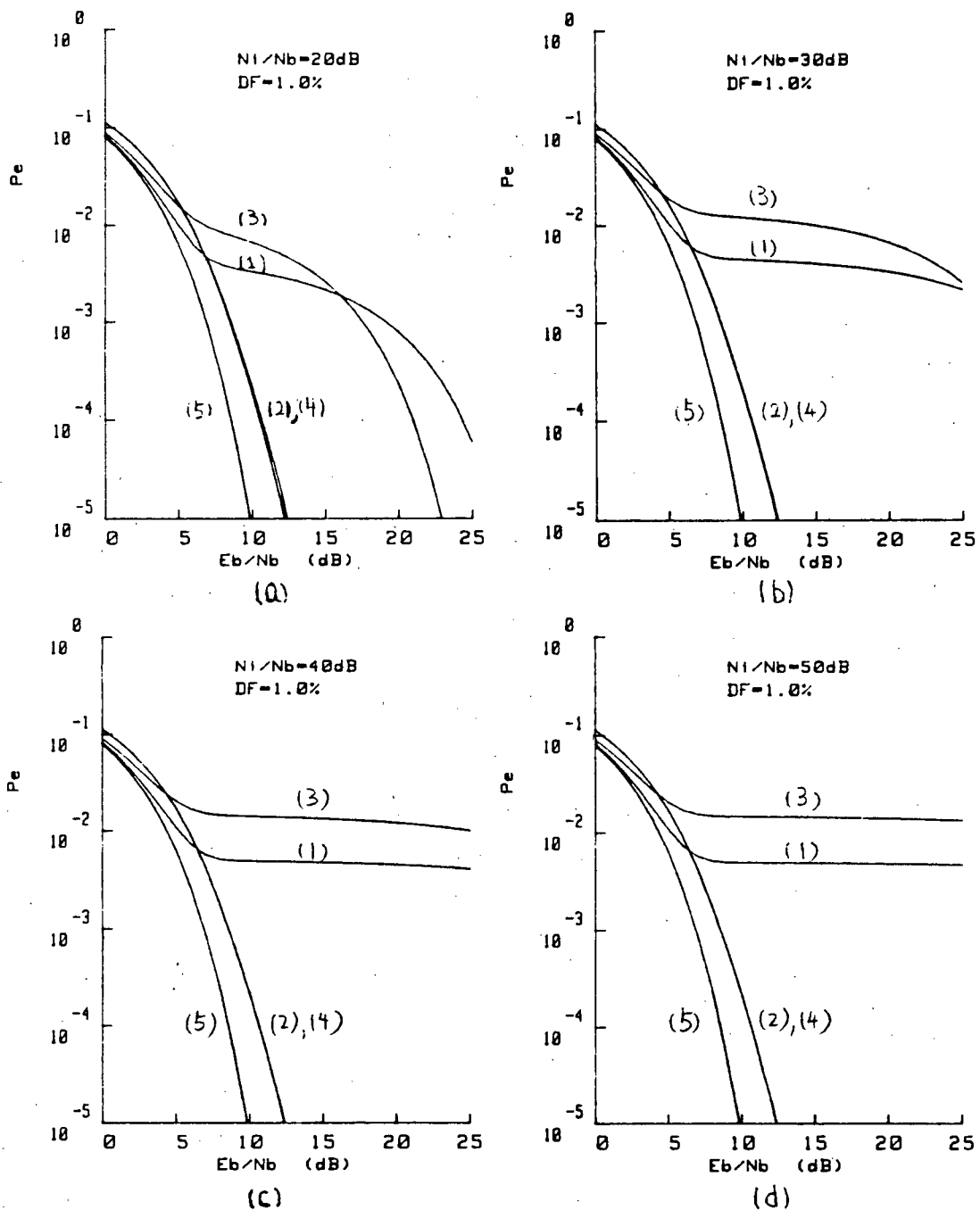
(1) Uncoded transmission. (2) Interleaved hard decision. (3) Interleaved soft decision. (4) Interleaved hard decision with erasure. (5) Interleaved soft decision with erasure.

Figure 5.1: Bit error probablity of uncoded and interleaved repetition coded transmissions at different $N_i/N_b$ values. Impulse noise duration equals or is an integer multiple of data bit duration.

66

the performance worse than with no coding.

In curves (2), (4) and (5), code bits badly damaged by impulse noise are prevented from damaging the entire data bit. These curves show considerable improvement in performance over that for uncoded transmission. Curve (2) results when hard binary decisions are made on each code bit, and these decisions are then used, under majority voting, to make a decision on the data bit. Curves (4) and (5) are obtained by discarding the code bits received during impulse noise from the decision making process. With hard decision, a tie situation may occur when only two code bits remain as the other code bit is erased. When this happens, "a fair coin toss" decides the data bit. This situation increases the error rate and curve (4) does not show appreciable performance improvement over curve (2) without erasure. Curve (5) clearly demonstrates the benefit obtained by erasing the unreliable bit, and is the best of the five. The results on hard decision are very different from what would be obtained for the frequently considered Gaussian noise channel for which hard decision repetition coding for cases (2) and (4) would always degrade performance relative to uncoded transmission. On a Gaussian noise channel, the gain obtained from repetition coding could not compensate for the error rate increase in detecting the shorter (faster) code bits.

We note here that a 1% duty factor with 120 Hz impulse noise implies

a data rate of 12 kbits/s when the data bit duration equals the duration of the impulse noise. Similary, the same 12 kbits/s date rate implies a 0.5% and a 2% duty factors with 60 Hz or 240 Hz impulse noise respectively.

Fig. 5.1(a-d) also shows the effects of impulse noise strength on system performance. As $N_i/N_b$ increases, curves (1) and (3) level out more quickly while curves (2) , (4) and (5) indicate very effective code performance regardless of the increase of the impulse noise power. Figs. 5.1(b) and 5.2 show the effects of impulse noise duration on system performance. Again as DF increases, curves (1) and (3) level out more quickly, while curves (2), (4) and (5) indicate a good performance regardless of the change of the impulse noise duration or period for a fixed impulse noise period or duration, respectively. All together , the above figures show that interleaved repetition codings for cases (2), (4) and (5) are robust against fluctuation of the noise process parameters from nominal levels.

Figs. 5.3 and 5.4 show the performances when the impulse noise duration is a fraction f of the data bit duration. The equations appear in Appendix A. Again, curves (2), (4) and (5) show much better performance and curve (3) shows a worse performance than that of curve (1).
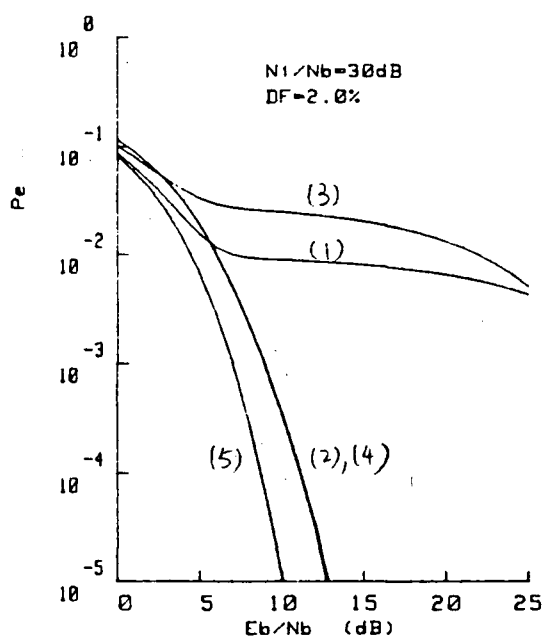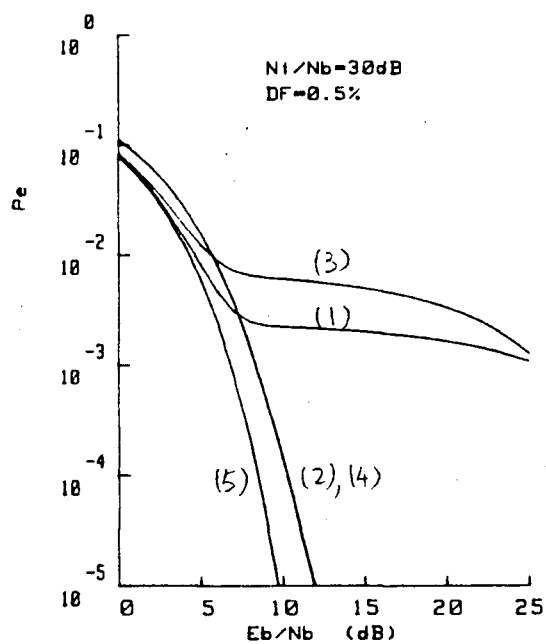
Figure 5.2: Bit error probablity of uncoded and interleaved repetition coded transmissions at different DF values. Impulse noise duration equals or is an integer multiple of data bit duration. (1)-(5) as in Fig.5.1.
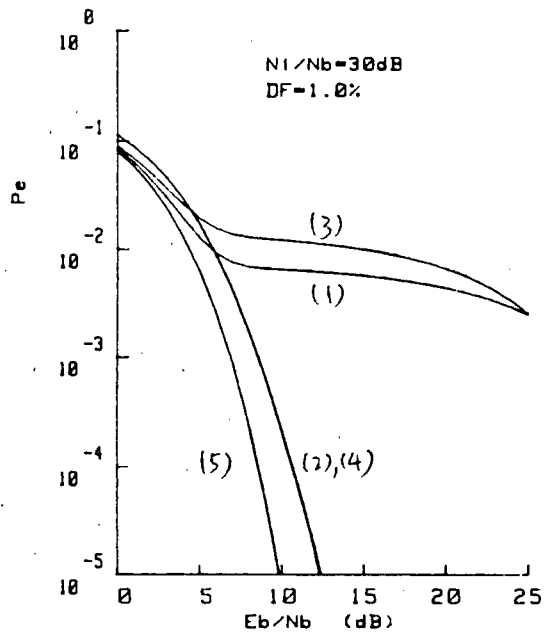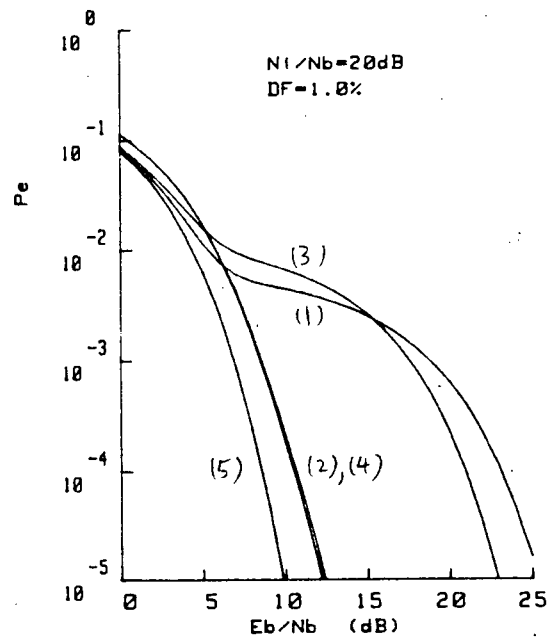
Figure 5.3: Bit error probablity of uncoded and interleaved repetition coded transmissions. Impulse noise duration equals 2/3 of the data bit duration. (1)-(5) as in Fig.5.1.

70
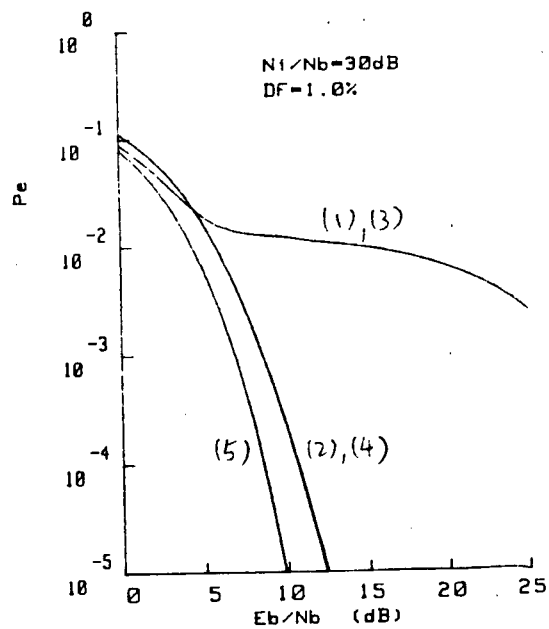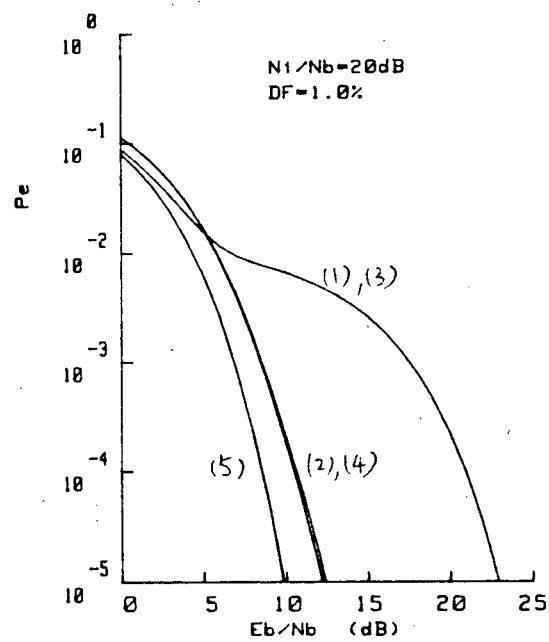
Figure 5.4: Bit error probablity of uncoded and interleaved repetition coded transmissions. Impulse noise duration equals 1/3 of the data bit duration. (1)-(5) as in Fig.5.1.

## 5.1.2 Packet Error Probability With or Without Bit Interleaving and Repetition Coding

In data communications, information bits are often transmitted in packets. To prevent data packet overheads from reducing throughput efficiency too much, packet lengths are typically in excess of few hundred bits, and often total 1000 bits or more. Under an ARQ protocol, incorrect packets are retransmitted. When the average channel bit error rate is small, such error detection and retransmission schemes are very effective. As the channel bit error rate increases, the packet retransmission rate becomes high and the thoughput of an ARQ protocol deteriorates quickly.

Fig. 5.5 shows the packet retransmission probability upper bound $P_r$ vs. $E_b/N_b$ for uncoded and interleaved repetition codings at packet length equal to 1000 bits. These curves were obtained as follows:

$$P_r = 1 - (1 - P_e)^l \qquad (5.8)$$

where $P_e$ is given by Eqns. (5.1)-(5.5) and $l$ is the packet length in bits. Curve (1) clearly indicates that with uncoded transmission, packets are retramsmitted with probability near unity. With interleaved repetition codings, curves (2), (4), and (5) show that a high successful packet reception rate can be readily achieved. Fig. 5.6 shows the effect of packet length $l$ on $P_r$ as a function of $E_b/N_b$ when using interleaved hard decision repetition coding, at

72
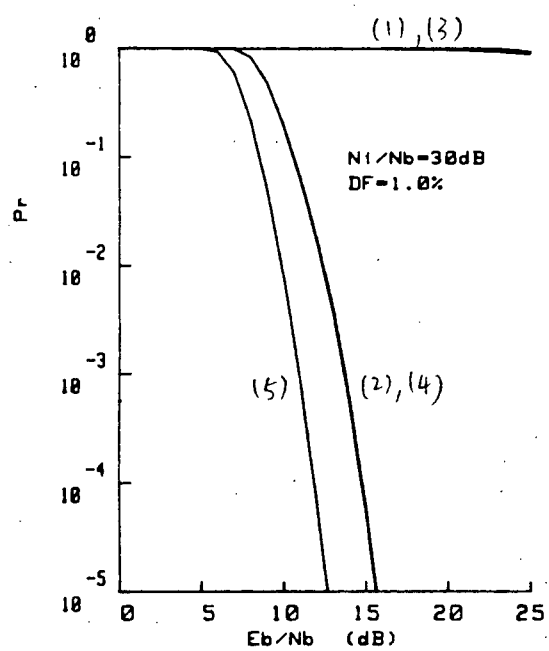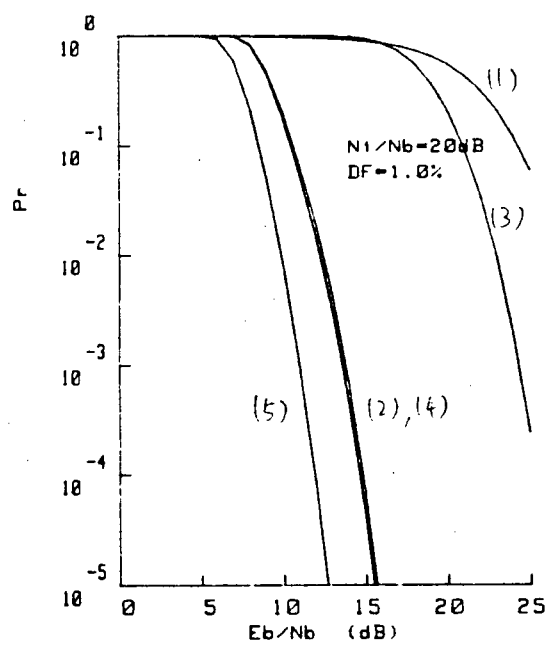
Figure 5.5: Packet error probablity of uncoded and interleaved repetition coded transmissions. (1)-(5) as in Fig.5.1.

73

the packet lengths of 100, 500, 1000, 2000, 3000, 4000 and 5000 bits. Fig. 5.7 shows the variation of $P_r$ as a function of packet length $l$ for all five cases at $E_b/N_b$ equal to 15 dB.

## 5.2   Overcoming Signal Fading

As shown in Chapter 3, periodic signal fades will sometimes occur on power line channels. This periodic signal degradation is analogous to periodic impulse noise impairment. Indeed, the occurrence of either signal drop-out or impulse noise results in signal-to-noise degradation. Therefore, interleaved repetition coding discussed in this chapter for combating power line impulse noise is similarly effective in handling periodic signal fading.

In an actual operating power line communication system, the signal level is usually well above the background noise level. Occurrences of periodic signal fades cause small degradations in performance unless the degree of fading is severe enough that the signal energy level becomes close to the background noise level. Occurrence of a deep fade is very rare, and over 90% of all fading occurrences are less than a few dB from the median level. However, a deep fade can last for a very long time if it occurs. The use of bit interleaving in combating the always present power line impulse noise simultaneously provides protection against impairments caused by this rare
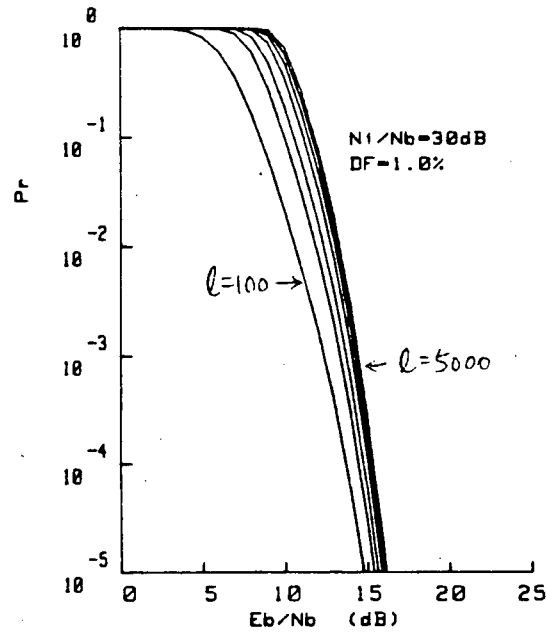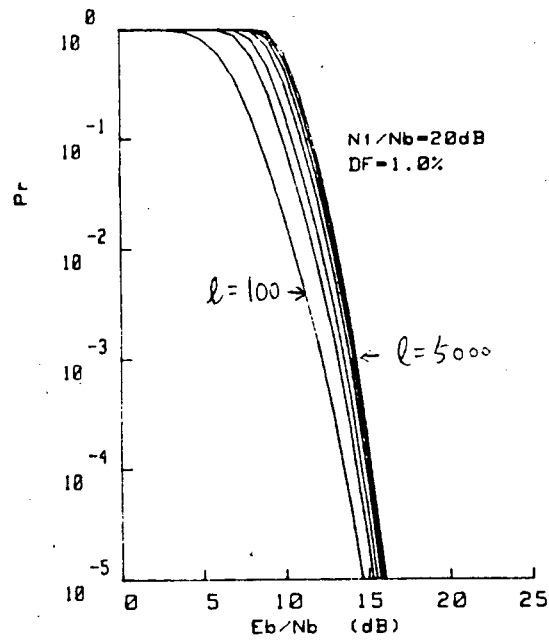
Figure 5.6: Packet error probablity of uncoded and interleaved repetition coded transmissions for different packet length $l$. (1)-(5) as in Fig.5.1.
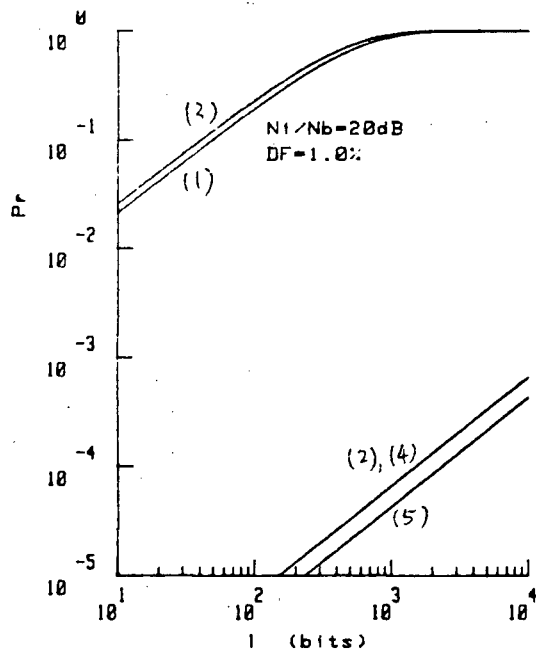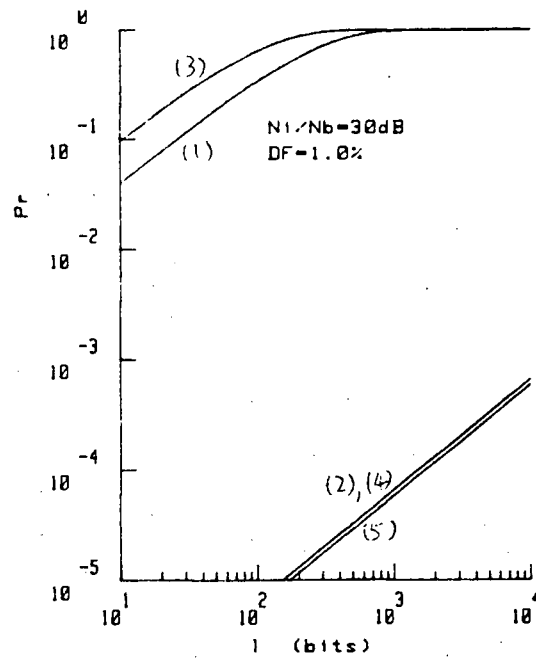
Figure 5.7: Packet error probablity of uncoded and repetition coded transmissions vs. packet length $l$. (1)-(5) as in Fig. 5.1.

but severe signal fading.

To obtain results similar to those of Fig. 5.1 when data communication systems are subjected to severe periodic power line signal fading instead of impulse noise, one simply replaces $E_b/N_i$ with $E_f/N_b$ in Eqns. (5.1)-(5.5) where $E_f$ is the energy per data bit at the receiver during fading, and use $E_b/E_f$ instead of $N_i/N_b$ as the parameter. In accordance with actual power line fading behaviour, $E_b/E_f$ can be tens of dB during the relatively rare occurrence of severe fading, and DF usually varies from 10 to 20%.

As well, bit interleaving also provides protection against the extremely rare occurrence of phase distortion errors caused by a step change in the signal amplitude, as mentioned in Chapter 3.

## 5.3 Summary

Intrabuilding power lines present hostile and complex communication channels for which an accurate and useful noise model is unavailable for analysis or simulation. The work in this chapter as well as in [6,7] uses a simple first order noise model to show that coding and bit interleaving is an important component in combatting power line impulse noise, periodic signal fading and other bursty impairments, greatly improving the performance of a data communication system. While the modelling is somewhat idealistic,

the analysis provides some useful initial results demonstrating the potential performance advantages to be realized with error correction. Fairly simple repetition coding techniques can eliminate the error floor of an uncoded system. Later, we show that better performance is readily possible with more complex and powerful codes.

In terms of practical realization, only hard decisions would be considered for low cost implementation. A short interleaver with an interleaving period no longer than the period of the impulsive disturbance should provide suitable bit interleaving. The use of erasure requires additional channel state information. The obvious way of implementation requires a comparator at the front end of the receiver to monitor the incoming voltage amplitude level. If the incoming signal plus noise level during the duration of a code bit exceeds a certain threshold relative to the average level computed, the code bit is likely to be impaired by noise impulse and would be discarded.

# Chapter 6

# Evaluation of Error Correction Block Codes for High Speed Power Line Data Communications

The benefits of using interleaving and repetition coding techniques in combatting power line impulse noise are shown in Chapter 5. In this chapter as well as in [7,8], some random and burst error correcting block codes whose efficiency exceeds the 33% efficiency of the three-bit repetition code are considered. Actual bit error patterns recorded in a computer during power line data transmission experiments were used to determine code performance. The error data was obtained by transmission of an 11th-order maximum length Pseudo Noise (PN) data sequence and observing the error bits in the received sequence. Results are given at a channel bit transmission rate of

79

28.8 kbits/s using coherent FSK at 115 kHz carrier frequency under various types of channel impairments. The FSK transceiver was implemented using standard FSK circuits based on IC's XR-2206 and XR-2211 [11,12]. Block error rates were measured for these codes to determine appropriate error correction capability, block size and depth of interleaving. Although typical codes have been used as illustrations, the investigation has been general, to enable the effect of parameter variation to be seen, to assist the selection of a code to meet a specified performance, and to permit assessments of possible trade-offs. The results will enable the application of appropriate error control codings required to achieve reliable data communications.

# 6.1 Forward Error Correction (FEC) Coding

Depending on the specific application, selection of a code or a decoding algorithm can be a complicated task; the choice is affected by numerous overall system design parameters. To determine whether an error control coding scheme is justified for a particular application, the following factors have to be taken into consideration:

- channel requirements and constraints

- decoding performance

- cost and complexity

- coding delay

- coding efficiency

- speed of codec operation

- storage requirements

- nature of data traffic

- message size and format

- availability of a feedback channel

- location of the codec in the transmission link and code transparency

From the system design standpoint, the most important factor is decoding performance and delay. From the standpoint of practical implementation, cost and complexity are of primary concern.

## 6.1.1 Error Correcting Block Codes

The two different types of codes in common use today are block codes and convolutional codes. This chapter deals with the application of block codes for power line data communications. The following chapter deals with convolutional codes.

The encoder for a block code divides the information bits into groups of k bits and adds r redundant parity bits to each group. The parity checks depend on the information bits. The information plus parity bits form an n bit block or code word. The number of bit positions in which two code words differ is called the distance between the code words, and the minimum distance for a code is denoted d. The error correcting capability of a code is determined by it's minimum distance. A code having a minimum distance d is capable of correcting all patterns of $t = (d-1)/2$ or fewer errors in a code word, and is usually referred to as a (n,k,t) random error correcting code. For example, a code having a 15-bit code word with 5 information bits and a capability of correcting up to 3 errors would be referred to as a (15,5,3) random error correcting code. A (n,k,b) burst error correcting code can correct any error pattern spanning not more than b bits in a code word. Also, most codes are able to correct some error patterns beyond the guaranteed bounds described above, but whether this capability is employed or not depends on the type of decoder. The ratio $R = k/n$ is called the code rate, and is a measure of the throughput or efficiency of the code.

For a code to be useful, $R \leq 1$. For a fixed code rate R, more redundant bits can be added by increasing the block length n of the code while holding the ratio k/n constant. In reality, it may not be beneficial to use a very long code for some applications because of the types of errors encounted,

large storage requirements, long decoding delay and increased implementation complexity, and because of the nature of message type and size to be transmitted. On the other hand, for a fixed block (code word) length n, more redundant bits can be added by decreasing the number of information bits k, hence the code efficiency R of the code. Obviously, if R is too low the code is not practically useful.

## 6.1.2 Bit Interleaving

As shown in Chapter 5, bit interleaving is a technique for improving performance when more than a single code word is transmitted. It is a method for dispersing errors that occur in clusters. The interleaving process may be visualized as assembling i code words as rows of an $i \times n$ array and transmitting the bits by scanning the columns. Thus, adjacent bits in the same codeword are seperated in transmission by i-1 bits. The number of code words i which are interleaved is called the interleaving degree or depth, and the total number of bits, $i \times n$, is called the interleaving period I. At the receiving site, the interleaved bit stream is deinterleaved into the orginal code words for decoding. This can be accomplished by storing column by column the received bits into an $i \times n$ array and reading out the code words by rows. Interleaving does not involve adding more redundancy but does add decoding delay and storage costs.

In order to implement interleaving, an interleaving period and a code word length must be chosen. Interleaving should enable errors occuring during impulse noise and signal fading to be dispersed into the intervals between these impairments.

## 6.2 Methods of Evaluation

To assess the performance of a code, we need to know how often a code word is corrupted by errors and how often the correcting capability of the code is exceeded. To find this out, the measured error patterns have been divided into blocks of bits and the number of errors in each block counted. The results of this are used to compute the block error rate upper-bound, $P_{bk}$, after decoding for random error correcting code which is

$$P_{bk1} = ( \sum_{i=t+1}^{n} iB_i)/(N/n) \tag{6.1}$$

where n is the block length, $B_i$ is the number of blocks containing i error bits, t is the number of correctable error bits in a block, and N is the total number of bits used. Typical values of N used are at least $1 \times 10^7$ bits.

For burst error correcting codes, it is necessary to determine the distribution of error burst lengths within code words. The results are used to

compute the $P_{bk}$ for burst error correctng code which is

$$P_{bk2} = ( \sum_{l=b+1}^{n} lB_l)/(N/n) \qquad (6.2)$$

where $B_l$ is the number of error-blocks containing an error burst of length $l$, and b is the correctable burst length in a block. When errors occur only near the ends of a block they have been regarded as an "end around burst", thus resulting in a shorter burst than one spanning almost the whole block length. One advantage of cyclic codes is the ability to manipulate code words cyclically in this fashion [25]. The use of $P_{bk}$ does not involve any assumptions on a particular decoding method, thus enabling a simple and effective analysis of error correction block codes.

For evaluation, a set of random error correcting block codes with block lengths ranging from 15 to 63 and with different error correcting capabilities and code rates was chosen from the class of BCH codes [25]. The BCH codes form a large class of powerful random error correcting cyclic block codes that occupy a prominent place in the theory and practice of forward error correction; and relatively simple decoding techniques are known for some of these. For burst error correction, some very efficient burst error correcting cyclic and shortened cyclic codes have been found analytically or with the aid of a computer [25]. A set of these codes with their burst error correcting capability is given in Table 6.1. They were chosen because of the similarity

| Code (n,k) | Burst-correcting capability b | k/n |
|---|---|---|
| 15,9 | 3 | 0.60 |
| 15,7 | 4 | 0.47 |
| 15,5 | 5 | 0.33 |
| 30,14 | 8 | 0.47 |
| 63,44 | 9 | 0.70 |

Table 6.1: Some burst-correcting cyclic and shortened cyclic codes.

of block lengths and code rates with the random error correcting BCH codes evaluated, thereby allowing a comparision of performance between burst and random error correcting codes.

These codes were evaluated for their performance under different types of impairment at different channel bit error rate p, with and without interleaving. The effect of interleaving has been investigated by rearranging the error patterns to simulate deinterleaving. The results of the evaluation are shown in Figs. 6.1-6.14 with p as the parameter; p is the dominant error measure. The error structure including burst error statistics is determined largely by the specific impairment encountered. Error distributions under different impairments at different p values have been obtained [4,5]. A higher value of p under the same impairment means longer error bursts would be expected when compared with a lower p value.

The results presented are selected from evaluations of error data for channels in which the conditions were bad. Results in these figures are presented starting from the smallest value of t and gradually increasing t to show the gradual change from poor performance obtained from a code having inadequate error correcting capability to significant improvement in performance obtained from codes having the right amount of error correcting capability. Although not shown, further improvement is generally incurred by a further increase in t, at the expense of efficiency.

## 6.3 Random Error Correcting Code Performance

### 6.3.1 Impulse Noise

Figs. 6.1-6.3 show the measured block error rate $P_{bk}$, after error correction for BCH codes when subjected to power line impulse noise, with $p = 1 \times 10^{-2}$. Without interleaving (i=1) and for t=1, $P_{bk}$ increases from $3 \times 10^{-2}$ to $1.5 \times 10^{-1}$ when n increases from 15 to 63, as shown in Figs. 6.1 and 6.3. Similary, for t=3, $P_{bk}$ increases from $5.5 \times 10^{-4}$ for the (15,5,3) code to $4.5 \times 10^{-3}$ for the (63,45,3) code.

However, with the code rate R fixed (say at $\cong 1/2$), $P_{bk}$ decreases from $5 \times 10^{-3}$ for the (15,7,2) code to $1.2 \times 10^{-4}$ for the (63,36,5) code.

87

Figure 6.1: Block error rate vs. interleaving degree for n=15 BCH codes, impulse channel. Channel bit error rate p=1 × 10⁻².

Figure 6.2: Block error rate vs. interleaving degree for n=31 BCH codes, impulse channel. Channel bit error rate $p = 1 \times 10^{-2}$.

Figure 6.3: Block error rate vs. interleaving degree for n=63 BCH codes, impulse channel. Channel bit error rate $p=1 \times 10^{-2}$.

For about the same code efficiency, increasing the code word length from 15 to 63 bits reduces the error rate by using the added redundant bits of the longer code. Also shown in Fig. 6.1 for comparision purposes is $P_{bk}$ for the (3,1,1) repetition code considered earlier. It is better than the single error correcting (15,11,1) code and is also better than the double error correcting (15,7,2) code. For repetition coding the decoded bit and block error rates are equal.

The effectiveness of interleaving in reducing $P_{bk}$ is seen to increase with t. For the (15,11,1) and (15,7,2) codes, for example, $P_{bk}$ decrease from $3 \times 10^{-2}$ and $5 \times 10^{-3}$ with no interleaving to $7 \times 10^{-3}$ and $2 \times 10^{-5}$ respectively, with interleaving to degree 10. With only single error correcting capability, interleaving lowers the error rate by about half an order of magnitude. But with double error correcting capacity, interleaving reduces the error rate by more than two orders of magnitude. To obtain $P_{bk} < 10^{-5}$ requires interleaving to degree i=5 using a (15,5,3) code.

The same kind of results are apparent for n=31 and n=63 BCH codes, as shown in Figs. 6.2-6.3. In these cases, interleaving the (31,11,5) code to degree 3 and interleaving the (63,24,7) code to degree 9 reduce $P_{bk}$ below $10^{-5}$. Fig. 6.3 also indicates that in this case, simply increasing the error correcting power from 5 to 10 bits as shown by the (63,36,5) and (63,18,10)

codes, does not give a much reduced $P_{bk}$ without some interleaving, while unnecessarily reducing throughput.

On the other hand, the effectiveness of interleaving in reducing $P_{bk}$ is seen to decrease as n increases. For $R \cong 1/2$ codes, for example, decrease in $P_{bk}$ is only gradual for the (63,36,5) code when the interleaving degree increases, as compared to the large decrease in $P_{bk}$ for the (15,7,2) code. This is because for large n, interleaving can bring in many additional errors into the interleaving block. It is noted that the more powerful (63,36,5) code starts from a better uninterleaved performance than the (15,7,2) code, however.

Figs. 6.4-6.6 show the performance of BCH codes when subjected to errors caused by periodic impulse noise and occasional signal drop outs, with $p = 2.7 \times 10^{-3}$. To reduce $P_{bk} < 10^{-5}$ requires interleaving to degree 3 using the (15,7,2) code, the (31,16,3) code or the (63,39,4) code. The (15,5,3) code indicated in Fig.6.4 gives $P_{bk} < 10^{-5}$ for all interleaving values from i=1 to 20. The (31,11,5) code and the (63,36,5) code in Figs. 6.5-6.6 give $P_{bk} < 10^{-5}$ with $i \geq 2$.

Figs. 6.1-6.6 show that there is a practical limit on a useful interleaving period. For a code with inadequate error correcting capability, even a very long interleaving period cannot improve its performance. For a code with
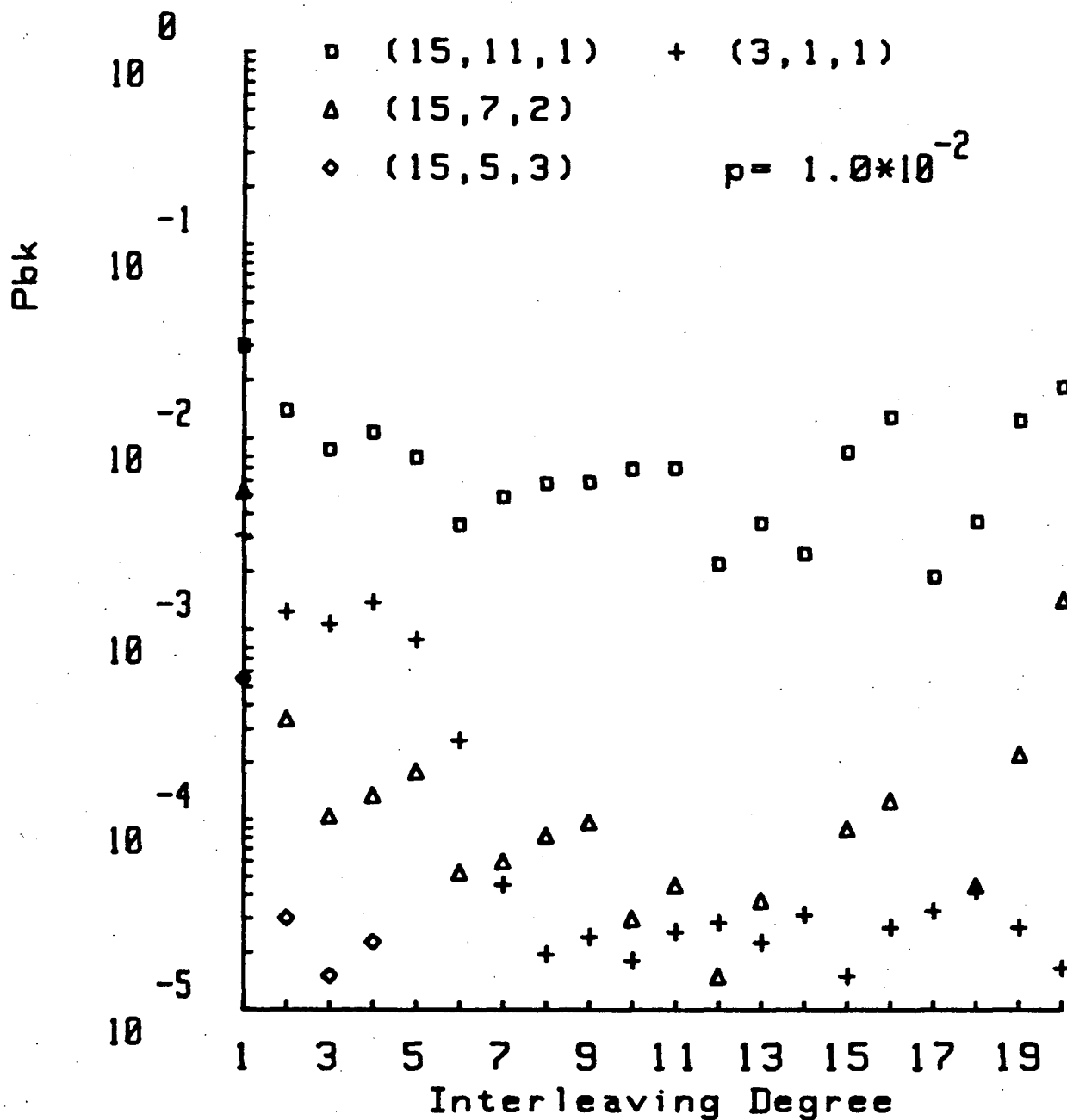
Figure 6.4: Block error rate vs. interleaving degree for n=15 BCH codes, impulse channel. Channel bit error rate p=2.7 × $10^{-3}$.

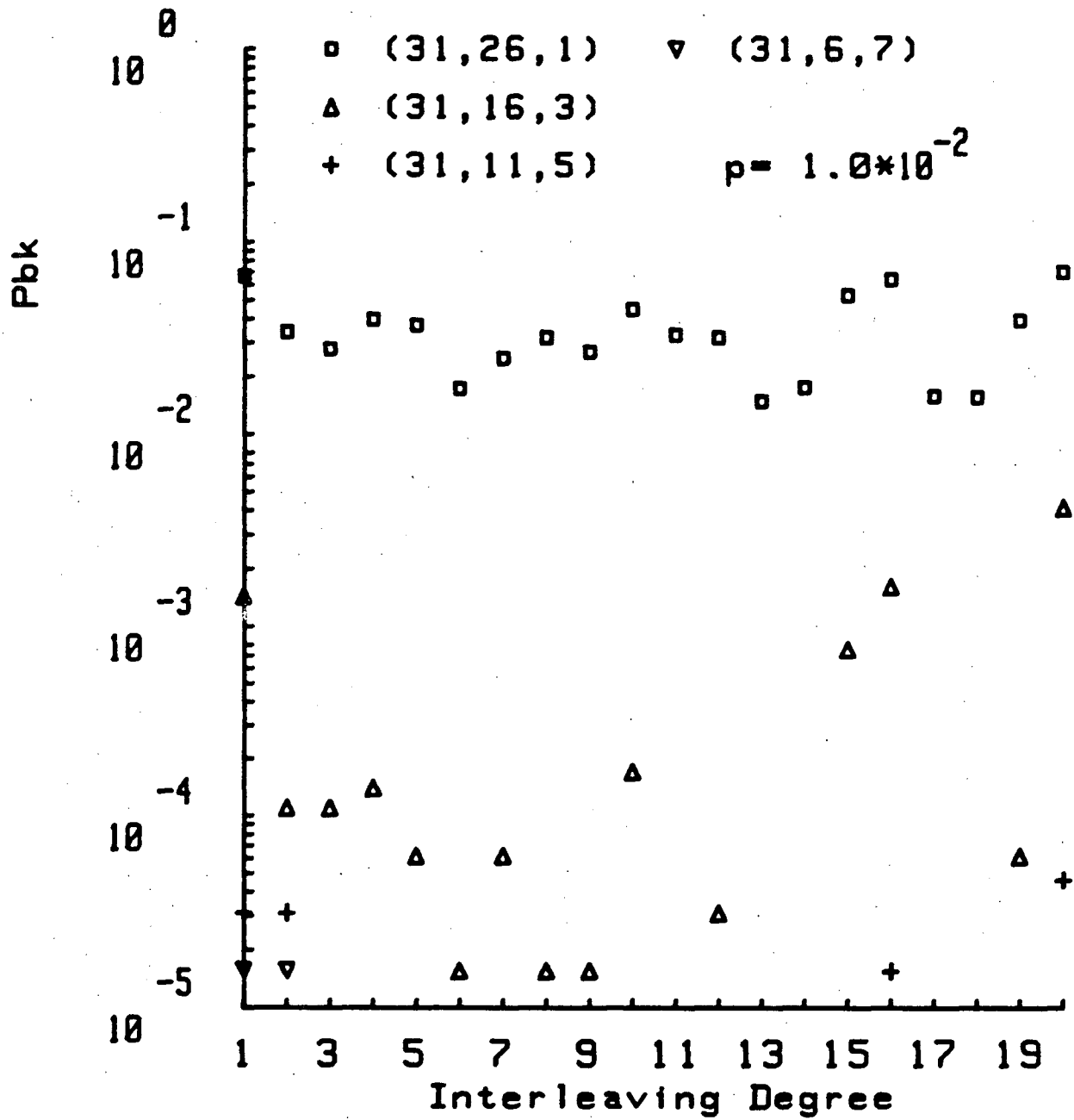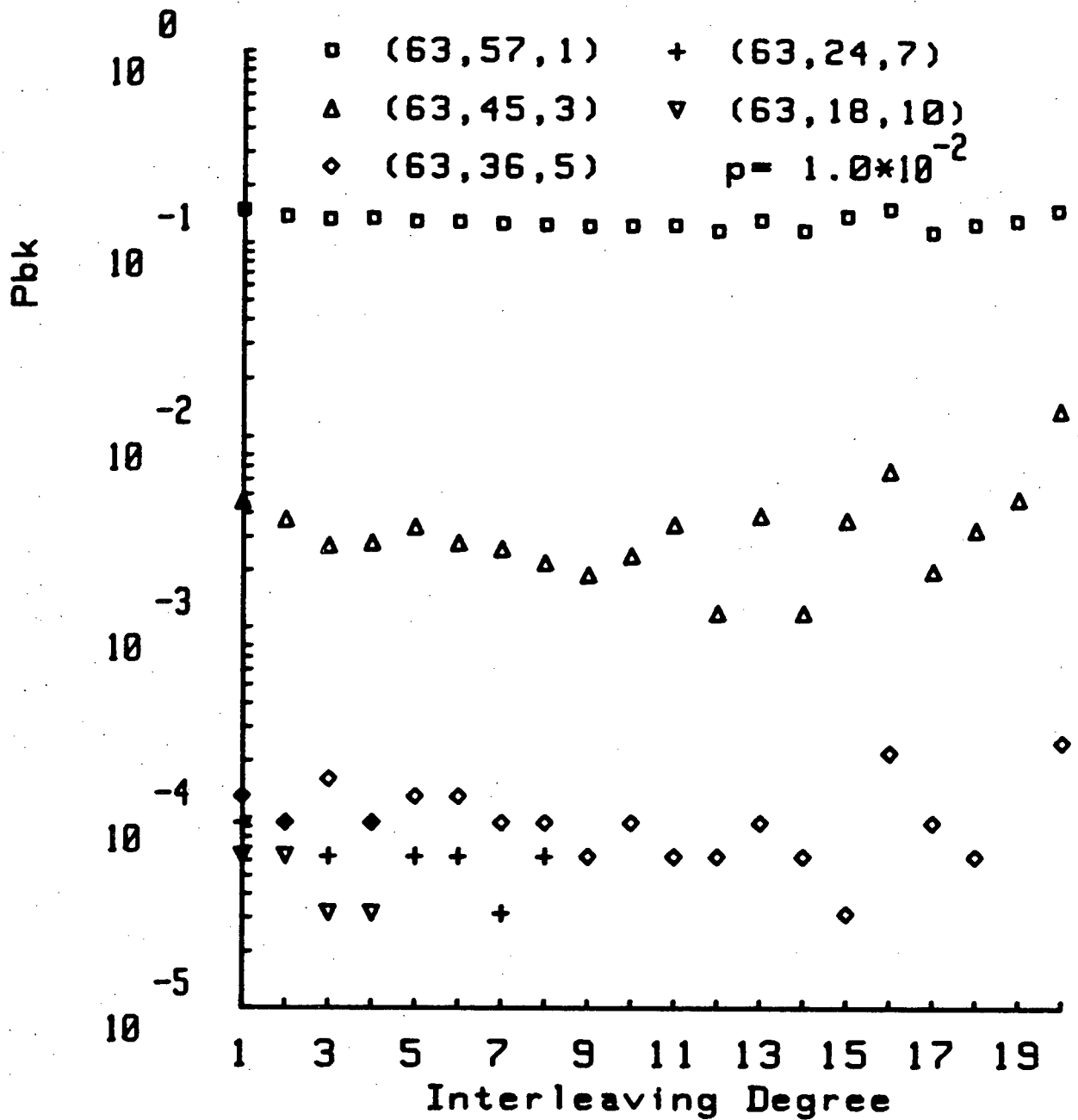Figure 6.5: Block error rate vs. interleaving degree for n=31 BCH codes, impulse channel. Channel bit error rate p=2.7 × 10⁻³.

Figure 6.6: Block error rate vs. interleaving degree for n=63 BCH codes, impulse channel. Channel bit error rate $p=2.7 \times 10^{-3}$.

suitable length and error correcting capability, a short interleaving delay is adequate to enable errors occuring during impulse noise to be dispersed into an adequate number of code blocks for correction. It may not be beneficial to use a much longer period as interleaving over many adjacent periodic noise impulses brings in significantly more errors into the interleaving block, which can reduce code performance. When the interleaver length is inadvertently selected at some multiples of periodic error as indicated by the (63,45,3) code in Fig. 6.6 at interleaving degrees 8, 12, 16 and 20, the error correction performance of this inadequate code is drastically reduced. Since the impulse noise frequency is quite high, a code with a shorter block length is more likely to be adequately interleaved without extending beyond one impulse period. As an example, there are about sixteen n=15 code blocks within one 240 bits long 120 Hz impulse noise period, at 28.8 kbits/s bit transmission rate. For n=63, there are four such code blocks.

The important results from Figs. 6.1-6.6 are summarized in Table 6.2 which shows the minimum value for i, the n(min i) value and the corresponding code rate k/n to obtain $P_{bk} < 10^{-5}$. For the two values of p shown, the required error correcting capability t and the interleaving delay n(min i) needed are less for all n at the lower p value, as fewer errors have to be corrected. The code rate in Table 6.2 increases with n, but so does the n(min i) product. Since decoding cannot begin until all $n \times i$ bits have been received,

| p | n | k | t | min i | n(min i) | k/n |
|---|---|---|---|---|---|---|
| $1 \times 10^{-2}$ | 63 | 24 | 7 | 9 | 567 | 0.38 |
| $1 \times 10^{-2}$ | 31 | 11 | 5 | 3 | 93 | 0.35 |
| $1 \times 10^{-2}$ | 15 | 5 | 3 | 5 | 75 | 0.33 |
| $2.7 \times 10^{-3}$ | 63 | 39 | 4 | 3 | 189 | 0.62 |
| $2.7 \times 10^{-3}$ | 31 | 16 | 3 | 3 | 93 | 0.52 |
| $2.7 \times 10^{-3}$ | 15 | 7 | 2 | 3 | 45 | 0.47 |

Table 6.2: Mininum value for i to obtain $P_{bk} < 10^{-5}$ for BCH codes, impulse noise channels.

a large $n \times i$ value implies undesirable decoding delay and increased storage cost at the transmitter and receiver. A long delay can degrade the response time and throughput of a packet switched data network substantially.

## 6.3.2   Signal Fading

Figs. 6.7-6.10 show the performance of BCH codes when subjected to severe periodic signal fading, as mentioned in Chapter 3. Under this type of rare but severe signal distortion, long error bursts proportional to fade durations occurred. To obtain $P_{bk} < 10^{-5}$ requires interleaving to degree 17 using the (15,5,3) code with $p = 8.8 \times 10^{-3}$, and to degree 9 with $p = 4.4 \times 10^{-3}$. Similarly, to reduce $P_{bk} < 10^{-5}$ needs interleaving to degree 10 using the

Figure 6.7: Block error rate vs. interleaving degree for n=15 BCH codes, fading channel. Channel bit error rate $p=8.8 \times 10^{-3}$.
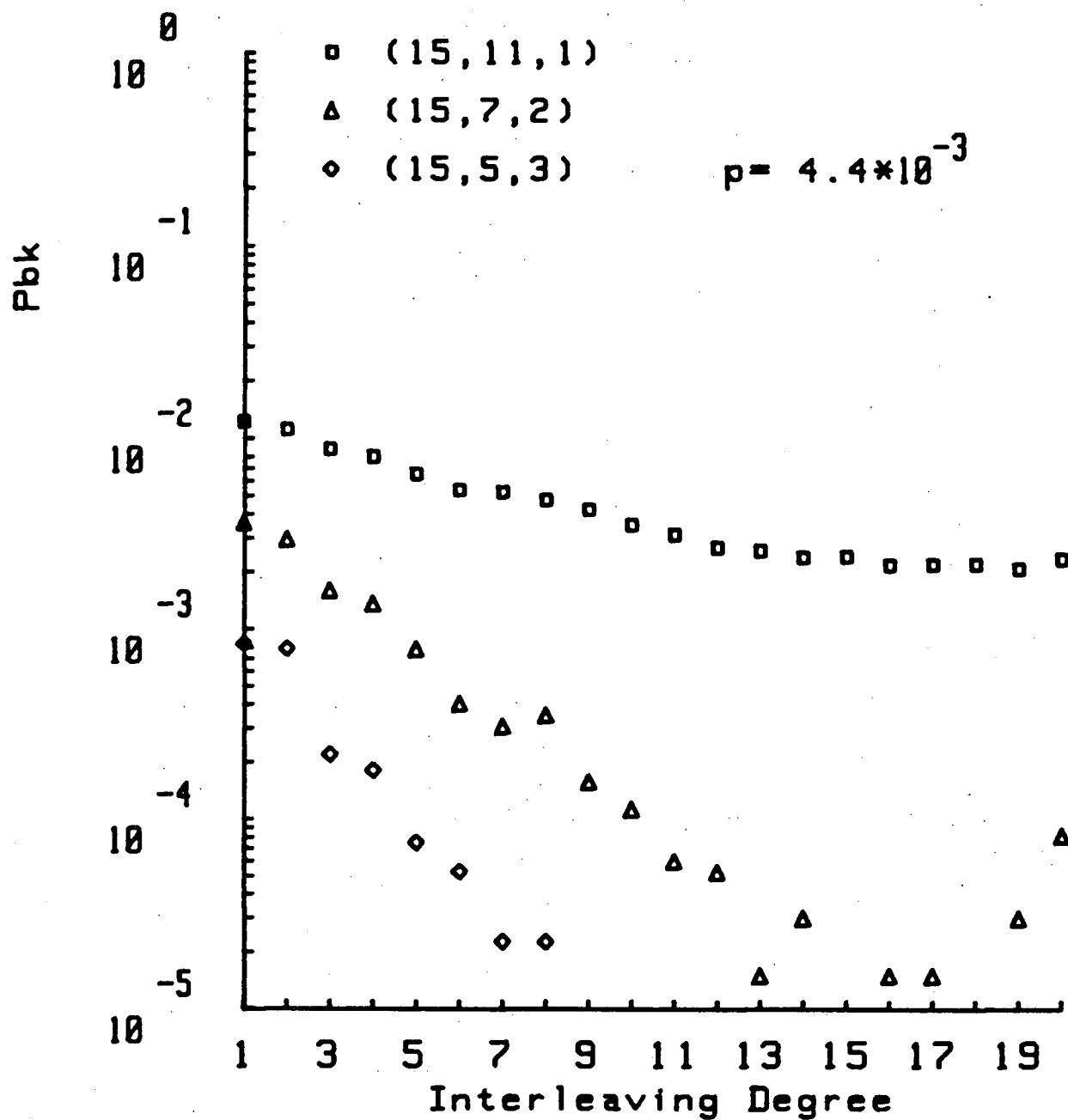
Figure 6.8: Block error rate vs. interleaving degree for n=15 BCH codes, fading channel. Channel bit error rate $p=4.4 \times 10^{-3}$.
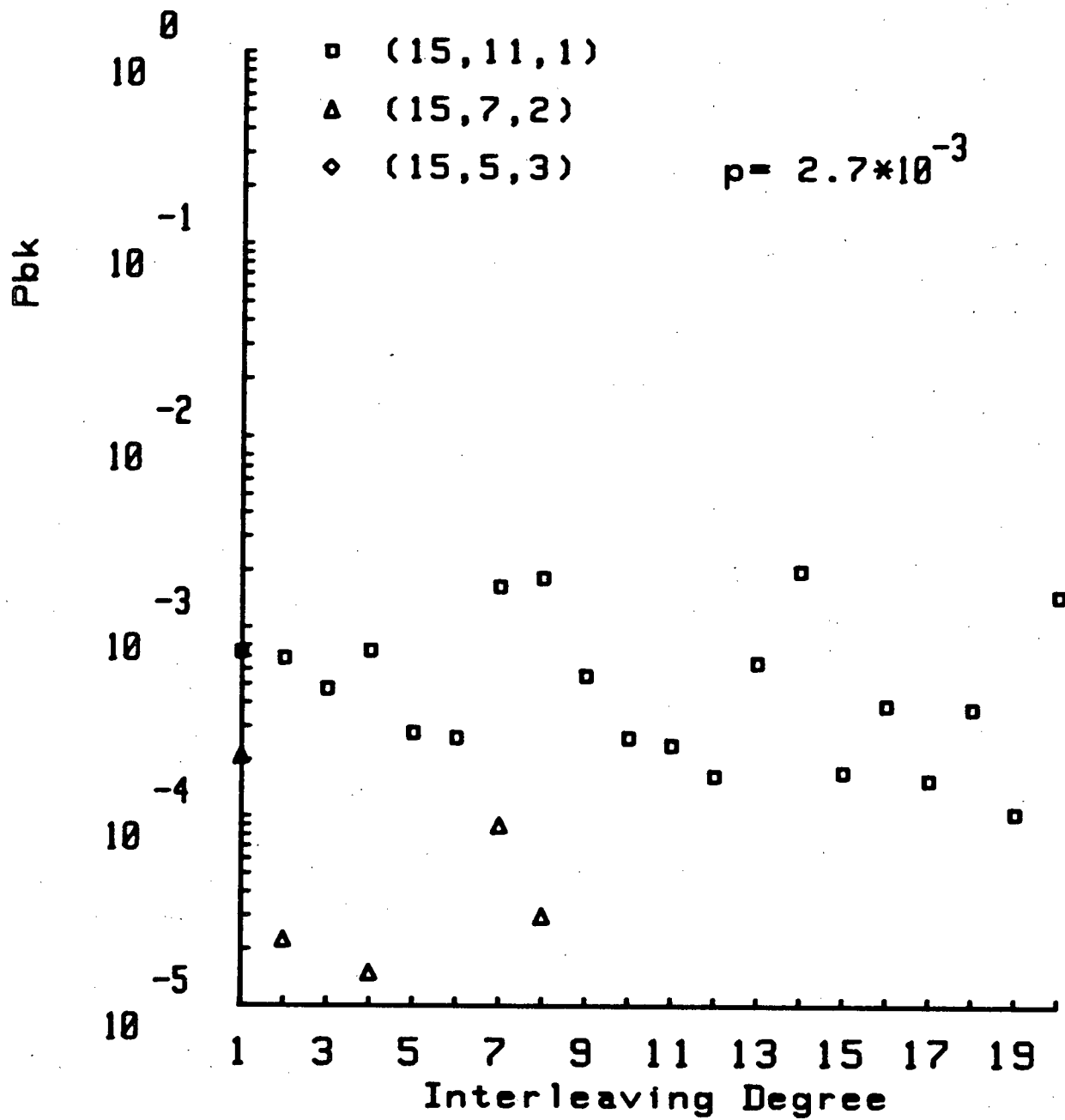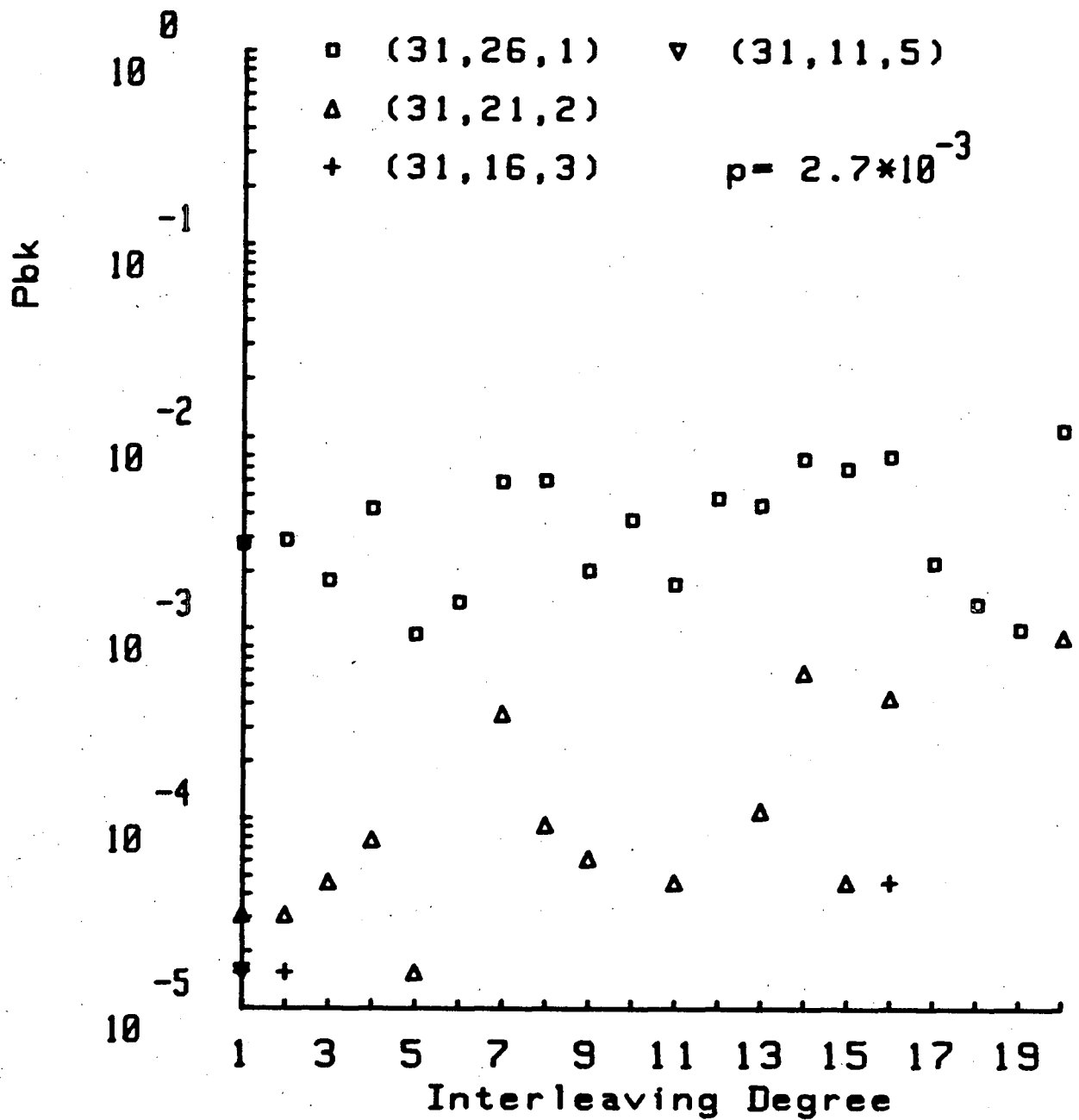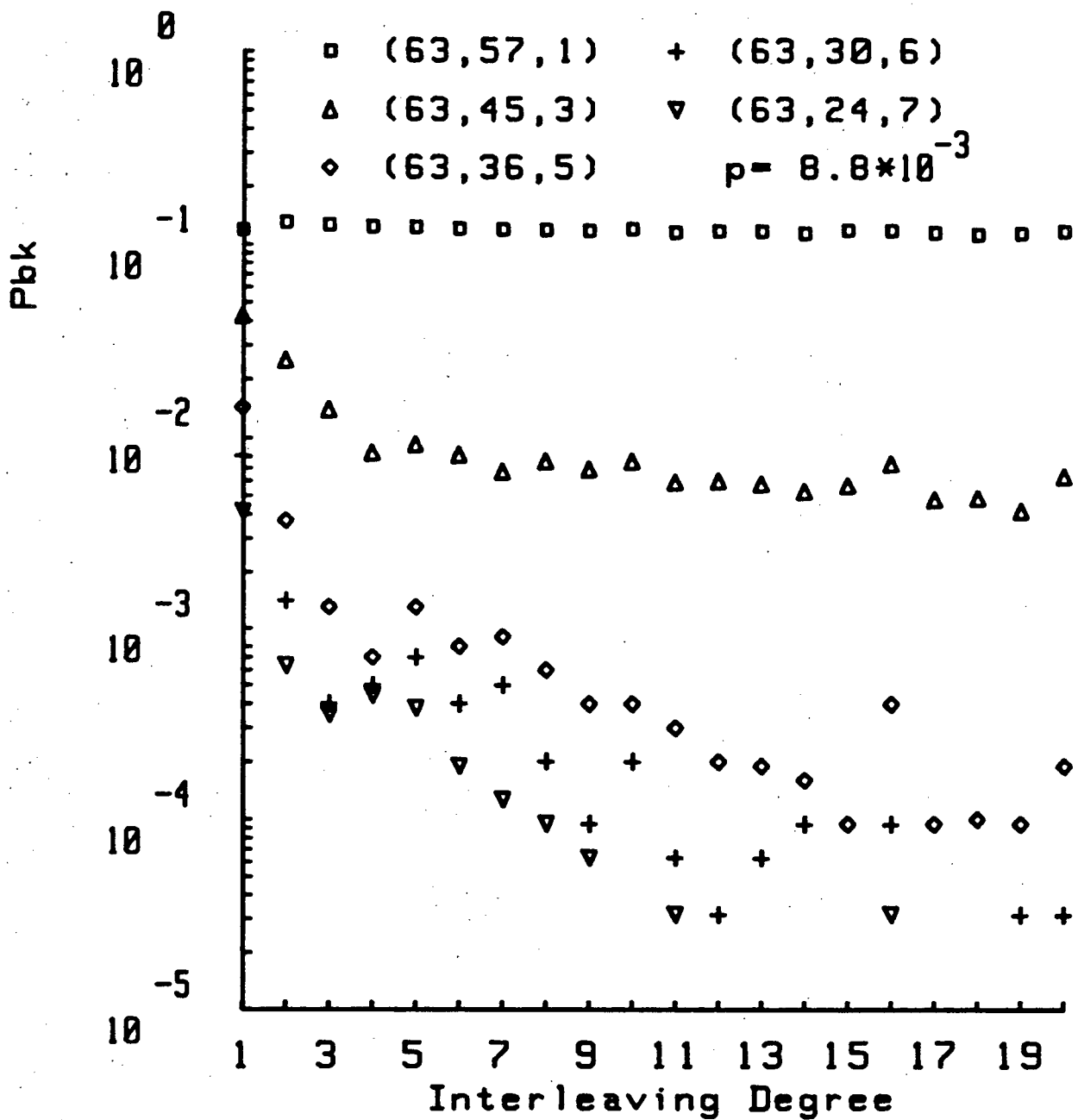
Figure 6.9: Block error rate vs. interleaving degree for n=63 BCH codes, fading channel. Channel bit error rate $p=8.8 \times 10^{-3}$.
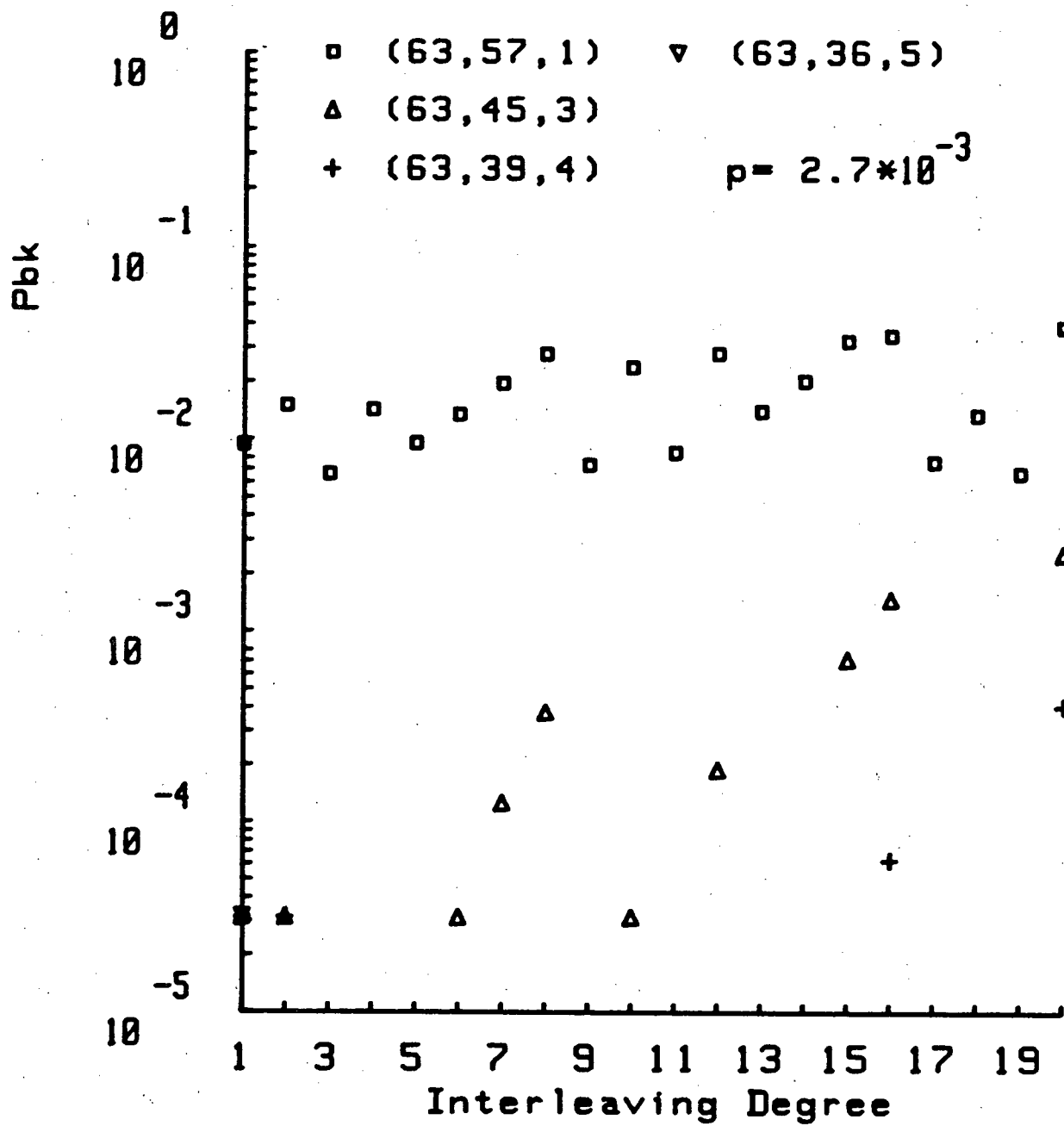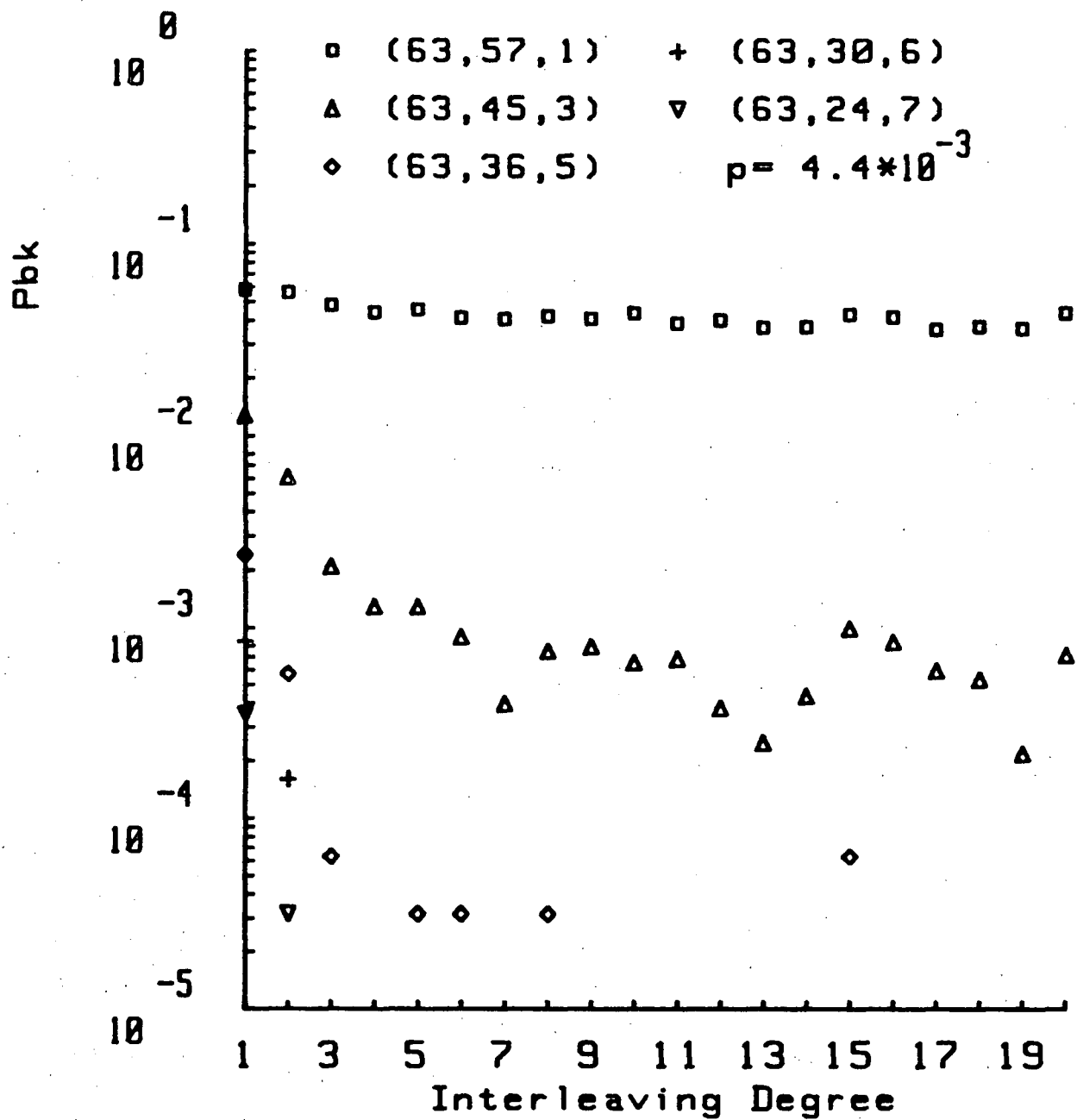
Figure 6.10: Block error rate vs. interleaving degree for n=63 BCH codes, fading channel. Channel bit error rate p=4.4 × 10⁻³.

(63,24,7) code, and to degree 4 using the (63,36,5) code, with $p = 8.8 \times 10^{-3}$ and $4.4 \times 10^{-3}$, respectively.

Also shown in Fig. 6.7 for comparison purposes is the (3,1,1) code. However, because of different block lengths, it would be fairer to compare these codes on an alternative basis. Fig. 6.11 shows the performance of the (3,1,1) code and the (15,5,3) code, on the basis of equal interleaver size (period) I. Under this comparison, the (3,1,1) repetition code is more powerful than the (15,5,3) code for interleaving period up to 180 bits. The short (3,1,1) repetition code can be more adequately interleaved than the (15,5,3) code, even with a short interleaving period. As an example, at interleaving period I=30 bits, ten (3,1,1) codes are interleaved. For the (15,5,3) code, only two such codes are interleaved.

The results of code evaluation when subjected to severe periodic signal fading are summarized in Table 6.3. The repetition code is effective in combating long error bursts encountered during fading with favourable delay characteristics and may be a preferred choice. Both Tables 6.2 and 6.3 also show that improvement in performance can be attained at a much shorter interleaving delay by using a shorter code.
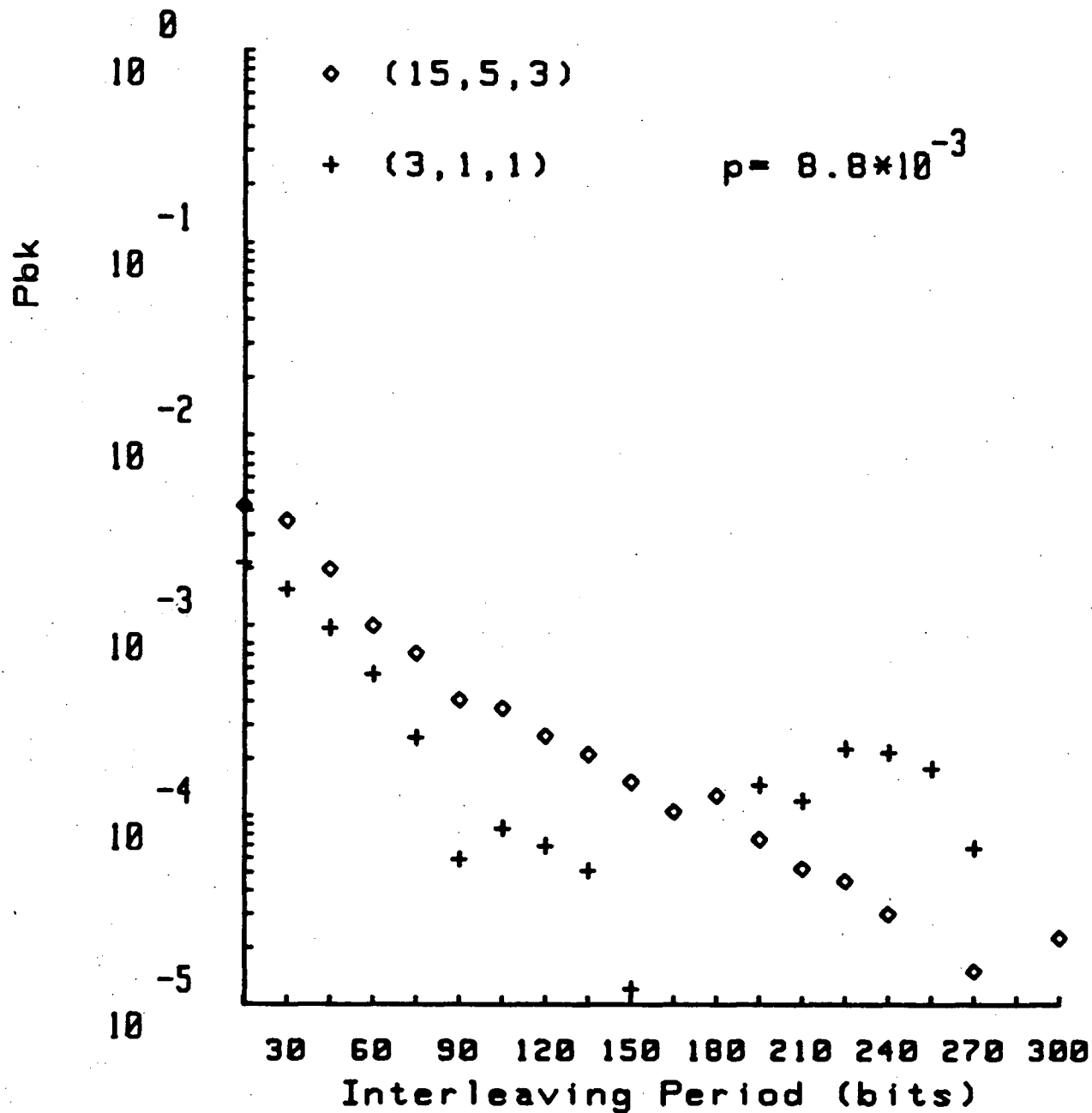
Figure 6.11: Block error rate vs. interleaving degree for n=15 BCH codes and n=3 repetition code, fading channel. Channel bit error rate $p=8.8 \times 10^{-3}$.

| p | n | k | t | min i | n(min i) | k/n |
|---|---|---|---|---|---|---|
| $8.8 \times 10^{-3}$ | 63 | 24 | 7 | 10 | 630 | 0.38 |
| $8.8 \times 10^{-3}$ | 15 | 5 | 3 | 17 | 255 | 0.33 |
| $8.8 \times 10^{-3}$ | 3 | 1 | 1 | 55 | 165 | 0.33 |
| $4.4 \times 10^{-3}$ | 63 | 36 | 5 | 4 | 252 | 0.57 |
| $4.4 \times 10^{-3}$ | 15 | 5 | 3 | 10 | 150 | 0.33 |
| $4.4 \times 10^{-3}$ | 3 | 1 | 1 | 30 | 90 | 0.33 |

Table 6.3: Minimum value for i to obtain $P_{bk} < 10^{-5}$ for BCH codes, fading channels.

## 6.4 Burst Error Correcting Code Performance

As the errors occuring on power line data channels are known to be clustered, the effectiveness of simple burst error correcting codes is of obvious interest since the "burst trapping" decoder for burst correction is one of the simplest decoding procedures available for error correction.

Burst error corrections are shown in Figs. 6.12-6.14. In none of the examples investigated, including those not shown, did the burst error correcting codes perform better than the equivalent (similar length and rate) random error correcting codes. It has been found that burst error correcting
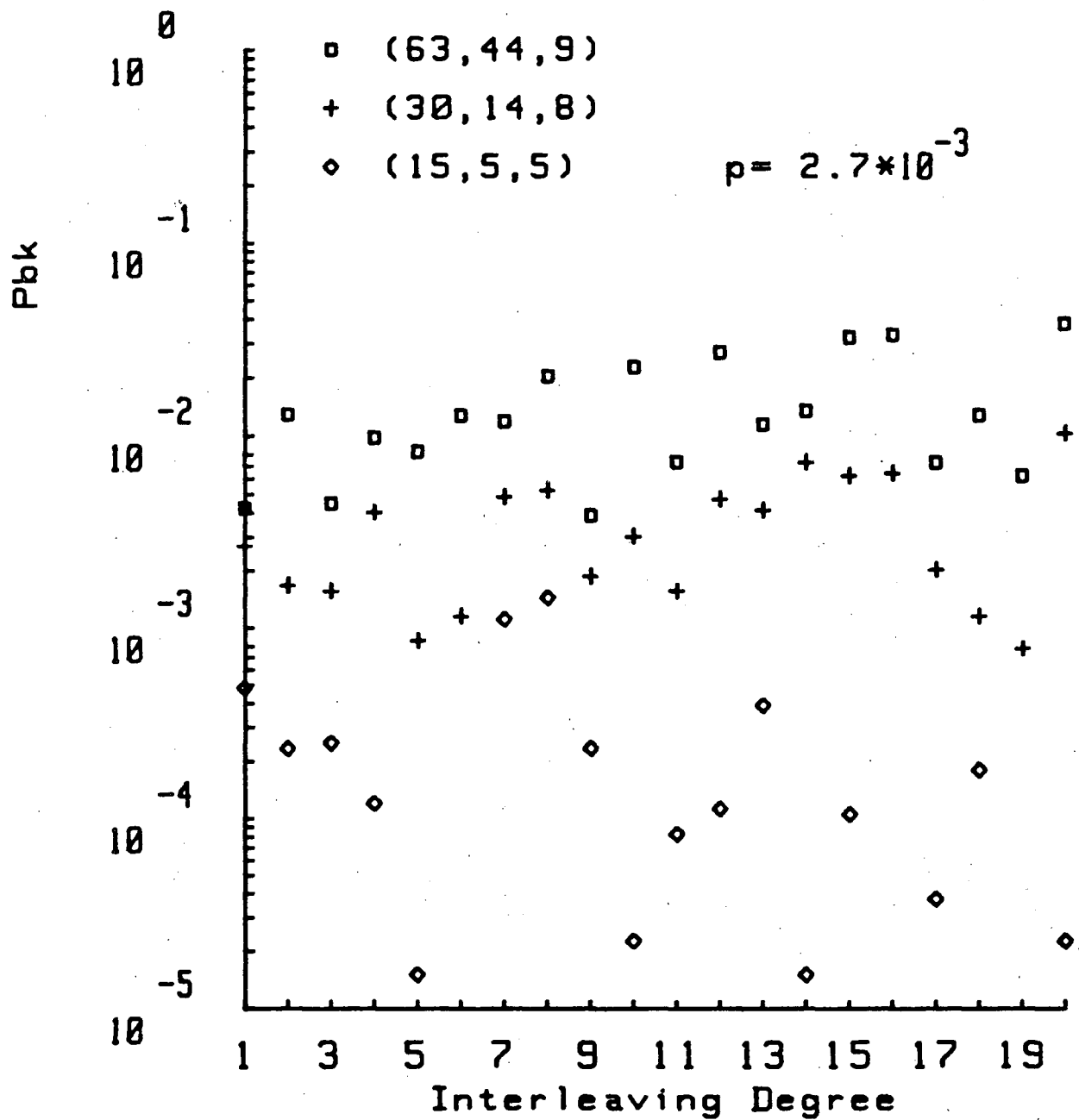
Figure 6.12: Block error rate vs. interleaving degree for burst error correcting codes of various length, impulse channel. Channel bit error rate p=$2.7 \times 10^{-3}$.
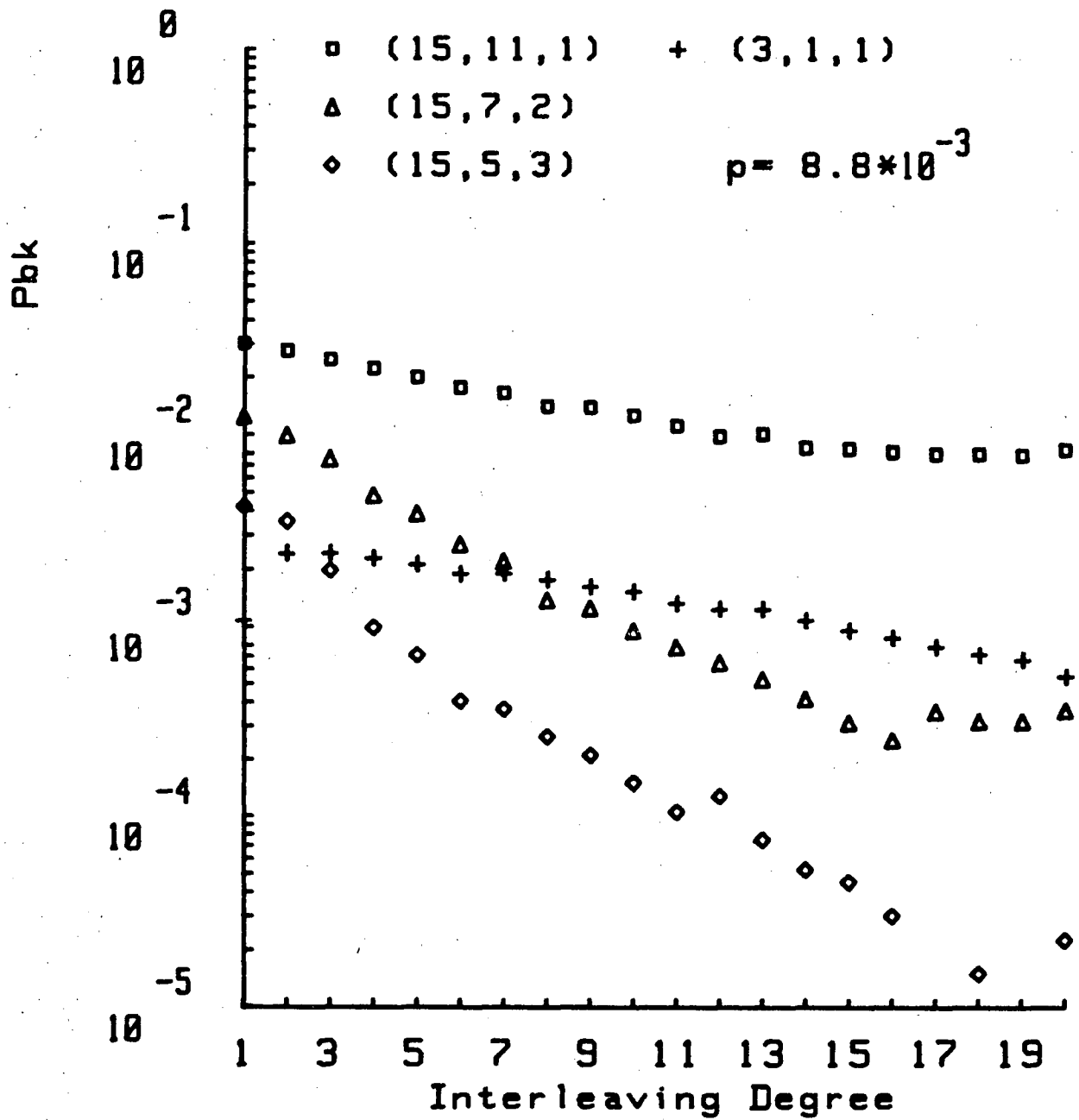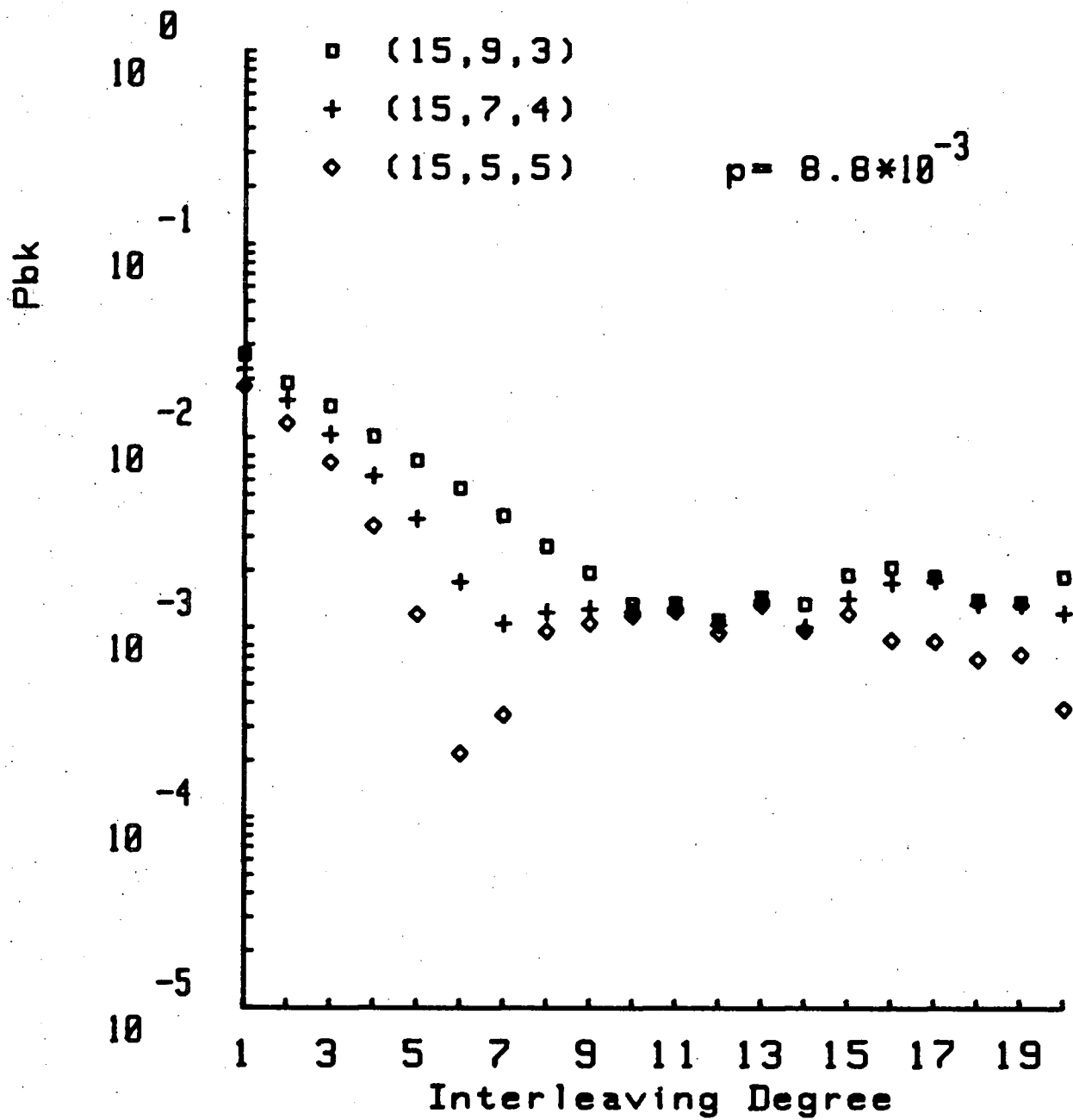
Figure 6.13: Block error rate vs. interleaving degree for n=15 burst error correcting codes, fading channel. Channel bit error rate p=8.8 × $10^{-3}$.
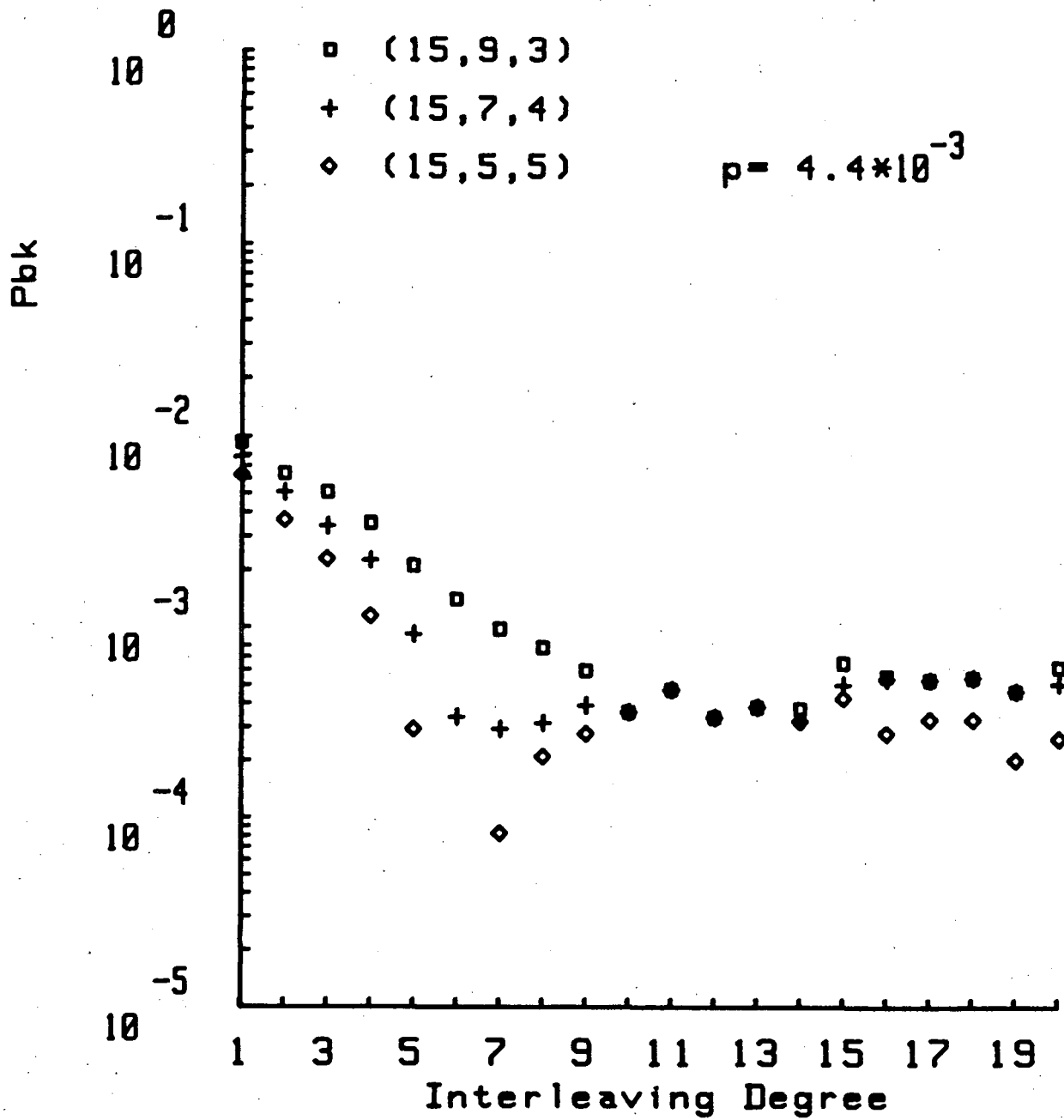
Figure 6.14: Block error rate vs. interleaving degree for n=15 burst error correcting codes, fading channel. Channel bit error rate p=4.4 × $10^{-3}$.

codes are generally no more effective than random error correcting codes, and that with long codes the performance can be significantly worse.

The restricted usefulness of burst codes on power line data channel deserves some explanation. Since burst codes are designed specifically for correcting burst errors, they perform well on the classic bursty channel [15] where error bursts never exceed certain length and are separated by error-free guard spaces which are never shorter than certain length. If even a single-bit error occurs outside the burst correcting span, the burst codes will not yield correct decoding.

On power line channels which may well be better described as "messy" than bursty, these very restricted requirements on burst codes obviously cannot be met. Although power line channel errors are mostly caused by impulse noise, the number of errors the noise impulses produce can become large depending on the impulse strength and duration. At times, impulse noise originating from other phases can become high and starts to cause errors which normally would not occur. Occassionally, fading of the received signal can lead to errors. At a low received signal level, a shallow fade is enough to produce many errors. At a high received signal level, a fade of even quite long duration may not produce errors. Also, single-event impulse noise from lightening and random load switching leads to errors which scatter

themselves through periodic impulse and non-impulse periods.

## 6.5 Summary

The results of the evaluation indicate that a proper combination of a suitable error correction code and appropriate amount of interleaving can provide an inexpensive and effective means to substantially improve the performance of power line data communications. The important effects of parameter variation in code selection have been obtained and summaried below.

When compared on the basis of fixed code rate R and varying block length n, interleaving of short random codes appears to be an attractive and reliable means of improving the reliability of this channel. Since errors appear mostly on a periodic basis, a realistic interleaving period should not be unnecessarily long compared to the period of the impulsive disturbance. As a result of the periodicity, a short code with a moderate amount of interleaving or a moderate long but more powerful code with less interleaving would be the preferred choices. However, a code with a short block length is more likely to be adequately interleaved with a small interleaving delay, providing a very effective and robust coding scheme for the periodic, bursty power line channels.

When compared on the basis of fixed block length n and varying code

rate R, the effect of interleaving is seen to increase with t. However, an increase in t also means a decrease in throughput R. It becomes apparent that a compromise must be made between choosing an adequate value for t and a high enough R when selecting a proper code to use. For a code with inadequate error correcting capability t, interleaving will not help very much. For a code with nearly adequate error correcting capability, interleaving can substantially improve its performance even at a very small interleaving delay. Although increased interleaving will generally improve code performance, depending on the code's correcting capability, it may also reduce the error correction performance at some multiples of the error period when the interleaving block encompasses additional periodic impulses. If a long interleaving length is needed for additional improvement, the interleaver length should be chosen at reasonable distance from multiples of periodicities. For a code with more than adequate error correcting capability, error correction performance improves monotonically with interleaving. The loss of throughput when using excessive redundancy is often too large, however.

# Chapter 7

# Convolutional Coding for High Speed Power Line Data Communications

The performance of error correcting block codes was evaluated in Chapter 6, based on simulations using error pattern statistics measured during field experiments. In this chapter and in [8,9], a number of recent coding applications for power line communications are presented. An actual low cost FEC coded power line communication system was successfully designed, implemented and tested; and real time performance results on typical power lines were determined. Convolutional codes are emphasized. Practical coding gains attained on power line channels were determined for these codes. The results include channel bit transmission rate up to 57.6 kbits/s. It is successfully demonstrated that with suitable FEC coding, reliable high speed

111

data transmission over power lines is feasible, even at very small interleaving delay.

## 7.1 Introduction to Convolutional Coding

### 7.1.1 Encoding of Convolutional Codes

Unlike block encoding in which the data stream is processed in blocks independent of each other, a convolutional encoder processes the information in a continuous fashion. The encoder for a convolutional code accepts k-bit blocks of the information sequence and produce encoded sequence of n-bit blocks. However, each encoded block depends not only on the corresponding k-bit information block, but also on m previous information blocks. Hence, the encoder has a memory of order m. The encoded data stream produced by a k-input, n-output encoder of memory order m is called an (n,k,m) convolutional code. The memory order m also determines the constraint length[1] of the code which for one definition is equal to n(m+1) [25].

For a convolutional code, redundant bits for combating channel impairments can be added to the information sequence when $k < n$. Typically, k and n are very small integers and more redundancy is added by increasing the memory order m or equivalently the constraint length of the code while

---

[1]Several slightly different definitions of constraint length are in use.

holding k and n, and hence the code rate R, constant.

## 7.1.2   Decoding of Convolutional Codes

Unlike block decoding in which the code bits are processed in blocks indenpent of each other, a decoder for a convolutional code has to know the history of the decoded stream before being able to decode a particular bit. In other words, the outcome of decoding a bit influences the decision on subsequent bits. Furthermore, the decoder has to look at subsequent blocks that follow before it can decode a presently received block.

The performance of convolutional codes depends on the techniques used in decoding. The three principal ways of decoding convolutional codes, Viterbi decoding [48], sequential decoding [51], and threshold decoding [29], all have different characteristics. They can be compared on the basis of their error performance, decoding speed, decoding delay, storage requirement, and implementation complexity and cost. The choice depends on the application.

In this thesis, threshold decoding is employed for power line communications. Although threshold decoding achieves slightly lower coding gains than those provided by Viterbi or sequential decoding, its main advantage is that the decoder is much simpler to implement. This makes threshold decoding particularly attractive in low cost applications such as power line

data network, where a reasonably good amount of coding gain is desired at the lowest possible cost. A threshold decoder has a decoding delay of exactly one constraint length; that is, bits received at time unit t are decoded at time unit t+m. Viterbi and sequential decoding, on the other hand, have a decoding delay normally equal to the entire frame or packet length $l$; that is, no decoding decisions are made until the entire frame has been received [25]. Since typically $l \gg m$, the decoding delay as well as the storage requirements are substantial in these cases. For a packet switched data network, this long decoding delay would degrade thoughput considerably. Furthermore, threshold decoding is useful on burst error channels since interleaving and deinterleaving can be included internally in the encoder and decoder [18].

Threshold decoding has been used in numerous practical applications in satellite communications over the INTELSAT digital television system (DITEC), SPACE demand-assigned equipment system and single channel per carrier (SCPC) system [52,53], in terrestial telephone lines and airborne satellite system [38], in troposcatter and HF radio [24].

## 7.2  Codes for the Intrabuilding Power Line Communication Channel

Based on knowledge obtained from the evaluation results on the effects of variation of code parameters and interleaving depth in Chapter 6 on power line channel errors, three convolutional codes from the important and well known classes of self-orthogonal code and diffuse code [25,39] were chosen for implementation and subsequently tested on real power lines for their applicability and performance. The characteristic, capability, and principle of operation of these codes are described below.

### 7.2.1  Self-othogonal (2,1,6) Code

The encoder for this systematic rate 1/2 (2,1,6) code, with generator polynomials given by $g_1(x) = 1$ and $g_2(x) = 1 + x + x^4 + x^6$, is shown in Fig. 7.1. It consists of a shift register of m=6 delay units and n-1=1 modulo-2 adder. The generator polynomials which specify this code determine the connections between the shift register and the modulo-2 adder. At each clock cycle, k=1 information bit enters the shift register, and n=2 encoded bits are transmitted. This code guarantees correct decoding if there are t=2 or fewer errors in a constraint length of received bits [25]. A convolutional code is said to be systematic if the first k bits of each n encoded bits are the actual information

115
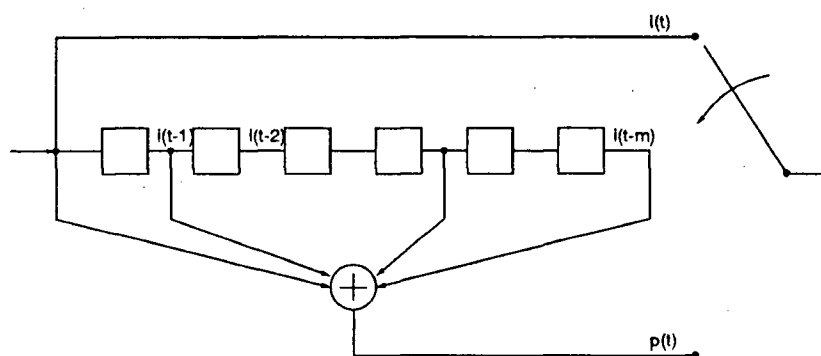
Figure 7.1: An encoder for the (2,1,6) code.

bits themselves.

A threshold decoder for this code is shown in Fig. 7.2. The operation of threshold decoding which was first proposed by Massey [29], is as follows. For a systematic rate 1/2 memory m code, at any time t an estimate $\hat{p}_t(t)$ of the transmitted parity digit $p_t(t)$ is constructed by re-encoding the corresponding received information bits $i_r(t)$. A syndrome bit $s(t)$ is then formed by comparing (modulo-2) the estimated parity bit $\hat{p}_t(t)$ to the corresponding received parity bit $p_r(t)$. These syndrome bits are accumulated in a syndrome register of length m properly connected to a threshold gate. The generator polynomials which specify a code determine the connections between the syndrome register and the threshold gate. When more than half of the inputs to the threshold gate have value 1, the output of the threshold gate is equal to 1. In this case, the leading information bit is estimated to

116
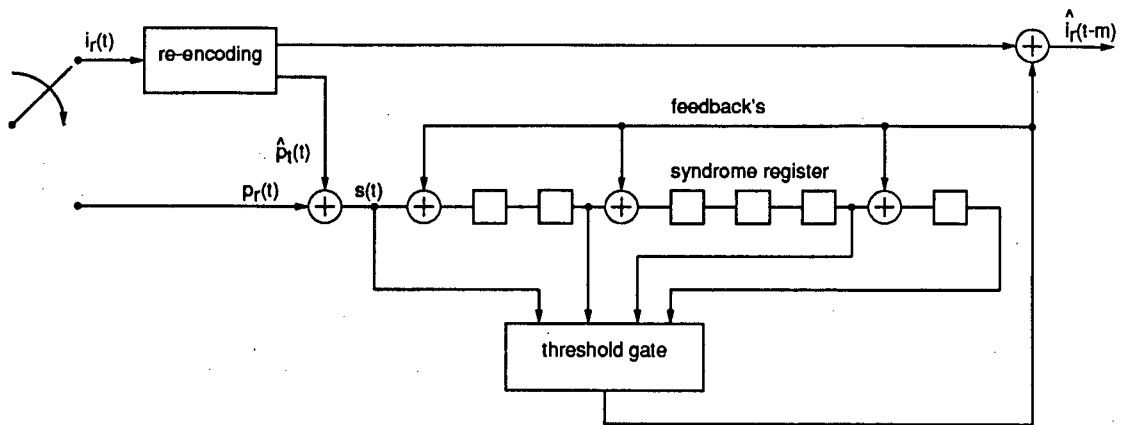
Figure 7.2: An threshold decoder for the (2,1,6) code.

be erroneous and is corrected by adding (modulo-2) to it the estimated error (noise) bit, which is the output of the threshold gate. This estimate $\hat{i}_r(t-m)$ is accepted as the decoded information bit at time unit (t-m) and is delivered to the user. The (2,1,6) code is called a self-orthogonal code since only single syndrome bits, and not sums of syndrome bits are fed to the threshold gate. Self-orthogonal codes form an important class of threshold decodable convolutional codes and are widely used in practice such as in INTELSAT's SCPC systems [52].

The decoder in Fig. 7.2 is said to be a feedback decoder since the estimate of the error bit is fed back to the syndrome register and subtracted from the syndrome to form a modified set of syndrome bits in order to remove the effects of the previously estimated error bits. This modified set

of syndrome bits along with a newly calculated syndrome bit are then used to estimate the next information error bit. Each successive information error bit is estimated in the same way.

In the above discussion of feedback decoding, it is assumed that the past estimates subtracted from the syndrome were all correct. Of course, this is not always true. When post-decoding errors are fed back to the syndrome, this has the same effect as additional transmission errors, and can cause further decoding errors which would not occur otherwise. This is called the error propagation effect. Self-orthogonal codes have the property that if the channel is error-free over a limited span of time units, the effect of past errors on the syndrome is automatically removed, thus halting error propagation [41].

The technique of interleaving short constraint length random error correcting convolutional codes as a practical means of correcting random and burst errors is investigated below. Unlike block codes which make use of a block interleaver, for convolutional codes, the idea is to multiplex the output of i separate encoders with certain constraint length for transmission over the channel. The received bits are then demulitplexed and sent to i separate decoders.

In a practical implementation, the interleaver is placed between the

118

| orginal encoder with each delay unit replaced by an i-stage delay unit |  | (i-1)/2 stages | (i-1)/2 stages | orginal decoder with each delay unit replaced by an i-stage delay unit |

(a)                                    (b)
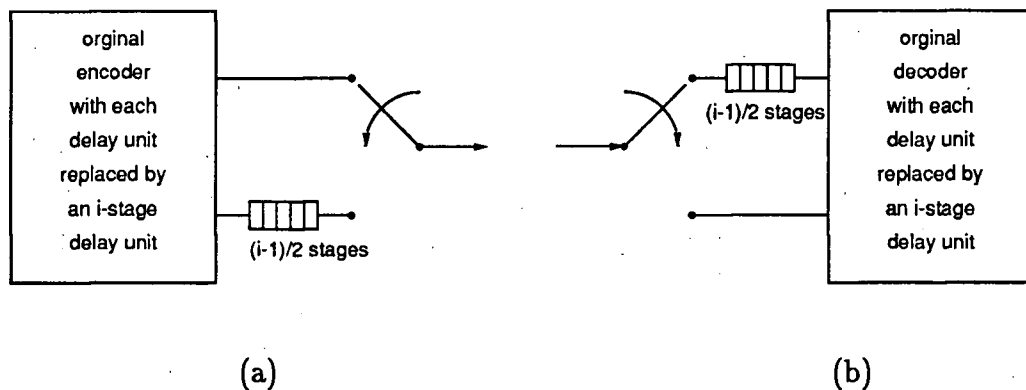
Figure 7.3: The (2,1,6) coder interleaved to degree i. (a) Encoder. (b) Decoder

encoder and the multiplexer, as shown in Fig. 7.3, where i is the interleaving

degree and i-1 is a multiple of n. The interleaver separates the n encoded bits

in a block by i-1 intervening bits prior to transmission over the channel. In

addition, the encoder is modified by replacing each delay unit with a string

of i delay units (an i-bit shift register). This makes the encoder equivalent

to i separate encoders whose n-bit encoded blocks are formed in succession.

The random error correcting (2,1,6) code was chosen for its short con-

straint length. Combined with a reasonable degree of interleaving, this code

is used to combat errors encountered on power line channels.

119

## 7.2.2   Self-orthogonal (2,1,35) Code

The generator polynomials which specify this code are $g_1(x) = 1$ and $g_2(x) = 1+x^7+x^{10}+x^{16}+x^{18}+x^{30}+x^{31}+x^{35}$. This systematic rate 1/2 code guarantees correct decoding of t=4 or less errors within one constraint length of received bits [25]. This code is chosen for its increased error correcting capability at a longer constraint length. Interleaving was not used with this more powerful but moderately long code.

## 7.2.3   Diffuse Code

It has been found in Chapter 6 that simple burst error correcting codes give poor performance when they are used to combat power line channel errors. In this chapter, a rate 1/2 self-orthogonal convolutional code from the class of diffuse codes of Kohlenberg and Massey [24,25,30], designed specifically to correct some burst and some random errors, is considered. The generator polynomials which specify this systematic (2,1,m) diffuse convolutional code with m=3d+1 are given by $g_1(x) = 1$ and $g_2(x) = 1 + x^d + x^{2d} + x^{3d+1}$, where d is any positive integer greater than 1. This code guarantees correct decoding when there are two or fewer random errors in a constraint length of received bits, or when there is a burst of length 2d or less with a guard space of 2(3d+1)=6d+2 [25].

## 7.3 A Power Line Data Communication System

A low cost data communication system for use on intrabuilding power lines was designed, implemented and used to obtain original measurement results of an actual system in operation, with bit transmission rates up to 57.6 kbits/s. A block diagram of the system is shown in Fig.7.4. The system accepts host data over a RS-232C serial computer interface, performs the necessary error encoding and interleaving and passes the encoded bit stream to the scrambler. The scrambler modulo-2 adds the incoming bit stream with a 11th order PN sequence to prevent the occurrence of a series of long "0" or "1" data, and to provide a constant output spectrum. If no provisions are made for the possible sequence of long "0" or "1", the demodulator would lose the bit timing information necessary to process the incoming bit stream. The scrambled data is then carrier modulated to 115 kHz frequency using differential phase-shift-keying (DPSK), bandlimited and power amplified. The amplified signal then passes through the line coupling network and out to the power line network.

At the receiving side, the received modulated signal is differentially detected (demodulated) after being passed through the receive band pass filter (BPF). A block diagram of a conventional DPSK demodulator is shown in
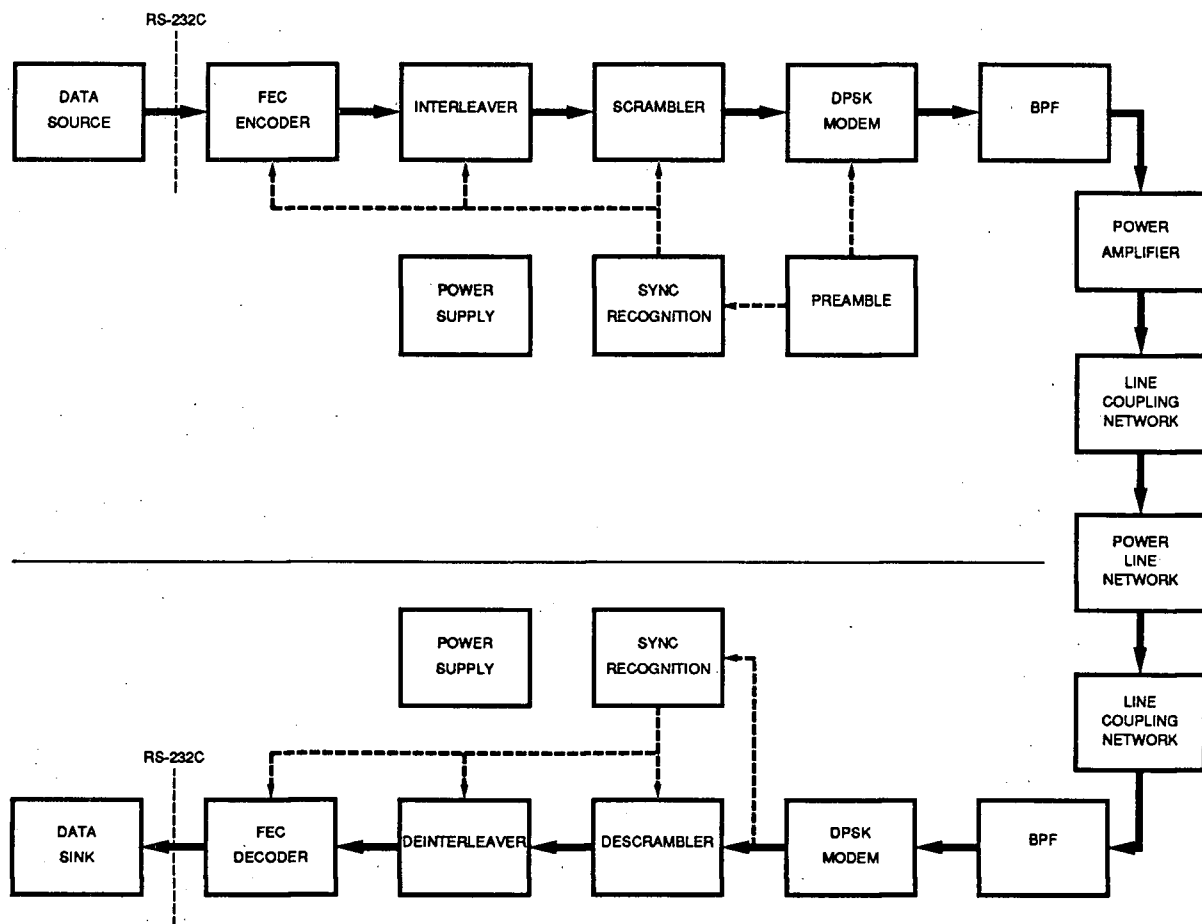
Figure 7.4: A FEC coded power line data communication system.

analog multiplier

received signal

LPF    "eye"    threshold detector    {0,1}

analog delay Tb

analog differential detection

bit clock recovery

(a)

ex-or

received signal    IF hard-limiter

to LPF in (a)

shift register delay

(b)
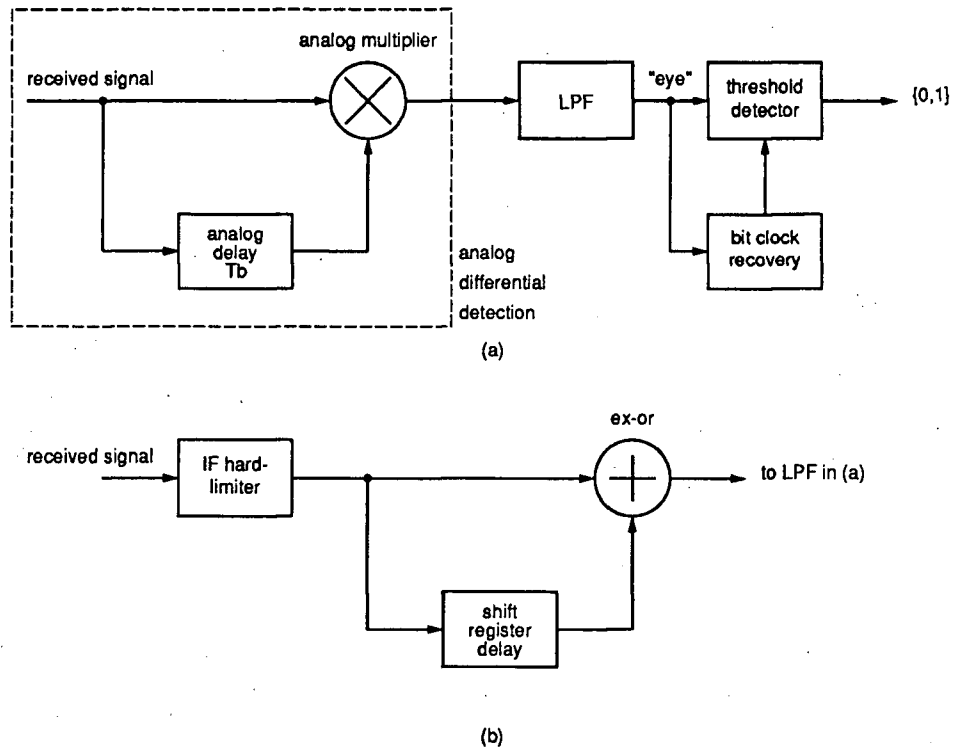
Figure 7.5: (a) A conventional DPSK demodulator. (b) A digital differential detector.

Fig. 7.5(a) [13]. The demodulated signal is low pass filtered by a 4th order Butterworth filter at the bit rate frequency. The output of the low pass filter is then sampled by the recovered bit clock at the centre of the eye (bit intervals) to regenerate the digital bit stream. Instead of using conventional analog differential detection as shown inside the dotted box in Fig. 7.5(a), the received signal is hard-limited by an IF hard-limiter and digitally delayed using shift registers, as shown in Fig. 7.5(b). A clock with frequency much higher than the carrier frequency is used to drive the shift registers. This digital relization of differential detection eliminates the complex and
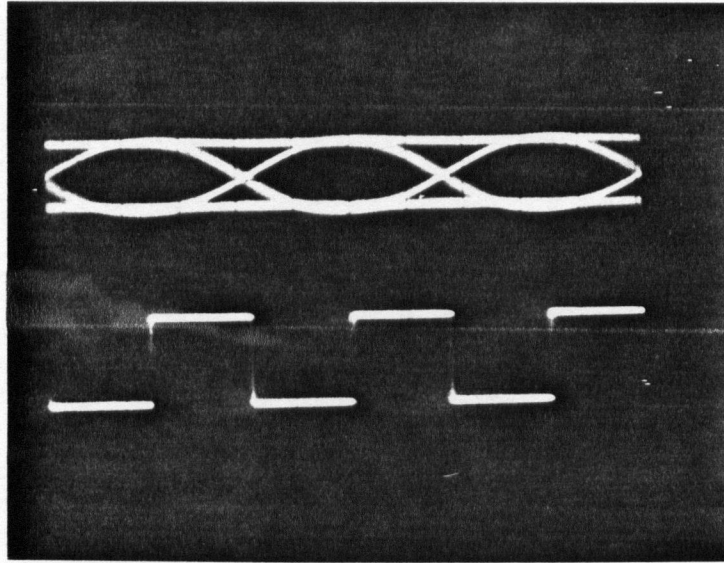
Figure 7.6: Demodulator eye patterns and recovered bit clock.

expensive analog delay circuit and multiplier used by an analog differential detector, and results in a simple low cost robust implementation which facilitates manufacture. In addition, hard limiting the received signal also helps to suppress the effects of impulse noise and signal amplitude variation encountered on power line channels. Fig. 7.6 shows the demodulated eye patterns at the output of the LPF and the corresponding sampling clock from the phase locked loop (PLL) based clock recovery circuit. The use of differential demodulation avoids carrier recovery and achieves fast carrier synchronization and resynchronization, minimizing detection delay and cost critical to a power line packet data network.

The recovered bit stream from the DPSK demodulator is then descram-

bled, deinterleaved, decoded and sent to the receiving host. The band pass filters used are 4th order Butterworth having a measured 3dB bandwidth of 70 kHz, which also determines the receiver noise bandwidth. The coupling network is the same as the one used in Chapters 3 and 4 in which the ac blocking capacitors and the isolation transformer perform 60 Hz rejection and ensure that network devices connected to it are completely isolated from the power line voltage.

## 7.3.1 System Operation

Upon request by the host (holding the Request to Send (RTS) line of the RS-232C interface at a high logic level) to transmit, the system will enter transmit mode if the channel is sensed idle (no carrier is detected). Upon entry into transmit mode, the transmit power amplifier output is connected to the line coupling network by a reed relay and a preamble of approximately 100 bits is sent over the channel. The first part of the preamble acts as a training sequence whose purpose is to allow the intended receiver's bit clock recovery circuit into bit clock synchronization with the demodulated bit stream. The second part of the preamble is a particular 56-bits long PN sequence called the "SYNC" sequence. After this "SYNC" sequence has been sent, the Clear to Send (CTS) line of the RS-232C interface is held high by the system, thereby instructing the host to transmit data. At the same

time, the FEC encoder, interleaver and scrambler are set into operation and in frame synchronization with the intended FEC decoder, deinterleaver and descrambler.

At the receiving site, after this "SYNC" sequence is recognized, the system is in the frame synchronized mode. The descrambler, deinterleaver and the FEC decoder are set into operation. Recovered data from the demodulator output is then descrambled, deinterleaved and decoded before it is sent to the receiving host via the RS-232C interface. During the whole reception period, any RTS is ignored. Thus, operation is half-duplex.

Photographs together with a discussion of the cost of the system appears in Appendix B.

## 7.4 Performance of Uncoded and Convolutional Coded Data Transmissions on Intrabuilding Power Lines

Since the signal transmission characteristic and noise structure of power lines can be extremely complex and load dependent, it is difficult to determine how well a power line communication system will work. Communication signals on power lines are subjected to channel attenuation, distortion, intersymbol interference (ISI), frequency and time fading, and both impulse

and random noise; however, impulse noise is the dominant error source. A realistic test procedure for any power line communication system will involve actual operation on real-world power line channels.

## 7.4.1 Bit Error Rate Performance

The BER versus $E_b/N_o$ performances of the system were obtained, where $E_b$ is the energy per data bit and $N_o$ is the noise power spectral density, as measured at the receiver. The energy per data bit $E_b$ is given by

$$E_b = \bar{V}_s^2/R_D \qquad (7.1)$$

where $V_s^2$ is the received signal power and $R_D$ is the data rate after decoding. The noise power spectral density $N_o$ is given by

$$N_o = \bar{V}_n^2/W_R \qquad (7.2)$$

where $V_n^2$ is the received noise power and $W_R$ is the receiver noise bandwidith. The overbar denotes a time average. A Brüel and Kjaer model 2426 true rms electronic voltmeter was used to obtain all voltage measurements while the BER results were obtained using a Hewlett Packard (HP) 1645A data error analyzer. The transmitter section of the HP 1645A was also used as the data source supplying the pseudo random binary sequence (PRBS) test data. All tests were run until more than 100 bit errors were accumulated.

The exceptions were when some BER measurements reached the $10^{-6} - 10^{-8}$ BER ranges and were stopped regardless of the number of errors.

Fig. 7.7 shows the results of an initial modem test with white noise. The system was subsequently tested on various power line channels. Extensive tests were performed in the Electrical Engineering Building of the University of British Columbia, an industrial/commercial building having a very hostile channel environment for power line communications. The tests were taken across all three phases of the power line network and were run mostly between 9:00 am to 5:00 p.m. during weekdays when the loading of the building's power lines was the heaviest.

Fig. 7.8 shows the results of comparative experiments on the different coding schemes at a decoded data rate of 14.4 kbits/s for an across phase signal transmission path of unknown length in the Electrical Engineering Building. Fig. 7.8 shows that without coding, impulse noise can severely degrade the BER performance and a substantial increase in signal power is required in order to reduce the BER. However, coding substantially reduces BER without increasing signal power. The diffuse code with d=8 is less powerful than the double error correcting self-orthogonal code interleaved to degree i=3 or i=7, and is also less powerful than the four-error correcting self-orthogonal code with no interleaving. The moderate performance of the
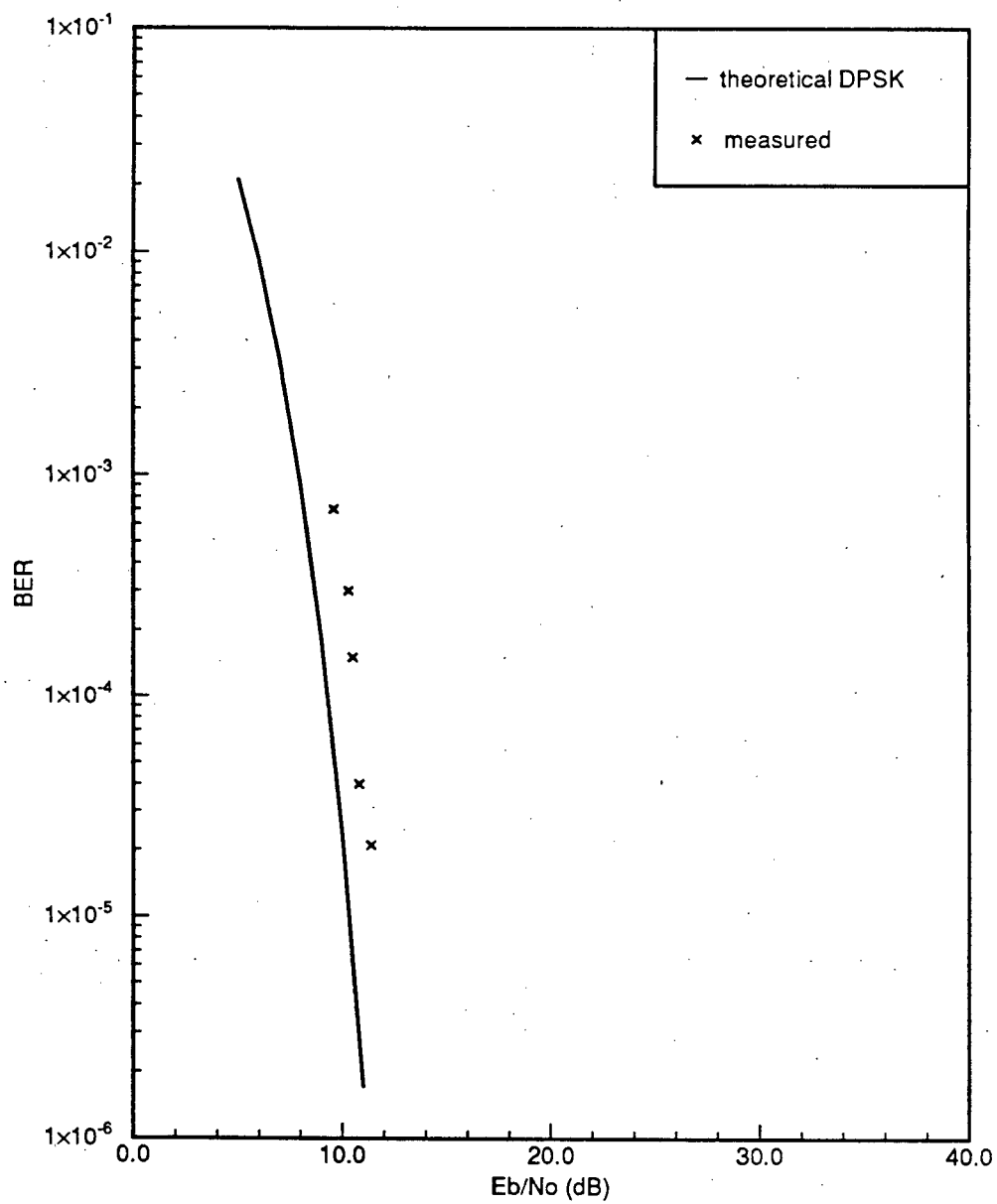
128

Figure 7.7: BER performance for white noise test. Bit rate equals 57.6 kbits/s.
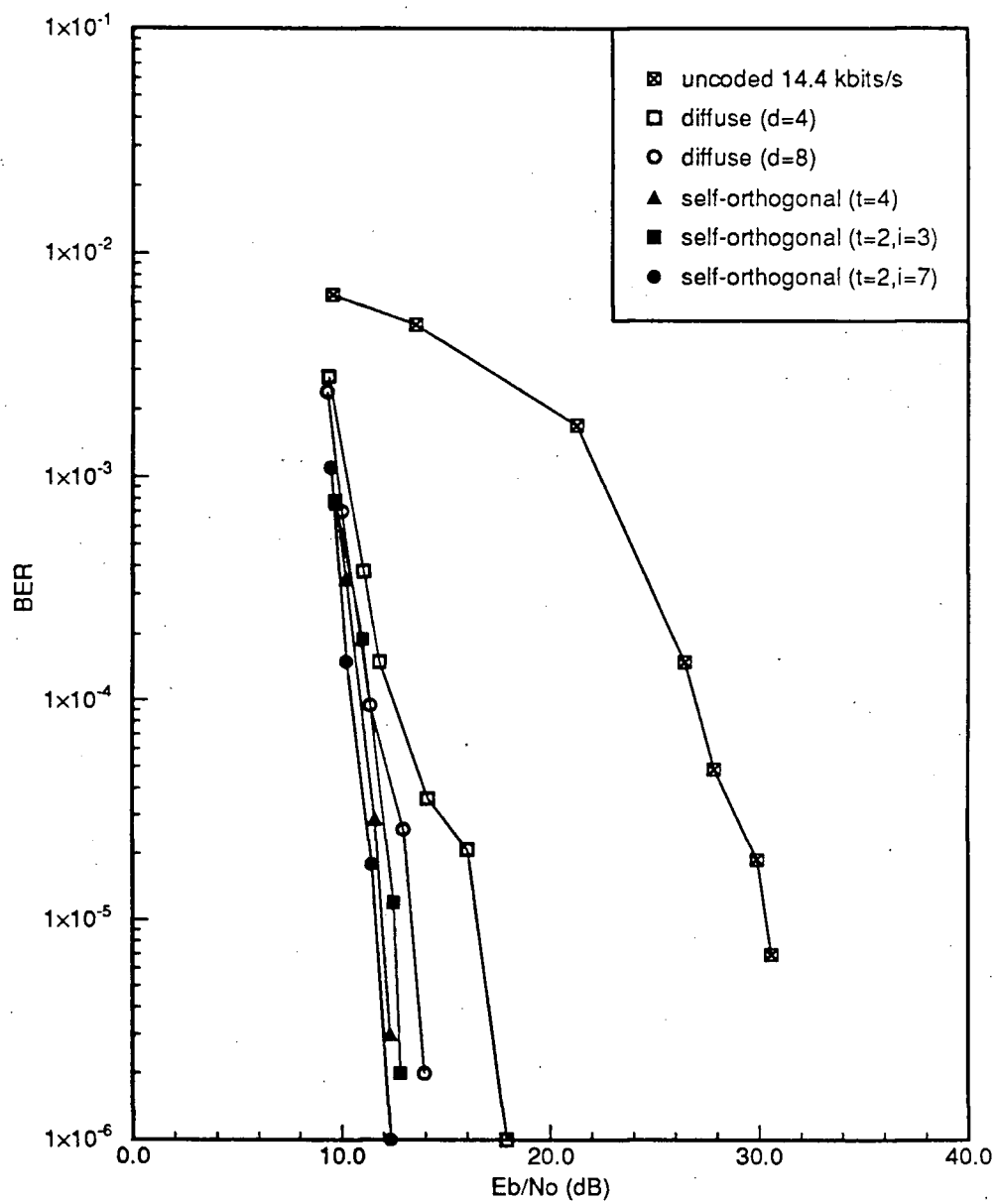
Figure 7.8: Uncoded and convolutional coded BER performances at 14.4 kbits/s data rate.

diffuse code is caused primarily by scattered random errors which occasionally occured with error bursts. Although the diffuse code can handle burst errors, it will not operate properly if a single-bit error then occurs outside the burst error correcting span of the code. A diffuse code with d=8 offers several dB advantage over one with d=4.

Among the five coding schemes shown, the double error correcting self-orthogonal code interleaved to degree i=7 offers the best performance. The more powerful four-error correcting self-orthogonal code with no interleaving is better than the double error correcting code interleaved to degree i=3. The required $E_b/N_o$ to achieve a BER of $10^{-5}$ for the five schemes is in the range of 11 to 16 dB. Compared to uncoded transmission, practical coding gains (the difference in $E_b/N_o$ between coded and uncoded transmissions at a given bit error rate and data rate) from about 14 to 16 dB have been obtained for this particular power line channel, at $10^{-4}$ BER.

Fig. 7.9 shows more BER results, obtained at a decoded data rate of 28.8 kbits/s for another across-phase signal transmission path. The channel bit transmission rate, in this case, equals 57.6 kbits/s. At this higher data rate, the system becomes even more susceptible to impulse noise. Without coding, the required increase of signal power to achieve a sufficiently low BER cannot be tolerated. When compared with Fig. 7.8, the required $E_b/N_o$ to
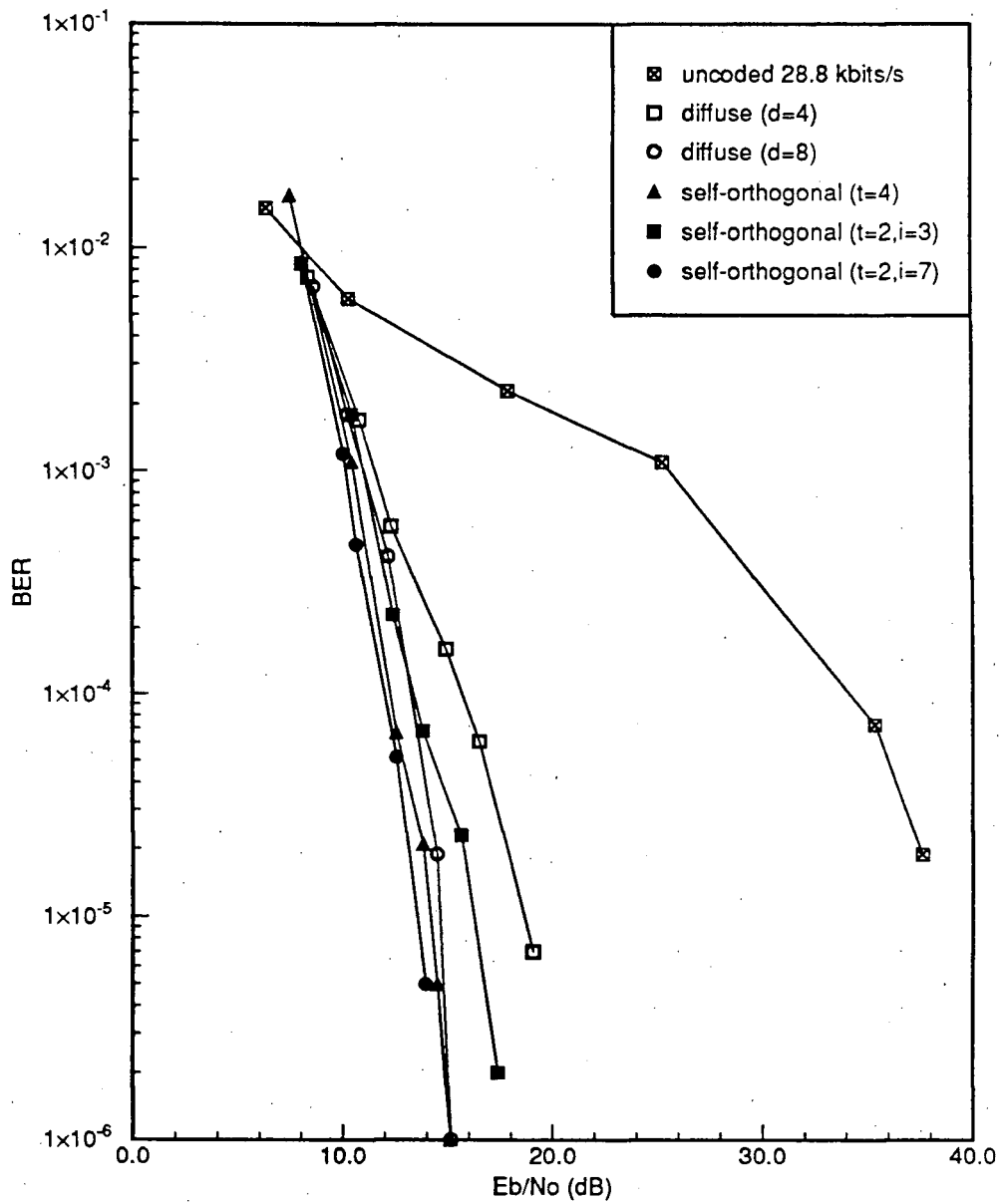
131

Figure 7.9: Uncoded and convolutional coded BER performances at 28.8 kbits/s data rate.

achieve a certain BER is higher for both uncoded and coded transmission. However, with appropriate coding, a larger coding gain from about 18 to 22 dB is attained with coded transmission, at $10^{-4}$ BER. At 28.8 kbits/s data rate, the relative performance of the five coding schemes remains almost the same. In this case, the d=8 burst error correcting diffuse code gives better performance than the double error correcting self-orthogonal code interleaved to degree i=3. It is because the receive signal level required to obtain the same $E_b/N_o$ value increases as the data rate doubles. This higher receive signal level implies that a higher percentage of all errors occurred will be caused by the regular periodic noise impulses and relatively fewer errors by the background disturbances which scattered among the error bursts. This makes the burst correcting diffuse code more effective.

To examine the effect of interleaving on code performance, Figs. 7.10 and 7.11 were obtained for the double error correcting self-orthogonal code which shows the decoded BER as a function of input BER for different interleaving degrees, at channel bit transmission rates of 57.6 kbits/s and 28.8 kbits/s respectively. Fig. 7.10 shows that there is a significant improvement in performance from no interleaving to interleaving degree i=7. For $i > 7$ the improvement becomes more gradual. Although in general, more interleaving (and more interleaving delay) results in better performance, it is more economical to use only a moderate amount of interleaving to take
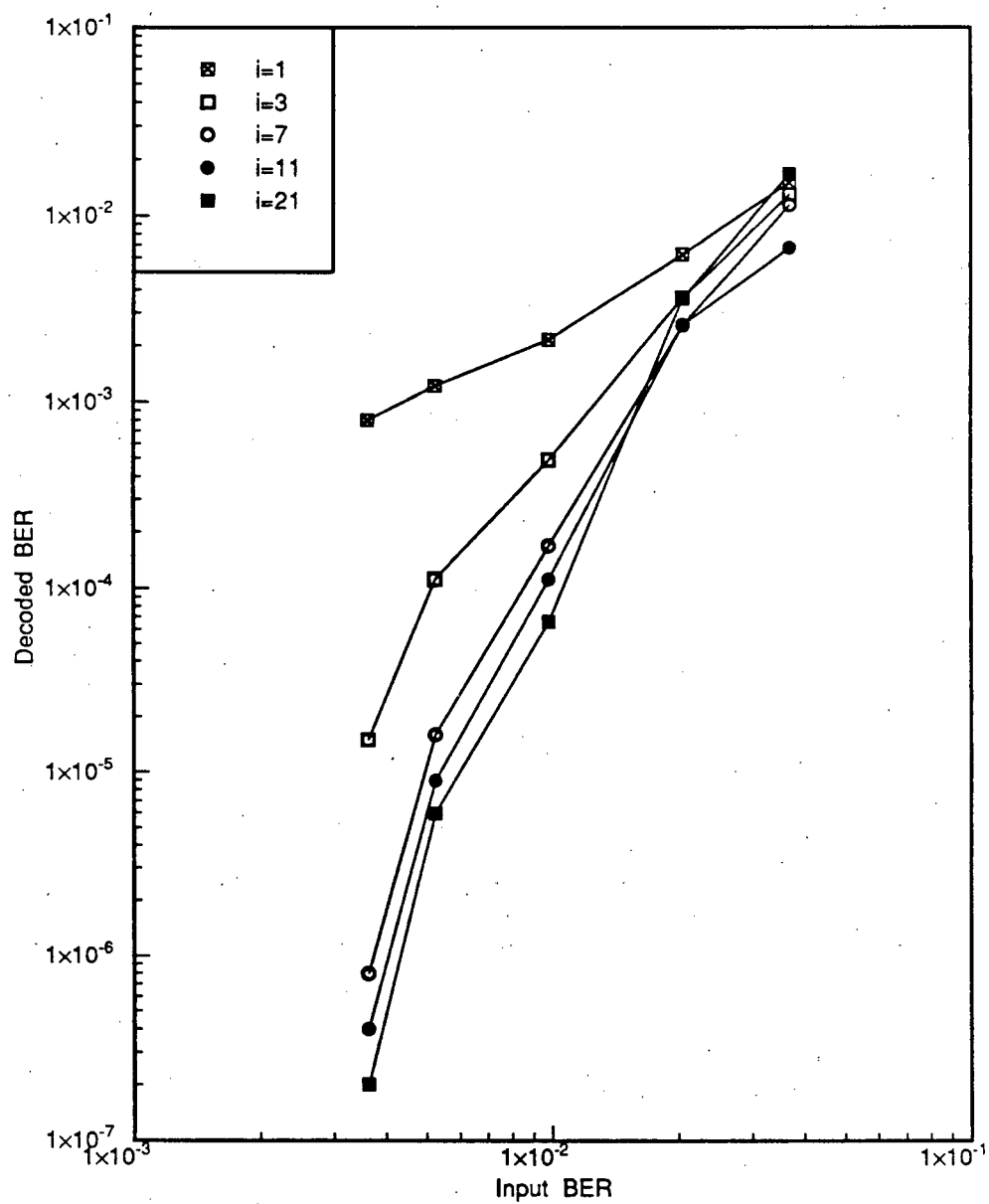
Figure 7.10: Decoded BER vs. input BER for different interleaving degree i at 57.6 kbits/s bit transmission rate.
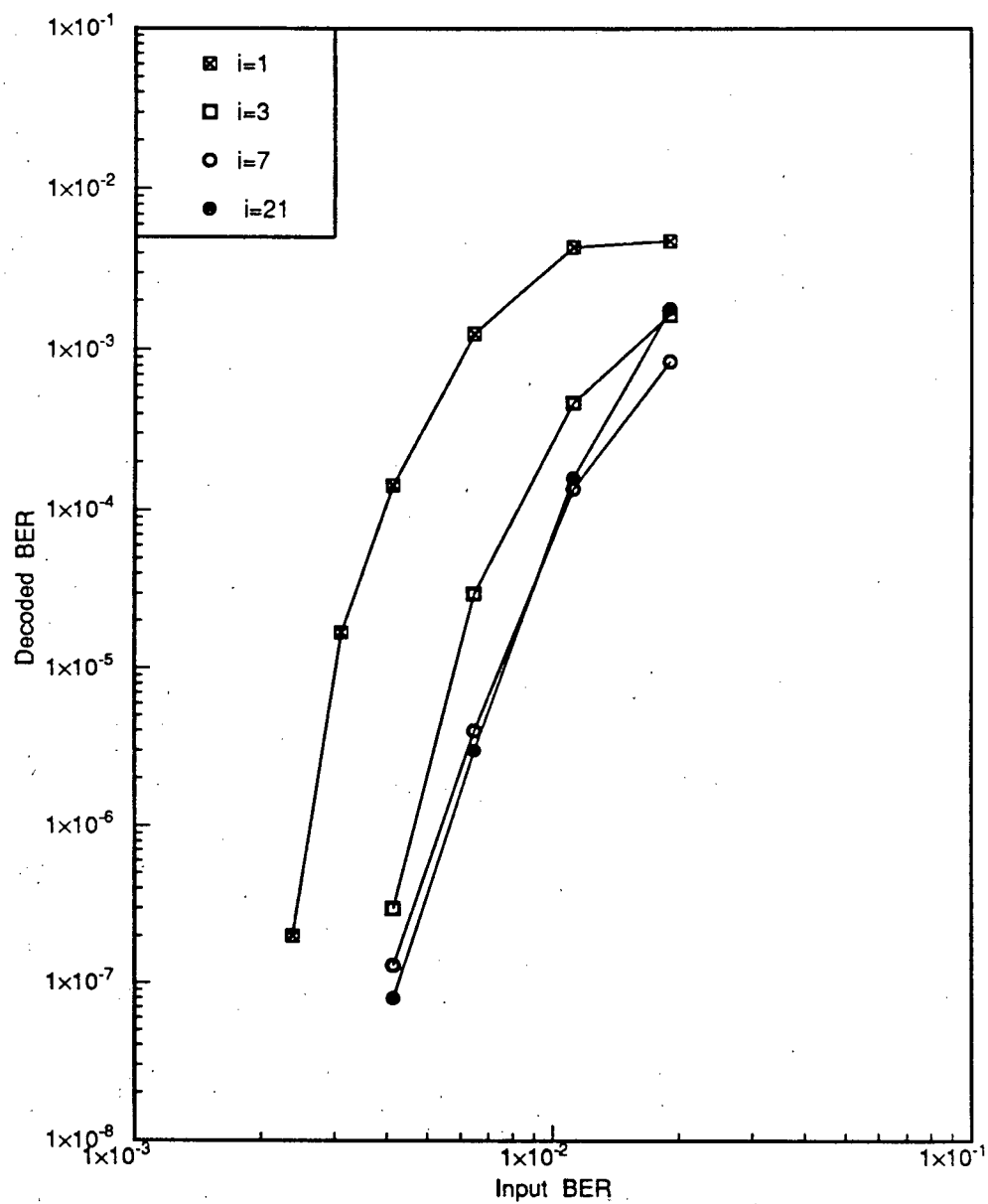
134

Figure 7.11: Decoded BER vs. input BER for different interleaving degree i
at 28.8 kbits/s bit transmission rate.

advantage of the initial large gain in performance improvement at a minimal interleaving delay. Fig. 7.11 shows similar results at 28.8 kbits/s channel bit transmission rate. In addition, this figure also indicates that the use of an excessively long interleaving period degrades the BER at certain interleaving degrees, as revealed in Chapter 6. When compared with Fig.7.10, the decrease in decoded BER is much more rapid with decreasing input BER at this lower 28.8 kbits/s channel bit transmission rate.

Figs. 7.8-7.11 above show the performance of the system under typical power line conditions. In the presence of some very strong noise impulses generated by a light dimmer, the performance of the system was measured and shown in Fig. 7.12. The data rate was 14.4 kbits/s. These curves were obtained under controlled conditions in a single family residence where no specific loads were energized except the light dimmer set at moderate brightness. The transmission and reception were on opposite phases of the house's power lines with the receiver placed on the same power phase as the light dimmer. This light dimmer generated strong 120 Hz periodic impulse spikes with amplitude levels 30-40 dB above the background noise level. The accuracy of signal reception under this badly impaired channel was greatly degraded. When compared with Fig. 7.8 with ordinary noise impulses, the uncoded transmission is very much worse. When appropriate error control codings were used, the system remained unaffected by the strong impulses
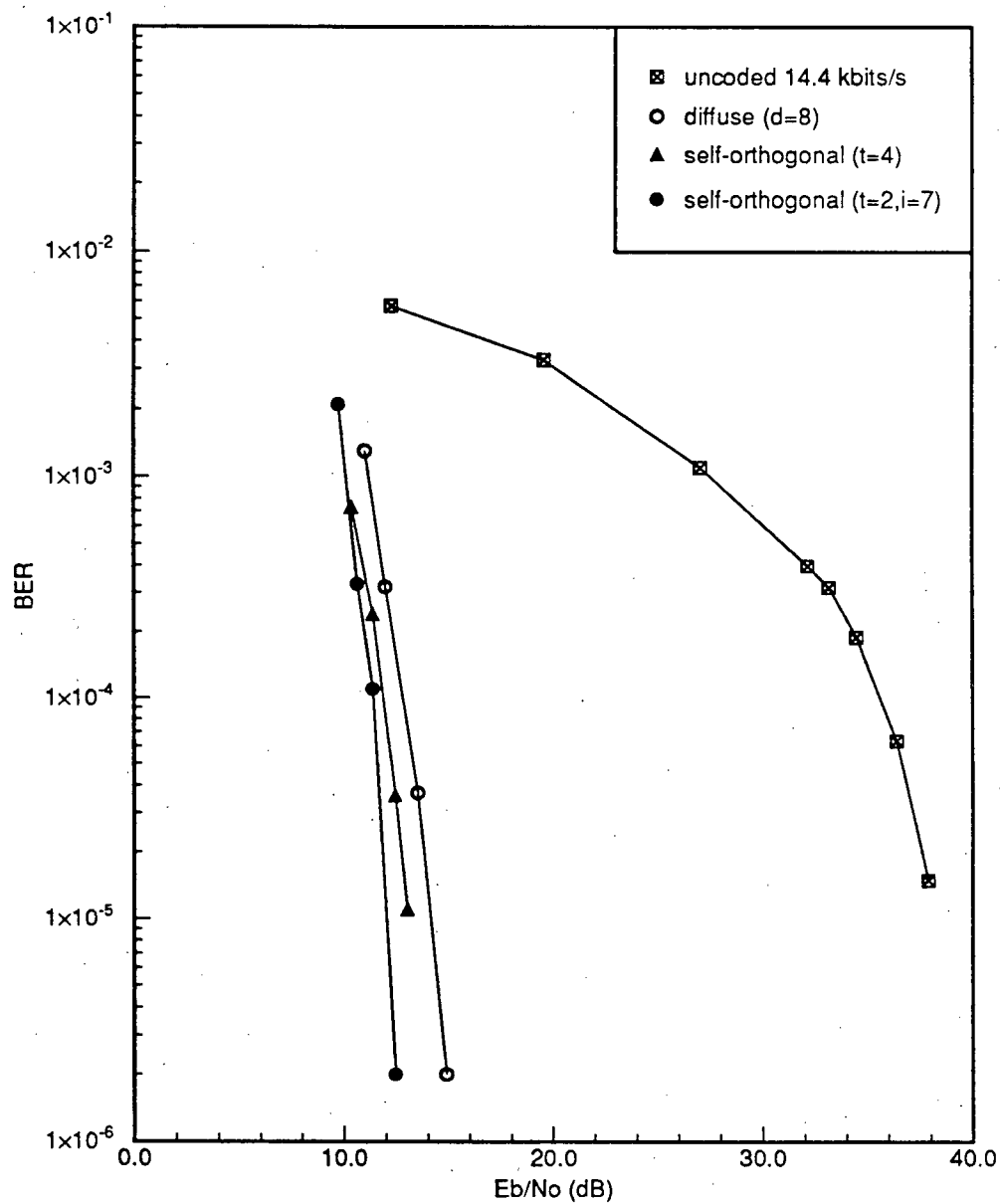
Figure 7.12: Uncoded and convolutional coded BER performances at 14.4 kbits/s data rate, light dimmer active.

and achieved a significant coding gain of about 23 dB at $10^{-4}$ BER. The comparative performance of the three coding schemes used remains unchanged from Fig.7.8. The double error correcting self-orthogonal code interleaved to degree i=7 provides the best protection.

However, at a higher data rate of 28.8 kbits/s, the strong impulses from the light dimmer produced long error bursts. Under this situation, the self-orthogonal code with its four-error correcting capability was inadequate to correct the errors. Its performance became significantly worse than at 14.4 kbit/s. This and other results are shown in Fig. 7.13. The performances of the d=8 diffuse code and the i=7 double error correcting self-orthogonal code are maintained however, even under very severe impulse noise impairments.

## 7.4.2  Correct Reception Rate (CRR)

As pointed out earlier, in data communications, information data are often transmitted in packets. As incorrect packets have to be retransmitted, the rate at which data packets received correctly is another important measure of system performance. A low packet reception rate means long response time and low throughput for a packet data network. Figs. 7.14 and 7.15 show the correct packet reception rate of the system as a function of $E_b/N_o$ with and without coding, at a data rate of 14.4 kbits/s and 28.8 kbits/s,
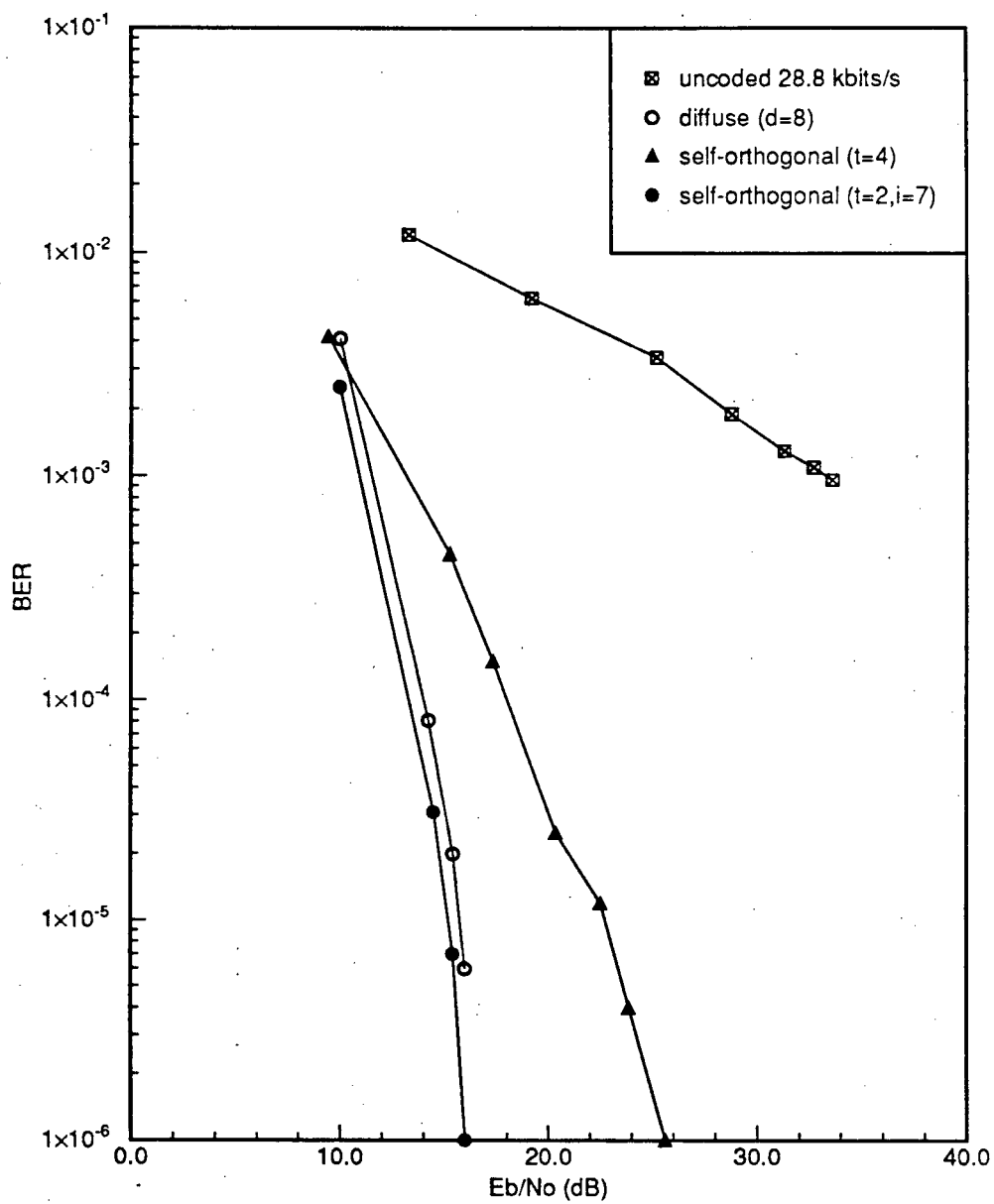
Figure 7.13: Uncoded and convolutional coded BER performances at 28.8 kbits/s data rate, light dimmer active.
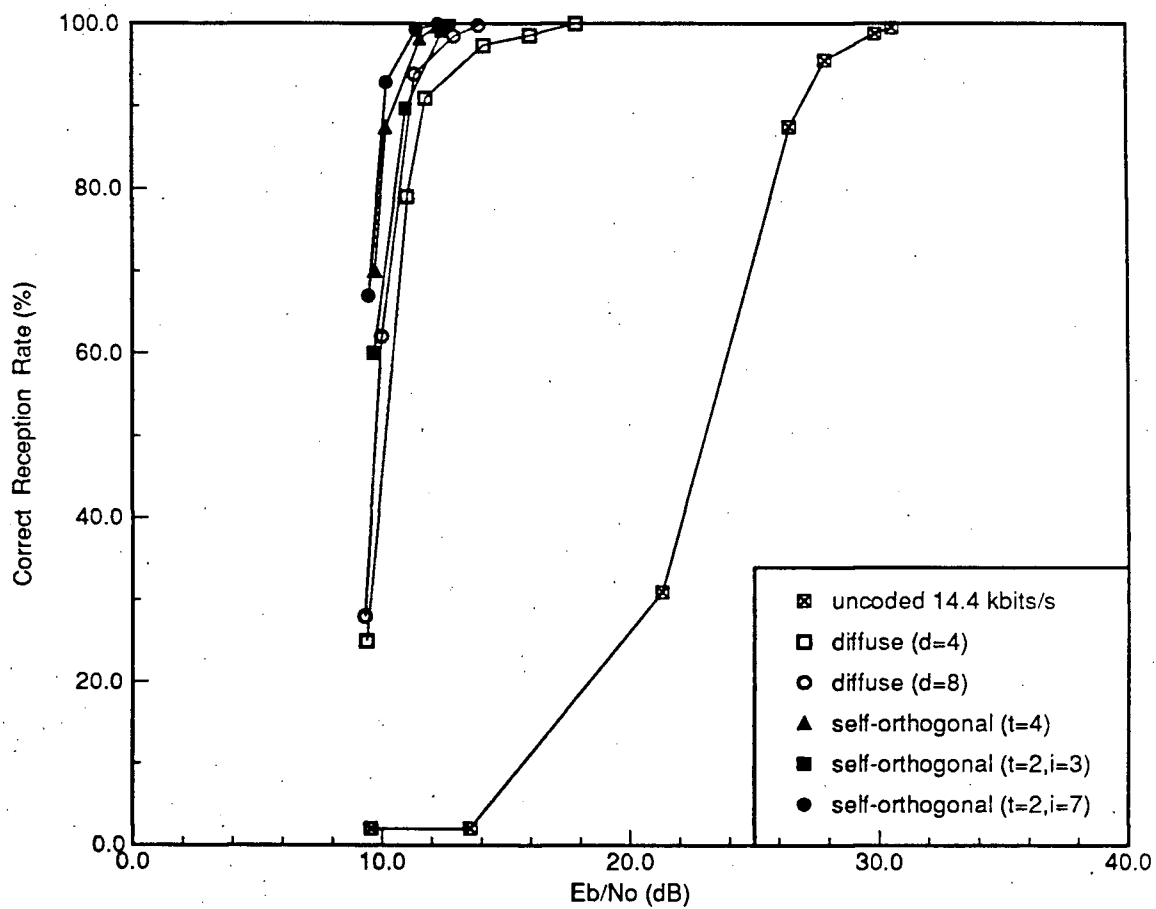
Figure 7.14: CCR for uncoded and convolutional coded transmissions at 14.4 kbits/s data rate.
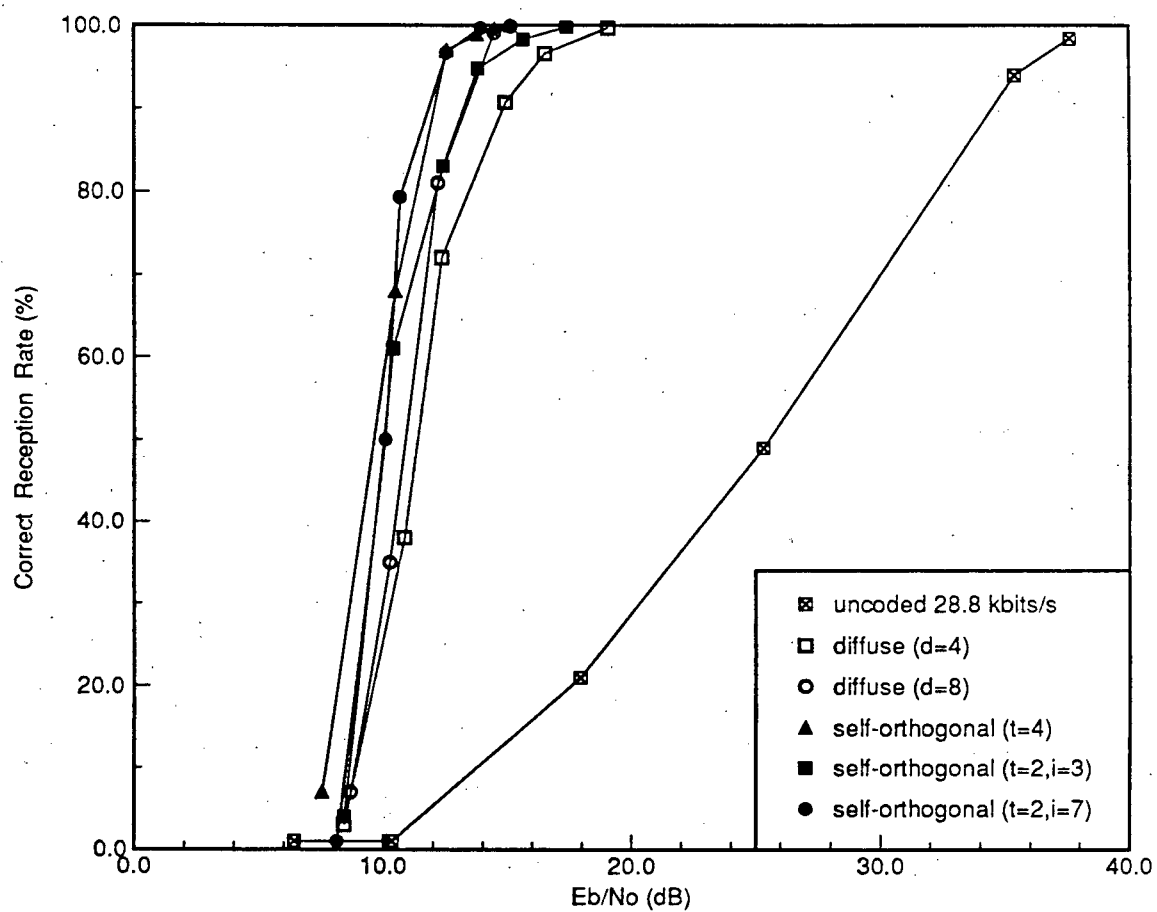
Figure 7.15: CCR for uncoded and convolutional coded transmissions at 28.8 kbits/s data rate.

141

respectively. The packet length was 1000 bits. The channel conditions were that of Fig. 7.8 and 7.9 in which impulse noise and other impairments were causes of errors. At 14.4 kbits/s, Fig. 7.14 shows that for coded transmission, CCR varies from 90-99% when $E_b/N_o$ is equal to 11 dB. However, without coding, it is close to 0%. Similarly, Fig. 7.15 indicates that the required $E_b/N_0$ to acheive a CCR of 90% with coding is in the range of 11 to 14 dB, as compared to more than 30 dB without coding.

## 7.5 Performance of Uncoded and Repetition Coded Data Transmissions on Intrabuilding Power Lines

Interleaved repetition coding discussed in Chapter 5 has been implemented and tested over actual power lines. For simplicity and cost, only hard decision decoding was realized and with a block interleaver of 3 x 8 bits long. A major concern during the implementation was to find a simple practical erasure mechanism.

An approach based on the eye opening of the demodulated bit stream from the digital DPSK receiver was used. Impulse hits caused severe closings of the eye which would otherwise be wide open. Because of this close correspondence between impulse noise and eye opening, a recovered code bit

142

was considered unreliable if during the sampling instant the eye level was below a certain threshold. A channel status bit was turned on to indicate this situation. Both the recovered code bit and the channel status bit were deinterleaved and passed to the decoder. The decoder could then make use of the channel status information to erase an unreliable code bit from the majority logic decoding process.

Figs. 7.16 and 7.17 show the BER performance of repetition coding at decoded data rates of 19.2 kbits/s and 9.6 kbits/s respectively with or without using erasure. The measurements were taken in the Electrical Engineering building on two across-phase signal transmission paths. These results agree sufficiently well with the theoretical calculations as shown in Fig. 5.1. The results show that even with limited interleaving, significant improvements in performance are achieved, although they are less than those provided by the convolutional codes. As predicted in Chapter 5, the measured performance of the three bit repetition code with and without erasure are almost the same for hard decision decoding. One would expect additional gains to be achieved if soft decision and erasure are used, as shown in Chapter 5.

The threshold setting used for erasure was found to be uncritical and could easily be set midway between wide opening and closing of the eye, for
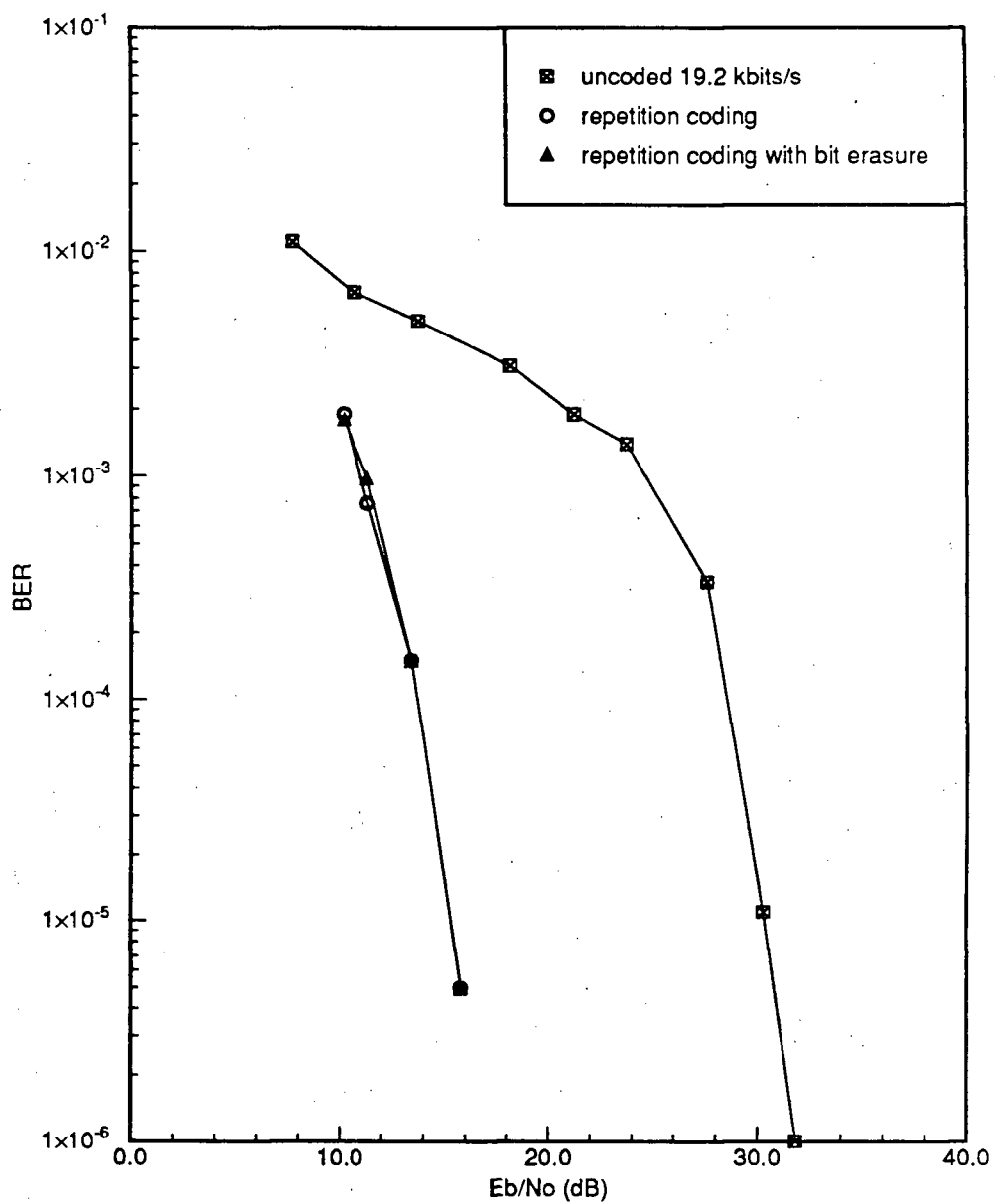
Figure 7.16: Uncoded and repetition coded BER performances at 19.2 kbits/s data rate.
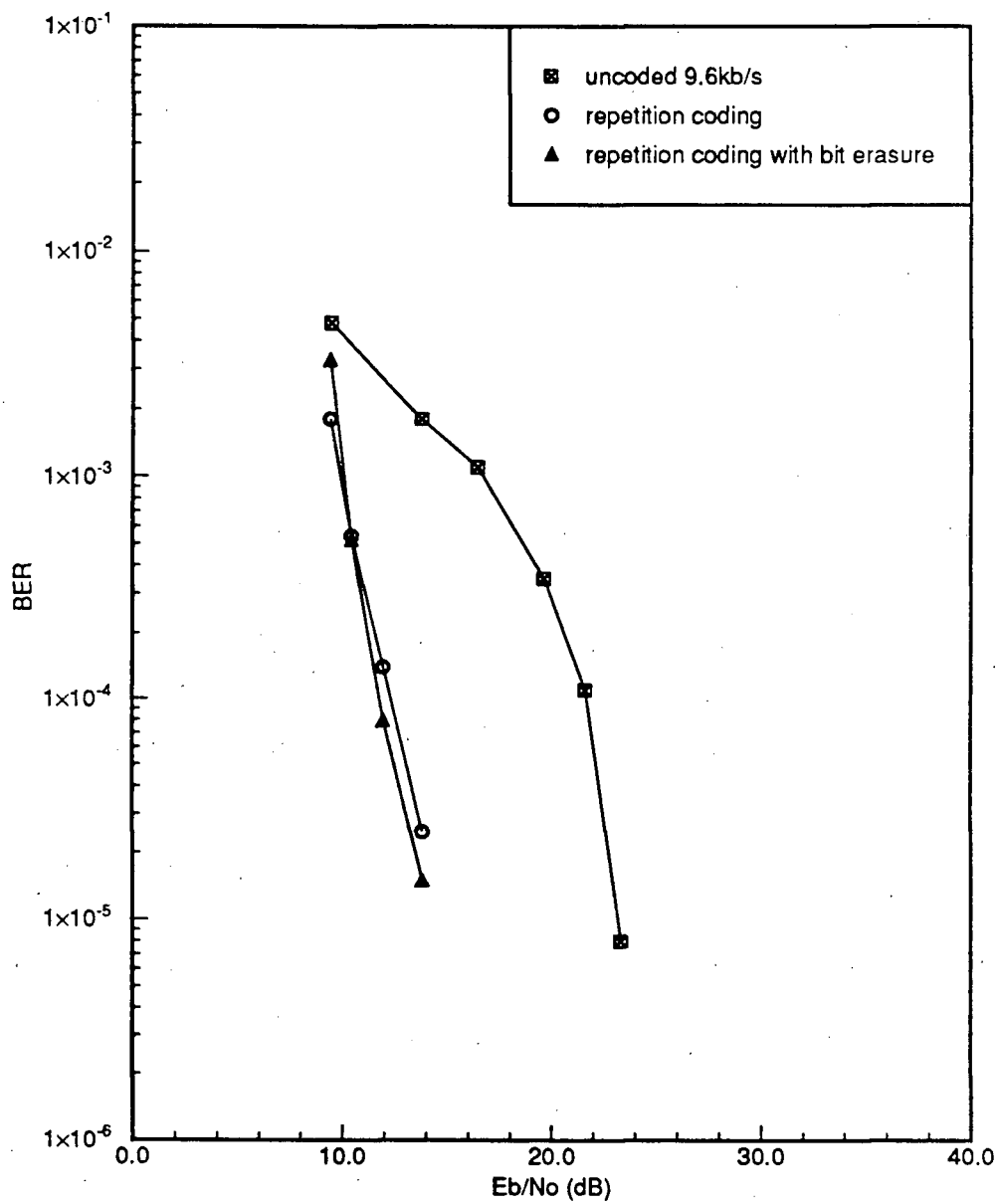
Figure 7.17: Uncoded and repetition coded BER performances at 9.6 kbits/s data rate.

the impulse noise impaired channels. Defining and evaluating an optimum threshold level is a formidable task. The correct packet reception rate for uncoded and repetition coded data transmission were also measured and shown in Figs.7.18 and 7.19. The packet length was 1,000 bits.

## 7.6   Summary

Unlike many other communication channels, power line networks exhibit high error rate. Suitable FEC coding is necessary to reduce these error rates to an acceptable level. A series of measurements were made on real power line channels in order to determine what improvements in performance could be obtained with the use of simple convolutional codes as well as with repetition coding and modest amounts of interleaving. The error correction effectiveness of these codes against periodic impulse noise, random noise, signal distortion, phase distortion and other impairments possibly encountered on typical power lines are experimentally determined.

The results of the measurements presented indicate that the use of a simple short constraint length convolutional code and threshold decoding can reduce decoded bit error rate several orders of magnitude below uncoded transmission, even under minimal interleaving delay insufficient to render the channel memoryless. This initial delay with coding is negligible
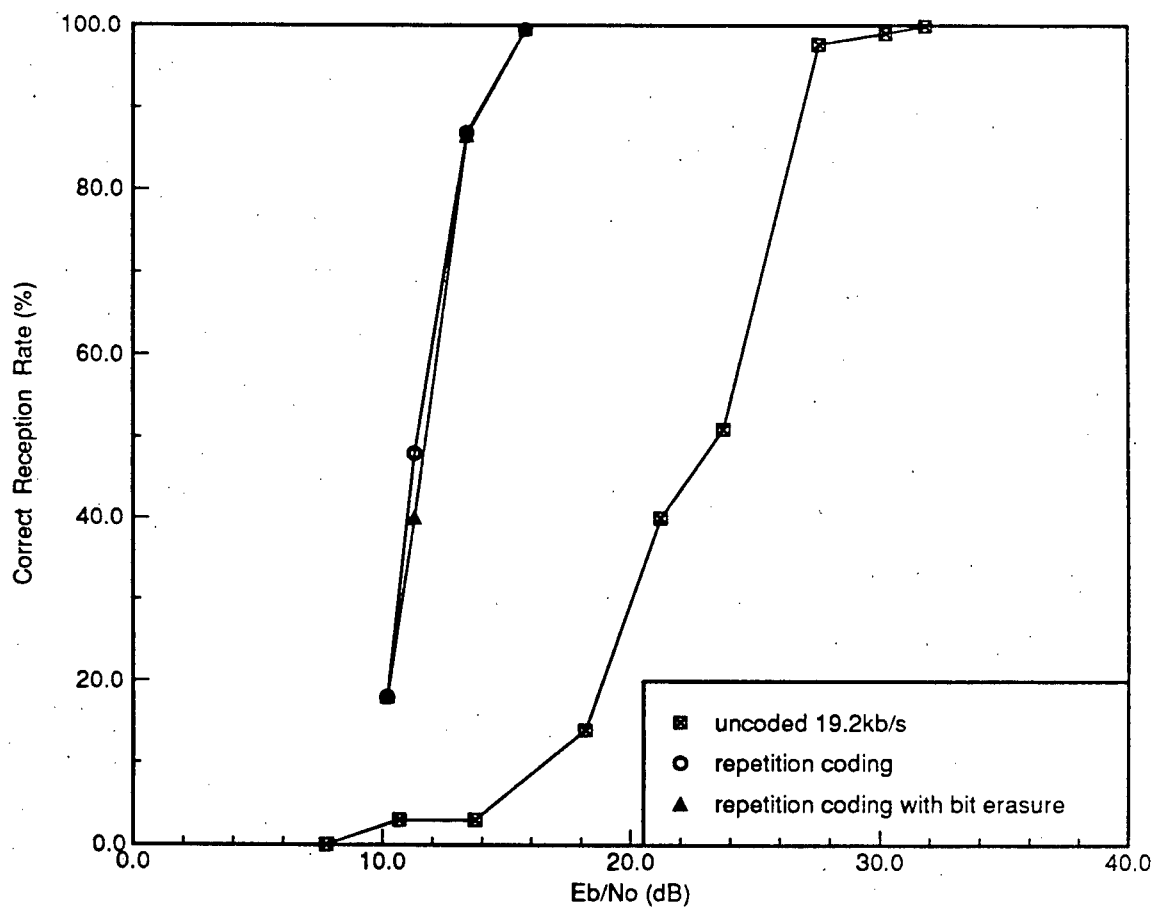
Figure 7.18: CCR for uncoded and repetition coded transmissions at 19.2 kbits/s data rate.
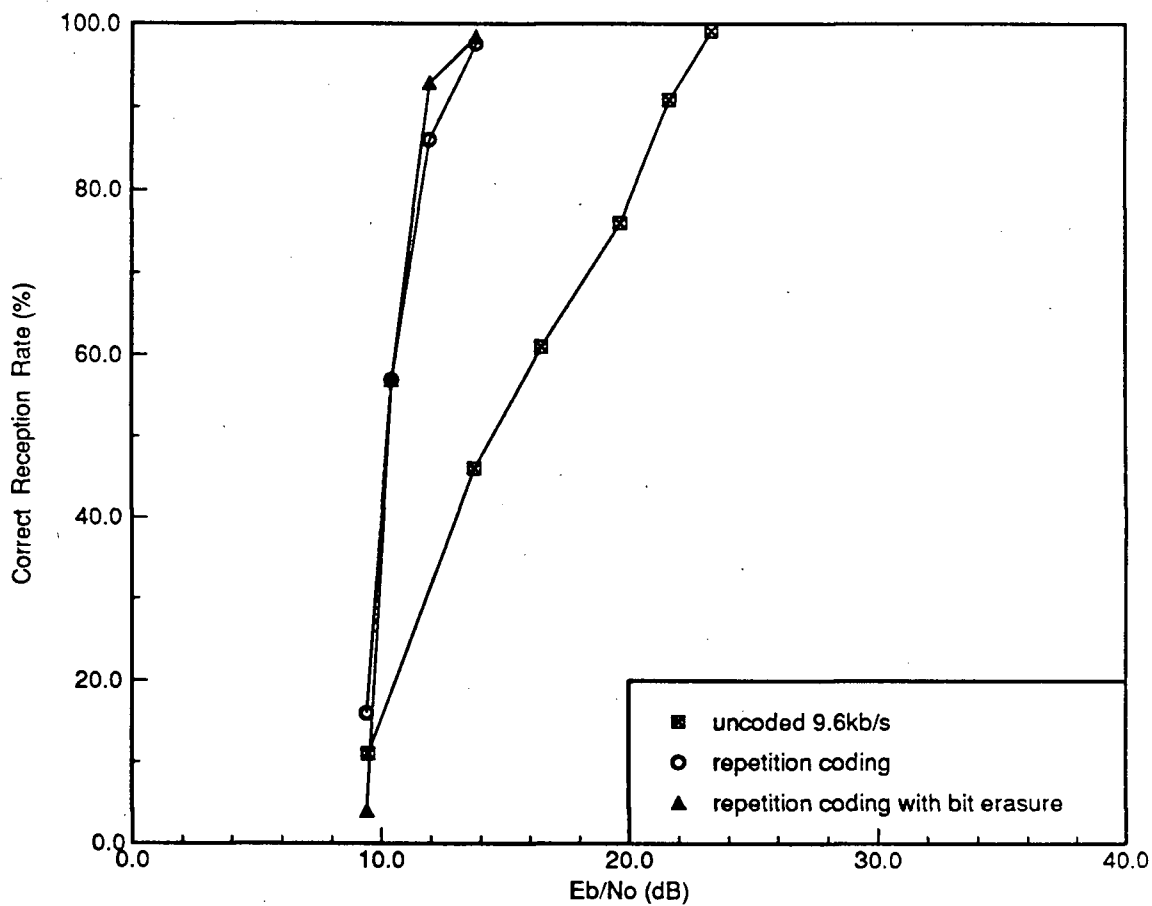
Figure 7.19: CCR for uncoded and repetition coded transmissions at 9.6 kbits/s data rate.

as compared with the delay with retransmissions of errored packets which are often thousands of bits long. The FEC coded system also increased the packet reception rate from close to 0% to over 90 %, greatly improving the throughput of any retransmission schemes. Even under strong interference levels generated by a light dimmer, appropriate coding reduced BER substantially. Rather than resorting to the use of particular codes to correct a fixed number or type of errors, interleaving a random error correcting code provides a very effective and robust means to combat both burst and random errors encountered on the highly varying power line communication channels. It is successfully demonstrated that utilization of a suitable, inexpensive FEC coding scheme enables transmissions on otherwise unreliable power line channels at acceptable decoded bit error rates. Retransmission of those packets with uncorrected errors can ensure highly reliable communication services on intrabuilding power line communication networks.

# Chapter 8

# Conclusions

## 8.1 Concluding Remarks

Apart from the inherent communication limitations, the key obstacles to power line communications are insufficient understanding of this complex and hostile communication channel as well as limited performance of present systems. The situation is further compounded by cost constraints imposed for low cost applications.

Through our experimental research program, practical constraints, limitations and requirements of the power line communication channels have been identified and studied, leading to design considerations essential for successful implementation of future generations of power line communication systems. While detailed conclusions are given at the end of each chapter, some general conclusions are drawn from this thesis and presented below.

The results of our signal transmission study reveal wide variations in attenuation vs. frequency behaviour and in actual attenuation levels at any given frequency, in different buildings. The differences arise because of substantial variations in the length and layout of the actual physical power line wiring. Within a given building, large attenuation differences arise in transmission between different node pairs or between the same node pair at different times. The differences over node pairs arise because of variations in actual transmission path, while the differences over time arise because of variations in network loading. Except over short transmission distances, signal attenuation typically exceeds 20 dB even when the transmitter and receiver use the same power phase. The high and varying propagation losses suggest the need for a large transmit signal power; however, this approach is not practical because attenuation can become extremely high. In addition, a high transmit signal level increases modem cost and power consumption, and also increases interference levels which may be subjected to government regulations.

Power line communication signals also experience periodic enhancements and fades about the median signal level. When these fades exceed a specific margin, system performance can be seriously degraded. The degree of degradation will depend on the magnitude of fading, the duration of the fade and the fading rate. This rate is normally 120 Hz although other rates

such as 6 Hz are possible and do occur.

Noise on power lines has a highly structured form, characterized by significant probabilities of large interference levels which can drastically degrade system performance. In particular, 120 Hz periodic impulse noise is the most dominant source of errors of all the impairments found on power lines. Impulse amplitude is typically more than 10 dB above the background noise level. However, specific noise sources located close to the receiving point can significantly add to the received noise process, and impulse amplitude 30-40 dB above the background noise level is possible. Also, impulses can appear in pairs leading to very long error bursts on power lines.

To enable reliable communications, FEC coding is used to combat power line impulse noise and periodic signal fading, to compensate for severe received signal power limitations, and to overcome potential narrow band fades, phase distortion and other impairments. Through mathematical analysis, it is shown that the performance advantages to be realized with error correction and interleaving can be substantial. Further testing of different random and burst error correcting block codes against actual recorded error patterns have shown that by careful choice of an error control coding scheme, it is possible to drastically reduce the effects of impulse noise. It is found that the combination of interleaving and random error correction provides

significantly better performance than error correction coding alone. However too long an interleaver, especially at some multiples of periodic error, may not be benefical. A code with a short block length can be effectively interleaved to provide an inexpensive and robust coding scheme for power line channels with periodic, bursty and random impairments.

The results from the study of the channel and error correction coding lead to the development of an operational FEC coded power line data communication system. Tests on actual channels show that through the use of simple short constraint length convolutional codes and threshold decoding or by use of repetition coding, the required $E_b/N_0$ for an acceptable BER is much reduced from uncoded transmission. Also, the rate that packets are correctly received is increased from close to 0% to over 90%. Even at strong interference levels generated by a light dimmer, appropriate coding reduced BER substantially. It is shown that suitably interleaving a random error correcting code appears to be an inexpensive and reliable mean for combating errors encountered on the complex and varying power line communication channels. The results include transmissions at bit transmission rates up to 57.6 kbits/s. It is successfully demonstrated that with suitable and inexpensive FEC coding, reliable high speed data transmission over power lines is feasible, even at very small interleaving delay.

153

In summary, this thesis presents important original fundamental studies and a much better understanding of the communication channel characteristics and behaviour of intrabuilding power line networks. The thesis also presents and demonstrates means to utilize such networks effectively in real operating envirnoments.

## 8.2  Some Suggestions for Further Work

The studies presented in this thesis provide quantitative measures and a better understanding of some of the most basic factors characterizing power line communication channels. These results add to an increasing data base for future analysis, and also help to the development of guidelines which would lead to the development of new regulations and standards governing the technical characteristics and operation of equipment and systems employing digital transmission of information over intrabuilding power line networks.

Some substantial work remains to be done in the future. Among these is implementation of the economically viable subsystems described in this thesis using various VLSI and application specific integrated circuit (ASIC) techonlogies. As well, multiple user access protocols needed to be designed and implemented.

The use of repeaters to overcome severe attenuation problems on par-

154

ticularly bad links is worthy of considerable investigation. Various questions arise. How many repeaters would be adequate and where should they be located? The highly variable attenuation characteristics make the choice of repeater locations difficult. A potential solution proposed by this author is that every network user would serve as a repeater upon request from other users, so that no explicit repeater is required. For a network of even moderate size, the number of repeaters available to each user would exceed what could be offered by installing explicit repeaters. A simple protocol which goes with this method follows.

With each user is a routing table which keeps track of the path conditions between itself and all other users as either good or bad. When user i wants to transmit to user j, a direct transmission will take place regardless of the path condition. If after a fixed number of unsuccessful trials, user i updates its own routing table regarding the path condition to user j as bad and then selects from the top of its table the first good user (user k) to serve as a repeater. User i then transmits to user j via user k who serves as a repeater. If a positive acknowledgement is not received by user i after some timeout period, user i again updates its routing table and looks for another good user to serve as a repeater. The process repeats until either a positive acknowledgement is received or all possible users are tried. If the later event occurs, then transmission is aborted. For the idle users, control

155

signals could be sent occasionally to determine the path conditions, and to use the information obtained to update their routing tables.

As more data becomes available, development of viable analytical channel models for system design is of interest. With regard to FEC coding, higher order models describing the error arrival process could be developed. But as pointed out by Brayer [1] in a guest editorial on HF data transmission, those who were studying error patterns divided into two camps, the coders and the modelers. The modelers are still doing modelling but the coders solved the problem.

The data rate of the system described in this thesis is high enough to support various types of digitized voice transmission. Subjective studies on the quality of digital voice communication over power lines would be interesting.

The above list of ideas for further studies is by no means exhaustive. Considerable work remains to be done at the data link, network and higher level protocol layers. Power line communications is potentially an active area for further research and product development. It is expected that there will be an expansion of activities as more is learned about the capabilities and limitations of power line channels, and about potential markets for power line communications technology.

# References

[1] K. Brayer, "Guest Editorial-HF Data Transmission: Lessons from the Past, Directions for the Future", *IEEE Journal on Selected Areas in Commun.*, vol. SAC-5, pp. 90-101, Feb. 1987.

[2] *BSR X-10 Owners Manual*, BSR (Canada) Ltd., 1978.

[3] *Canadian Electrical Code - Part I*, 14th ed. Rexdale, Ont., Canada: Cdn. Standards Assoc., 1982.

[4] M.H.L. Chan, F.F.K. Chiu and R.W. Donaldson, "Signalling and error control for data communications on intrabuilding electric power distribution circuits," in *Canadian Developments in Telecommunications: An overview of Significant Contributions*, T.L.McPhail and D.C. Coll, Eds., Calgary, Alta.: U. Calgary Press, 1986, pp. 165-212.

[5] M.H.L. Chan and R.W. Donaldson, "Attenuation of communication signals on residential and commercial intrabuilding power distribution circuits," *IEEE Trans. Electromagn. Compat.*, vol. EMC-28, pp. 220-230, Nov. 1986.

[6] M.H.L. Chan and R.W. Donaldson, "Local area networking on intrabuilding electric power distribution circuits - physical layer considerations", *Proc. of IEEE Pacific Rim Conf. on Communications, Computers and Signal Processing*, Victoria, Canada, June 4-7, 1987.

[7] M.H.L. Chan and R.W. Donaldson, "Amplitude, Width and Interarrival Distributions for Noise Impulses, and Bit Error Rates, on Intrabuilding Power Line Communication Networks", *IEEE Trans. Electromagn. Compat.*, submitted for publication, 1988.

[8] M.H.L. Chan and R.W. Donaldson, "FEC coding for Data Communications on Intrabuilding Electric Power Lines," to be submitted to *IEEE Trans. Commun.* for publication.

[9] M.H.L. Chan and R.W. Donaldson, "Convolutional Coding for Data Communications on Intrabuilding Power Lines," accepted for presentation at Canadian Information Theory Workshop, Victoria, B.C., May 29-31, 1989.

[10] A.C.M. Chen, "Automated Power Distribution", *IEEE Spectrum*, pp. 55-60, April 1982.

[11] F.K.K. Chiu, *Data Communications Using Coherent Minimum Frequency Shift Keying on Intrabuilding Polyphase Power Line Networks*, M.A.Sc. Thesis, Electrical Eng. Dept., University of British Columbia, Canada, December 1985.

[12] *Stable FSK Modems Featuring the XR-2206, XR-2207, and XR-2211, AN-01*, EXAR Integrated Systems, Inc., Synnyvale, CA., 1986.

[13] K. Feher, *Digital Communications: Satellite/Earth Station Engineering*, Englewood Cliffs, N.J.: Prentice Hall, 1983.

[14] D.G. Fink, Ed., *Standard Handbook for Electrical Engineerings*, 11th ed. New York: McGraw-Hill, 1978.

[15] G.D. Forney, Jr., "Burst-Correcting Codes for the Classic Bursty Channel", *IEEE Trans. Comm. Tech.*, pp. 772-781, Oct. 1971.

[16] P.K. van der Gracht, *A Spread Spectrum Modem for Use on Electrical Power Lines*, M.A.Sc. Thesis, Electrical Eng. Dept., University of British Columbia, Canada, January 1982.

[17] P.K. van der Gracht and R.W. Donaldson, "Communication using pseudonoise modulation on electric power distribution circuits", *IEEE Trans. Commun.*, vol. COM-33, pp. 964-974, Sept. 1985.

[18] J.A. Heller, "Feedback decoding of convolutional codes", in *Advances in Communication Systems*, vol.4, A. Viterbi Ed., New York: Academic, 1975, pp. 261-278.

[19] H.P. Hsu, R.M. Storwick, D.C. Schlick and G.L. Maxam, "Measured Amplitude Distribution of Automotive Ignition Noise", *IEEE Trans. Electromag. Compat.*, vol. EMC-16, pp.57-63, May 1974.

[20] A.G. Hudson, D.R. Beuerle and H.J. Fiedler, "SSB Carrier for Utility Control and Communication", *Proceedings of IEEE National Telecommunication Conference*, pp. 2.1.1-2.1.7, 1976.

[21] M. Kanda, "Time and Amplitude Statistics for Electromagnetic Noise in Mines", *IEEE Trans. Electromag. Compat.*, vol. EMC-17, pp. 122-129, Aug. 1975.

[22] W.R. Lauber, "Quasi-Peak Voltages Derived from Amplitude Probability Distributions", *IEEE Trans. Electromag. Compat.*, vol. EMC-23, pp. 98-100, May 1981.

[23] W.R. Lauber, "Amplitude Probability Distribution Measurements at the Apple Grove 775kV Project", *IEEE Trans. Power App. Syst.*, July/Aug., 1976.

[24] A. Kohlenberg and G.D. Forney, Jr., "Convolutional Coding for Channels with Memory," *IEEE Trans. Inf. Theory*, IT-14, pp. 618-626, Sept. 1968.

[25] S. Lin and D.T. Costello, Jr., *Error Control Coding: Fundamentals and Applications*. Englewood Cliffs, N.J.: Prentice Hall, 1983.

[26] Glen Lokken, Neil Jagoda, and Raymond J. D'Auteuil, "The Proposed Wisconsin Electric Power Company Load Management System Using Power Line Carrier Over Distribution Lines", *Proc. IEEE National Telecommunication Conference*, pp. 2.2.1-2.2.3, 1976.

[27] R. Lytle and S. Strom, "A new carrier current protocol utilizing an active repeater for consumer and industrial applications", *IEEE Trans. Cons. Electron.*, vol. CE-31, pp. 700-705, Nov. 1985.

[28] J.A. Malack and J.R. Engstrom, "R.F. impedance of United States and European power lines", *IEEE Trans. Electromagn. Compat.*, vol. EMC-18, pp. 36-38, Feb. 1976.

[29] J.L. Massey, *Threshold Decoding*. Cambridge, MA: M.I.T. Press, 1963.

[30] J.L. Massey, "Advances in Threshold Decoding," in *Advances in Communication Systems, vol.2*, A.V. Balakrishnan, ed., Academic Press, New York, 1968.

[31] R.J. Matheson, "Instrumentation Problems Encountered Making Man-Made Electromagnetic Noise Measurements for Predicting Communication System Performance", *IEEE Trans. Electromag. Compat.*, vol. EMC-12, pp. 151-158, Nov. 1970.

[32] T. Nakai and Z. Kawasaki, "Automotive Noise from a Motorway: Part I, Measurement", *IEEE Trans. Electromag. Compat.*, vol. EMC-26, pp. 169-174, Nov. 1984.

[33] T. Nakai and H. Ohba, "On the Graphical Method of Drawing APD's for Atmospheric Radio Nomethodise", *IEEE Trans. Electromag. Compat.*, vol. EMC-26, pp. 71-78, May 1984.

[34] *NE5050 Power Line Modem Data Sheet,* Signetics Corporation, Synnyvale, CA., U.S.A., 1988

[35] J.R. Nicholson and J.A. Malack, "R.F. impedance of power lines and line impedance stabilization networks in conducted interference measurements", *IEEE Trans. Electromagn. Compat.*, vol. EMC-15 pp. 84-86, May 1973.

[36] *NONWIRE Multipdrop Network Users Guide,* CYPLEX Division, Controlonics Corporation, Chelmsford, MA, U.S.A., 1985.

[37] H. Ochsner, "Data transmission on low voltage power distribution lines using spread spectrum techniques", *Proc. Can. Commun. Power Conf.*, Montreal, P.Q., Canada, Oct.15-17, 1980, pp. 236-239.

[38] J.P. Odenwalder and and A.J. Veterbi, "Overview of Existing and Projected Uses of Coding in Military Satellite Communications," *Proc. of NTC Conf. Rec.*, pp. 36:4.1-36:4.2, Los Angeles, Calif., Dec. 1977.

[39] W.W. Peterson and E.J. Weldon, *Error Correcting Codes,* Cambridge, MA: M.I.T. Press, 1972.

[40] *POWERLAN,* ExpertNet, Acton, MA, U.S.A., 1984.

[41] J.P. Robinson, "A class of binary recurrent codes with limited error propagation", *IEEE Trans. Inform. Theory,* vol. IT-13, pp. 106-113, Jan. 1967.

[42] R.B. Schulz and R.A. Southwick, "APD Measurements of V-8 Ignition Emanations", *IEEE Trans. Electromag. Compat.,* vol. EMC-16, pp. 63-70, May 1974.

[43] A.A. Smith, "Power line noise survey", *IEEE Trans. Electromagn. Compat.,* vol. EMC-14, pp. 31-32, Feb. 1972.

[44] H.J. Trussel and J.D. Wang, "The effect of hard limiters on signal detection in harmonic noise using adaptive noise cancellation," *IEEE Trans. Pwr. Del,* vol. PWRD-1, pp. 73-78, Jan. 1986.

[45] H.J. Trussel and J.D. Wang, "Cancellation of Harmonic Noise in Distribution Line Communication", *IEEE Trans. Pwr. Del.,* vol. PAS-104, pp.3338-3344, Dec. 1985.

[46] R.M. Vines, H.J. Trussel, L.J. Gales and J.B. O'Neal, Jr., "Noise on residential power distribution circuits", *IEEE Trans. Electromagn. Compat.,* vol. EMC-26, pp. 161-168, Nov. 1984.

[47] R.M. Vines, H.J. Trussel, K.C. Shuey and J.B. O'Neal, Jr., "Impedance of the residential power-distribution cirucit", *IEEE Trans. Electromagn. Compat.,* vol. EMC-27, pp. 6-12, Feb. 1985.

[48] A.J. Viterbi, "Error Bounds for Convolutional Codes and an Asymptotically Optimum Decoding Algorithm", *IEEE Tran. Inform. Theory,* IT-13, pp. 260-269, April 1967.

[49] R.E. Walpole and R.H. Meyers, *Probability and Statistics for Engineers and Scientists*, 2nd ed. New York: MacMillan, 1978, Ch. 9.

[50] J.M. Wozencraft and I.M. Jacobs, *Principles of Communication Engineering,* New York, Wiley, 1965.

[51] J.M. Wozencraft and B. Reiffen, *Sequential Decoding,* M.I.T. Press, Cambridge, Mass., 1961.

[52] W.W. Wu, "New Convolutional Codes - Part I," *IEEE Trans. Commun.,* COM-23, pp. 942-956, Sept. 1975.

[53] W.W. Wu , "New Convolutional Codes - Part II," *IEEE Trans. Commun.,* COM-23, pp. 19-33, Jan. 1976.

# Appendix A

# Equations for Interleaved Repetition Coding

For a simple additive white Gaussian noise channel of power spectral density $N_b/2$, the bit error probability $P_e$ of an integrate and dump receiver is $Q(\sqrt{2E_b/N_b})$ [50]. When the noise power spectral density alternates between $N_i/2$ and $N_b/2$, Eqns. (5.1-5.5) are obtained by multiplying the proportion of time with the bit error probability of a data bit when it is affected by each noise type.

In Eqn. (5.1), DF and 1-DF represent the proportion of time that a data bit is affected by impulse noise and background noise, respectively.

In Eqn. (5.2), when a data bit affected by impulse noise is interleaved, three data bits are affected. The proportion of time that a data bit is affected by impulse noise and background noise then becomes 3DF and 1-3DF,

respectively. For repetition codings, a data bit is in error when any two or all of the three code bits are in error. When all three code bits are affected by background noise, this probability of any two or all three code bits in error is given by the binomial expression in the equation. When one of the three code bits is affected by impulse noise, this probability of any two or all three code bits in error is written out explicitly as shown in the 2nd term of the equation.

In Eqn. (5.3), the 1st term is the probability of error when a data is affected by background noise only. The 2nd term is the probability of a data bit in error when 1/3 of the data bit is affected by impulse noise while the other 2/3 is affected by background noise.

In Eqn. (5.4), the first term is the same as in Eqn. (5.2). The 2nd term is the probability of a data bit in error when either one or all two of the unerased code bits are in error.

In Eqn. (5.5), the 1st term is the same as in Eqn.(5.3). The 2nd term is the probability of a data bit in error when the remaining 2/3 of the data bit is affected by background noise as the other 1/3 is erased.

When the impulse noise duration is a fraction f of the data bit duration, the bit error probability $P_e$ derivations follow the same aguements as with eqnations (5.1-5.5) and are straight forward. They are given below:

163

For $2/3 < f \le 1$

(1) Uncoded transmission.

$$P_e = (1 - \frac{DF}{f})Q(\sqrt{2E_b/N_b}) + \frac{DF}{f}Q(\sqrt{2E_b/(fN_i + (1-f)N_b)}) \quad \text{(A.1)}$$

(2) Interleaved hard decision.

$$
\begin{aligned}
P_e =\ & (1 - 3\frac{DF}{f})\sum_{k=2}^{3}\binom{3}{k}Q(\sqrt{2E_b/3N_i})^k\overline{Q}(\sqrt{2E_b/3N_b})^{3-k} \\
& +2\frac{DF}{f}[2Q(\sqrt{2E_b/3N_i})Q(\sqrt{2E_b/3N_b})\overline{Q}(\sqrt{2E_b/3N_b}) + Q(\sqrt{2E_b/3N_b})^2] \\
& +\frac{DF}{f}[2Q(\sqrt{2E_b/[3((3f-2)N_i + (3-3f)N_b)]})Q(\sqrt{2E_b/3N_b})\overline{Q}(\sqrt{2E_b/3N_b}) \\
& +Q(\sqrt{2E_b/3N_b})^2]
\end{aligned}
\quad \text{(A.2)}
$$

(3) Interleaved soft decision.

$$
\begin{aligned}
P_e =\ & (1 - 3\frac{DF}{f})Q(\sqrt{2E_b/N_b}) + 2\frac{DF}{f}Q(\sqrt{6E_b/(N_i + 2N_b)}) \\
& +\frac{DF}{f}Q(\sqrt{6E_b/((3f-2)N_i + (5-3f)N_b)})
\end{aligned}
\quad \text{(A.3)}
$$

(4) Interleaved hard decision with erasure.

$$
\begin{aligned}
P_e =\ & (1 - 3\frac{DF}{f})\sum_{k=2}^{3}\binom{3}{k}Q(\sqrt{2E_b/3N_b})^k\overline{Q}(\sqrt{2E_b/3N_b})^{3-k} \\
& +3\frac{DF}{f}Q(\sqrt{2E_b/3N_b})
\end{aligned}
\quad \text{(A.4)}
$$

(5) Interleaved soft decision with erasure.

$$P_e = (1 - 3\frac{DF}{f})Q(\sqrt{2E_b/N_b}) + 3\frac{DF}{f}Q(\sqrt{4E_b/3N_b}) \quad \text{(A.5)}$$

For $1/3 < f \leq 2/3$

(1) Uncoded transmission.

$$P_e = (1 - \frac{DF}{f})Q(\sqrt{2E_b/N_b}) + \frac{DF}{f}Q(\sqrt{2E_b/(fN_i + (1-f)N_b)}) \quad \text{(A.6)}$$

(2) Interleaved hard decision.

$$\begin{aligned}
P_e &= (1 - 2\frac{DF}{f})\sum_{k=2}^{3}\binom{3}{k}Q(\sqrt{2E_b/3N_b})^k\overline{Q}(\sqrt{2E_b/3N_b})^{3-k} \\
&+ \frac{DF}{f}[2Q(\sqrt{2E_b/3N_i})Q(\sqrt{2E_b/3N_b})\overline{Q}(\sqrt{2E_b/3N_b}) + Q(\sqrt{2E_b/3N_b})^2] \\
&+ \frac{DF}{f}[2Q(\sqrt{2E_b/[3((3f-1)N_i + (2-3f)N_b)]})Q(\sqrt{2E_b/3N_b})\overline{Q}(\sqrt{2E_b/3N_b}) \\
&+ Q(\sqrt{2E_b/3N_b})^2]
\end{aligned} \quad \text{(A.7)}$$

(3) Interleaved soft decision.

$$\begin{aligned}
P_e &= (1 - 2\frac{DF}{f})Q(\sqrt{2E_b/N_b}) + \frac{DF}{f}Q(\sqrt{6E_b/(N_i + 2N_b)}) \\
&+ \frac{DF}{f}Q(\sqrt{6E_b/((3f-1)N_i + (4-3f)N_b)})
\end{aligned} \quad \text{(A.8)}$$

(4) Interleaved hard decision with erasure.

$$\begin{aligned}
P_e &= (1 - 2\frac{DF}{f})\sum_{k=2}^{3}\binom{3}{k}Q(\sqrt{2E_b/3N_b})^k\overline{Q}(\sqrt{2E_b/3N_b})^{3-k} \\
&+ 2\frac{DF}{f}Q(\sqrt{2E_b/3N_b})
\end{aligned} \quad \text{(A.9)}$$

(5) Interleaved soft decision with erasure.

$$P_e = (1 - 2\frac{DF}{f})Q(\sqrt{2E_b/N_b}) + 2\frac{DF}{f}Q(\sqrt{4E_b/3N_b}) \quad \text{(A.10)}$$

165

For $0 < f \leq 1/3$

(1) Uncoded transmission.

$$P_e = (1 - \frac{DF}{f})Q(\sqrt{2E_b/N_b}) + \frac{DF}{f}Q(\sqrt{2E_b/(fN_i + (1-f)N_b)}) \quad \text{(A.11)}$$

(2) Interleaved hard decision.

$$\begin{aligned}
P_e &= (1 - \frac{DF}{f})\sum_{k=2}^{3}\binom{3}{k}Q(\sqrt{2E_b/3N_b})^k\overline{Q}(\sqrt{2E_b/3N_b})^{3-k} \\
&\quad + \frac{DF}{f}[2Q(\sqrt{2E_b/[3(3fN_i + (1-3f)N_b)]})Q(\sqrt{2E_b/3N_b})\overline{Q}(\sqrt{2E_b/3N_b}) \\
&\quad + Q(\sqrt{2E_b/3N_b})^2] \quad \text{(A.12)}
\end{aligned}$$

(3) Interleaved soft decision.

$$\begin{aligned}
P_e &= (1 - \frac{DF}{f})Q(\sqrt{2E_b/N_b}) \\
&\quad + \frac{DF}{f}Q(\sqrt{2E_b/(fN_i + (1-f)N_b)}) \quad \text{(A.13)}
\end{aligned}$$

(4) Interleaved hard decision with erasure.

$$\begin{aligned}
P_e &= (1 - \frac{DF}{f})\sum_{k=2}^{3}\binom{3}{k}Q(\sqrt{2E_b/3N_b})^k\overline{Q}(\sqrt{2E_b/3N_b})^{3-k} \\
&\quad + \frac{DF}{f}Q(\sqrt{2E_b/3N_b}) \quad \text{(A.14)}
\end{aligned}$$

(5) Interleaved soft decision with erasure.

$$P_e = (1 - \frac{DF}{f})Q(\sqrt{2E_b/N_b}) + \frac{DF}{f}Q(\sqrt{4E_b/3N_b}) \quad \text{(A.15)}$$

166

# Appendix B

# Hardware Photographs and Cost Discussions of the DPSK System

Photographs of the FEC coded DPSK system described in Chapter 7 are shown below. The implementation is based largely on standard off the shelf CMOS logic IC's which easily lends to VLSI implementation. Part cost per board is typically about five dollars with the exception of the power supply board which costs around twelve dollars. Quantity discounts and integrated circuit implemention would significantly reduce these costs.

In implementing the system, no attempt was made to optimize packaging. Instead, board layouts were designed to facililate experimental work and performance measurements. The various FEC codes used were implemented on different boards, which could be easily interchanged.
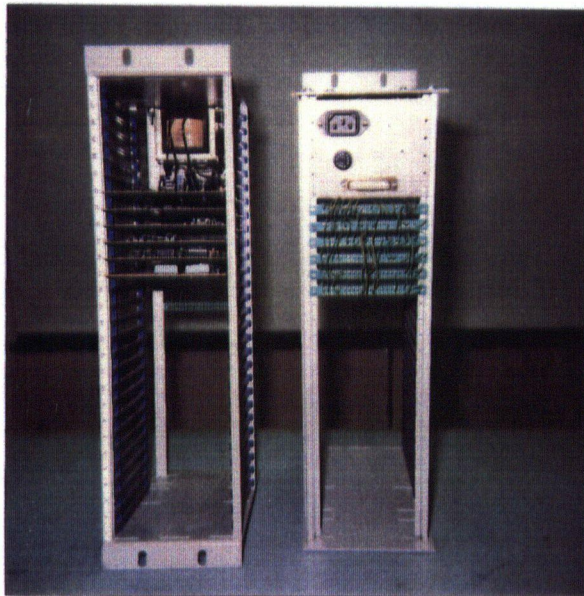
Figure B.1: A photograph of the front and rear view of the implementation of the FEC coded power line data communication system described in Chapter 7
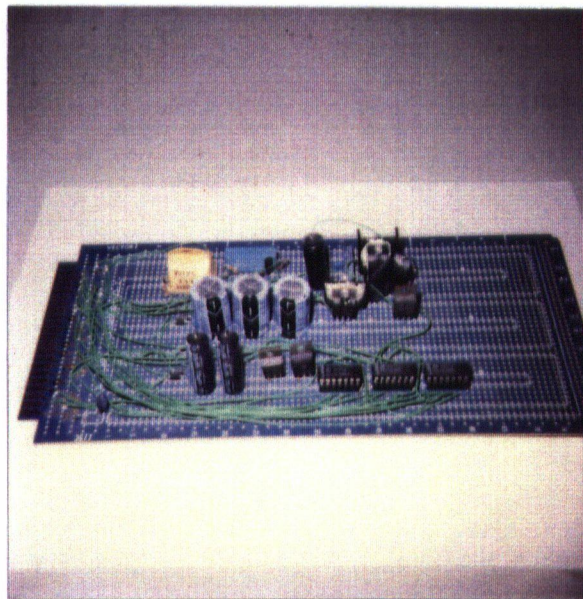


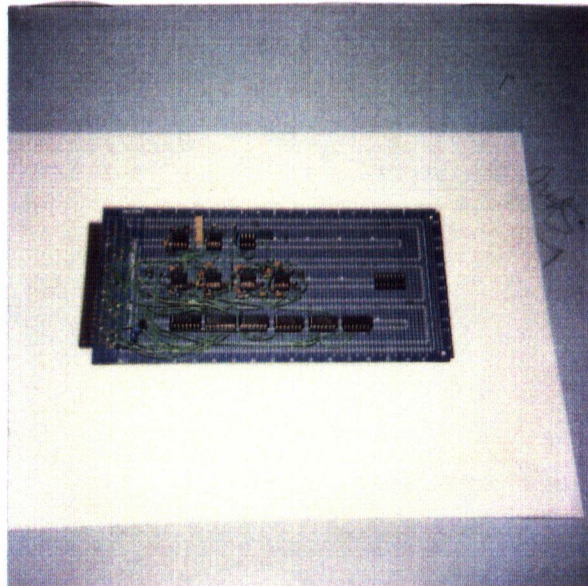Figure B.2: The Power Supply/Power Amplifier/TTL-RS-232C Level Shift/Line Coupling Network board.

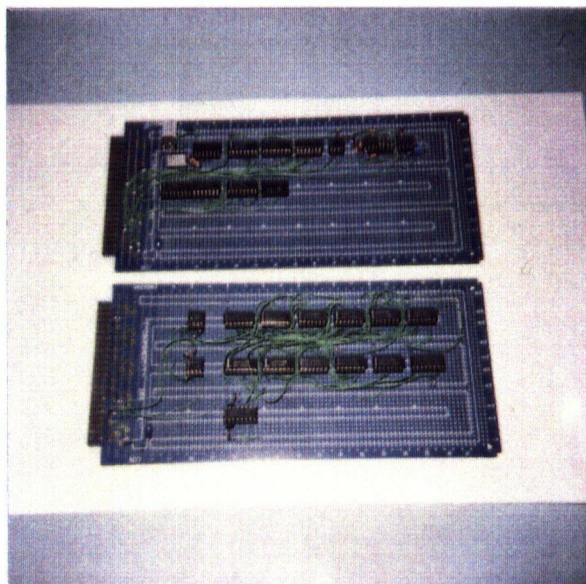Figure B.3: The BPF's/CMOS-TTL Level Shift/RS-232C signals board.


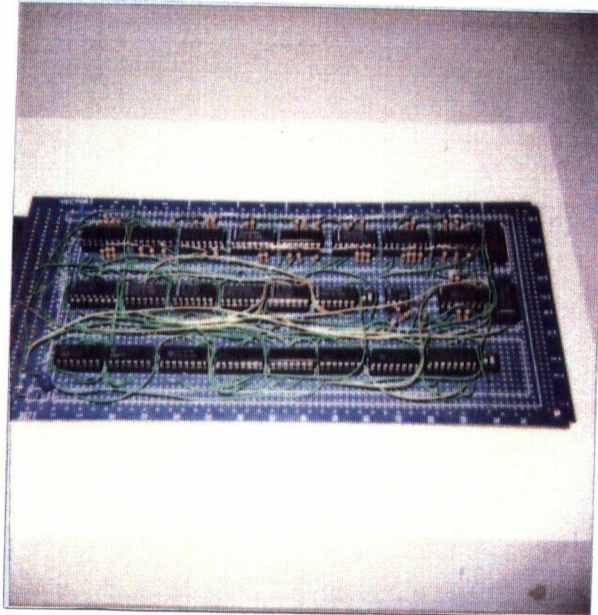
Figure B.4: The DPSK Modem boards.

169

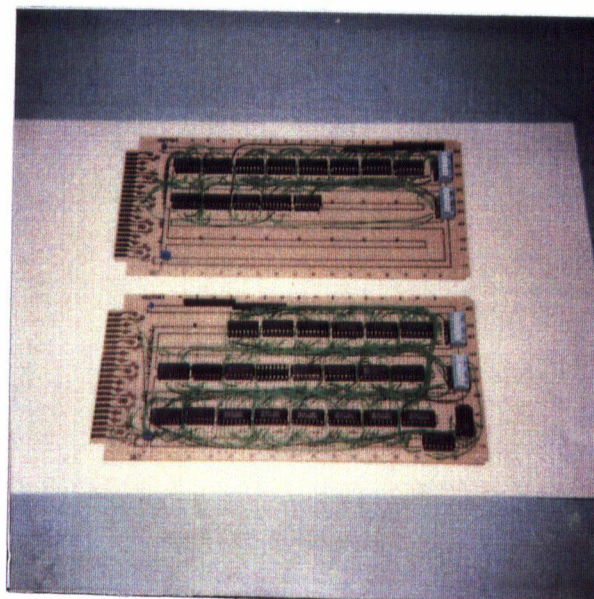Figure B.5: The Preamble/Sync Recognition/Scrambler/Decrambler board.



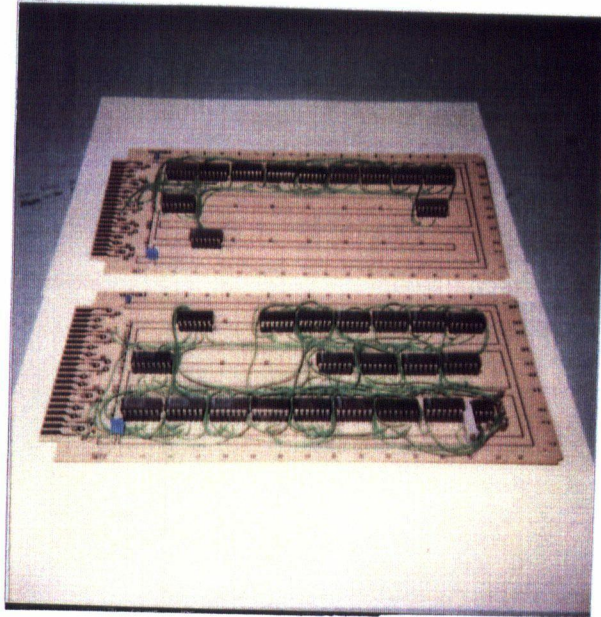Figure B.6: The (2,1,6) Encoder/Interleaver and Decoder/Deinterleaver boards.

170

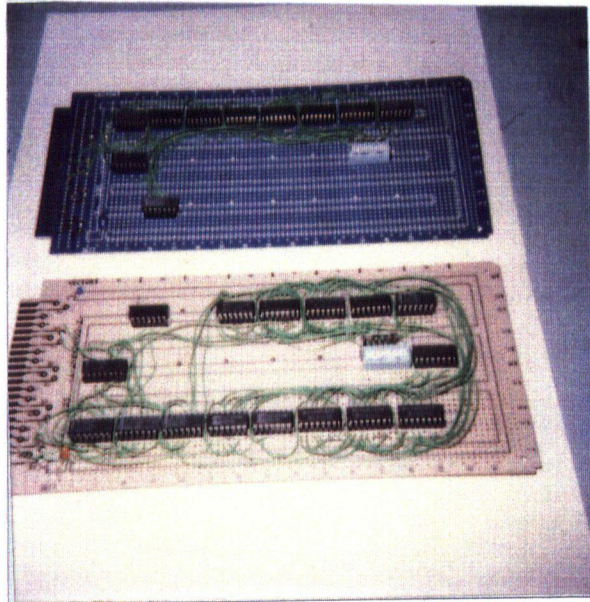Figure B.7: The (2,1,35) Encoder and Decoder boards.



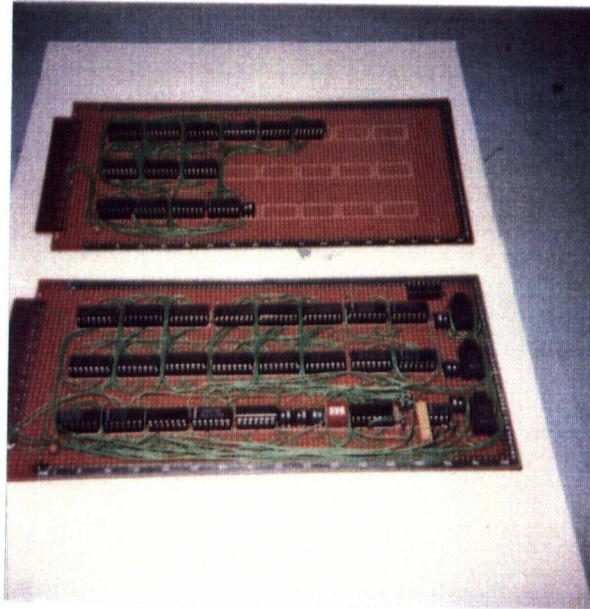Figure B.8: The Encoder and Decoder boards for the Diffuse Code.

171

Figure B.9: The Encoder/Interleaver and Decoder/Deinterleaver boards for the Repetition Code.